EFFECTS OF pH AND HYDROPHOBICITY ON THE TRANSPORT OF VIRUSES AND BACTERIA IN SATURATED MEDIA

by

Takashi Kinoshita

A Thesis Submitted to the Faculty of the

DEPARTMENT OF HYDROLOGY AND WATER RESOURCES

In Partial Fulfillment of the Requirements
For the Degree of

MASTER OF SCIENCE
WITH A MAJOR IN HYDROLOGY

In the Graduate College

THE UNIVERSITY OF ARIZONA

1991

STATEMENT BY AUTHOR

This thesis has been submitted in partial fulfillment of requirements for an advanced degree at The University of Arizona and is deposited in the University Library to be made available to borrowers under rules of the Library.

Brief quotations from this thesis are allowable without special permission, provided that accurate acknowledgment of source is made. Requests for permission for extended quotation from or reproduction of this manuscript in whole or in part may be granted by the head of the major department of the Dean of the Graduate College when in his or her judgment the proposed use of the material is in the interests of scholarship. In all other instances, however, permission must be obtained from the author.

SIGNED: Takashi Kinoshita

APPROVAL BY THESIS CO-DIRECTORS

This thesis has been approved on the date shown below:

R. C. Bales
Associate Professor of Hydrology

4/29/91
Date

C. P. Gerba
Professor of Microbiology

4/29/91
Date

ACKNOWLEDGMENTS

I would like to thank Dr. Roger Bales and Dr. Charles Gerba for their guidance and support throughout the project. I also wish to acknowledge Dr. Jim Yeh who demonstrated his interest and involvement as an examining advisor.

I would like to thank my partner Kimberly Mcguire who helped me to develop my assay technique and shared those unbearable experiments with me. I appreciate the support of Moyasar Yahya and all the people of the fourth floor of Microbiology. I am also grateful for the advice of Shimin Li, Robert Matzner, Tim Corley, and the other friends in the Water Chemistry laboratory in Hydrology.

I especially thank my roommate Michael Allen and all of his family, without whom I could not have finished my entire program at the University.

Finally, I wish to acknowledge Kunio Arai, Dr. Sol Resnick, Dr. Simon Ince, and my mother who gave me this great opportunity to come to the United States for these invaluable experiences in my life.

TABLE OF CONTENTS

TABLE OF CONTENTS — CONTINUED

LIST OF FIGURES

LIST OF TABLES

ABSTRACT

Effects of pH and hydrophobicity on attachment-detachment of PRD-1 and MS-2 in three different soils, and Pseudomonas fluorescens P17 and Bacillus subtilis TF-32 in 0.5-mm silica beads, were investigated in laboratory-column experiments. Attachment and detachment of hydrophobic virus PRD-1 may be predominantly controlled by hydrophobic interactions in soil media, while those of less-hydrophobic virus MS-2 may be mainly controlled by pH. Bacteria tend to exhibit hydrophobic interactions, since their surface contains hydrophobic substances. Soil media can exhibit strong hydrophobic interactions as well as electrostatic interactions. Parameters for three different transport models were estimated. The equilibrium model fits to the breakthrough curves of MS-2 in Cape-Cod soil resulted in dispersion coefficients similar to those of the conservative tracer (NaCl). The first-order and two-site model parameters indicated non-equilibrium conditions in all cases. Calculations of the two-site model were less stable than the first-order model for these breakthrough curves.

1. INTRODUCTION

1.1 Viruses and Bacteria in Groundwater

Land application of wastewater, private waste-disposal systems, and municipal sanitary landfills are common practices in the United States. Human pathogens, notably human enteric viruses, are among the most persistent of pathogens found in wastewater effluents and sludges. They are neither completely removed nor inactivated by conventional wastewater treatment methods [*Duboise et al., 1979*]. Furthermore, bacterial pathogen transport through aquifer materials of up to 830 m and virus migration to 400 m have been reported [*McDowell-Boyer et al., 1986*].

It has been assumed, however, that groundwater is safe for consumption without treatment because the soil acts as a filter to remove pollutants. Hence, private wells generally do not receive treatment, nor do a large number of public water-supply systems. As a result, the use of contaminated, untreated, or inadequately treated groundwater has been a major cause of waterborne disease outbreaks in the country since 1920. Between 1920 and 1980, 1405 waterborne outbreaks were reported in the U.S., involving over 386,000 people and resulting in 1083 deaths. From 1981 to 1983, there were 112 reported waterborne outbreaks and 28,791 cases of illness associated with drinking water [*Yates et al., 1988*].

Besides disease transmission, another area of interest is the behavior of viruses and bacteria as colloid particles. Viruses and most bacteria are classified as colloids. Colloids are particles with diameters less than 10 μm [*Stumm and Morgan, 1981*]. These small particles have high surface areas per unit mass, thus posing a significant sorption potential [*McDowell-Boyer et al., 1986*], and possibly enhance the transport of other contaminants.

It was demonstrated that submicrometer colloidal material in soil is important in binding radionuclides. Also, it was found that colloidal organic carbon (COC) competed with lake sediment for binding plutonium, such that measured distribution coefficients decreased with increasing COC concentration [*McDowell-Boyer et al., 1986*].

Bales et al. [*1989*] reported the inability of a solute tracer to provide estimates for dispersion and effective porosity that are applicable to a colloid. They suggested that bacteriophage can be used better to estimate the maximum subsurface transport rate of colloidal contaminants through a porous formation.

In addition, bioremediation of contaminated groundwater requires reliable and relatively cheap decontamination procedures. The study of microbial transport might provide additional information to optimize this practice.

1.2 Transport Mechanism of Viruses and Bacteria in Groundwater

The physical processes that control the flux of solutes are advection and hydrodynamic dispersion [*Freeze and Cherry, 1979*]. Advection is the process by which solutes are transported by the bulk motion of flowing groundwater. Hydrodynamic dispersion occurs by mechanical mixing during fluid advection and molecular diffusion. In addition to these mechanisms, the transport of viruses and bacteria in groundwater are governed by retention and survival.

Retention takes place because of straining and attachment to immobile substrates. Straining is a major limitation for bacterial travel through soil. When bacteria are larger than the pore openings, this phenomenon will be dominant [*Gerba et al., 1984*]. Generally, straining becomes negligible when one considers the retention of viruses, which are colloidal-size particles [*Bitton, 1980*]. However, aggregated or particulate-associated viruses may be removed by straining through the small pores [*Yates et al., 1988*].

Several factors contribute to the adhesion of viruses and other colloids to soil particles, such as electrostatic attraction and repulsion, van der Waals forces, covalent-ionic interactions, hydrogen bonding, and hydrophobic effects.

Viruses have a net positive charge at pH values less than their isoelectric point. Since most solids and membrane filters have a net negative charge at pH values less than three, virus retention at low pH can usually be explained as due to an attraction between oppositely charged groups [*Farrah et al., 1981*].

From the study of the adsorption of fifteen viruses to nine soils, it was found that, in general, soils with a saturation pH of less than five were good virus adsorbers. In a study of coliform bacteria movement through sand, it was demonstrated that the retention efficiency increased as the pH of the water decreased [*Yates et al., 1988*].

The important concept to explain electrostatic repulsion in colloid interactions is the electric double layer. A charged or electrified interface reflects an unequal distribution of charges at the phase boundary; that is, it results from a localized disturbance of electroneutrality. The spatial distribution of free charges in its neighborhood determines the electric state of a surface. This distribution is idealized as an electrochemical double layer. In 1924, *Stern* conceptualized this distribution with two layers. The first consists of a layer of ions specifically adsorbed at the surface forming the compact *Stern layer*. The second consists of the diffuse layer or the *Gouy layer* [*Stumm and Morgan, 1981*].

When two particles approach each other, the Gouy layer on one particle is repelled electrostatically by the Gouy layer on the other. Hence, the attachment or detachment of a colloidal particle to an immobile substrate depends on the thickness of the Gouy layer. As ionic strength increases, the Gouy layer becomes compressed close to the particle or a surface [*Drever, 1988*].

Van der Waals forces, which are always attractive, can be explained by considering that neutral molecules or atoms constitute systems of oscillating charges producing synchronized dipoles that attract each other [*Stumm and Morgan, 1981*].

The DLVO theory named after Derjaguin and Landau and Verwey and Overbeek combined the van der Waals forces (attractive) with electrostatic double-layer forces (repulsive) to explain the stability of lyophobic colloids. In the interaction of two colloidal particles, van der Waals forces dominate at short and long distances. At intermediate distances, electrostatic forces overcome van der Waals forces [*van de Ven, 1989*].

Murray and Parks [*1980*] conducted the adsorption of poliovirus to a variety of metal oxides and found that free energies agreed with potentials evaluated from the DLVO theory.

Van Loosdrecht et al. [*1989*] described the adhesion of bacteria (Pseudomonas strain 62) to negatively charged polystyrene by the DLVO theory.

Murray and Parks [*1980*] indicated that covalent-ionic interactions appear to be important in the adsorption of small molecules on various materials. These authors also stated that virus (bacteria) coat proteins have ionizing amino acid residues expressed on the exterior that might be able to participate in bonding to metal sites of an adsorbent; however, there is no clear evidence of this bonding between viruses (bacteria) and soil [*Gerba, 1991, pers. comm.*].

The binding of some proteins and viruses to clays appears to result primarily from hydrogen bonding [*Stotzky, 1985*]. In water bridging, another possible form of hydrogen bonding, appropriate anionic groups on the biological entity are hydrogen-bonded to water molecules in the primary hydration shell of a charge-compensating cation on the clay [*Stotzky, 1985*]. Hydrogen bonding is in the same energy range (10 to 40 $kJmol^{-1}$) as van der Walls interactions [*Stumm and Morgan, 1981*] ; therefore, this bonding is expected to play a role in virus and bacteria attachment to surfaces, but the existence of this interaction has not been well identified.

Hydrophobic substances are defined as substances that are readily soluble in many nonpolar solvents, but only sparingly soluble in water [*Tanford, 1973*]. The viruses or bacteria with nonpolar regions may be bound to other nonpolar regions of the surface (e.g., other viruses, bacteria, soil surface). *Farrah et al.* [*1981*] studied the effects of chaotropic and antichaotropic agents on elution of poliovirus adsorbed on membrane filters. Chaotropic agents disorder the structure of water and antichaotropic agents have the opposite effect. It was found that, at pH 9.5, the ability to elute viruses adsorbed on membrane filters parallels the ability to accommodate hydrophobic functions. They concluded that hydrophobic interactions are the major factor in virus-filter surface interactions at this pH.

Hydrophobicity of bacteria has also been investigated. For example, *Rosenberg et al.* [*1980*] developed a rapid quantitative assay for the hydrophobic interaction of bacterial cells with liquid hydrocarbons. The method is based on the degree of adherence of cells to various liquid hydrocarbons following a brief period of mixing.

A major factor in determining the survival of enteric bacteria in soil is moisture content. The survival time is longer in moist soils. Other factors that may affect the survival of bacteria in soil are temperature, pH, sunlight, organic matter, and other microorganisms. Cold temperatures favor the survival of most microorganisms. The survival time will be shorter in acid soils (pH 3-5) than in alkaline soils [*Gerba et al., 1984*].

In addition, some bacteria are also more susceptible to inactivation at highly alkaline pH values. Several enteric bacteria have been found to be rapidly inactivated in alkaline water, with an upper pH tolerance limit of 9.5 reported [*Yates et al., 1988*].

Bacteria will survive for shorter times at the soil surface because of the presence of ultraviolet light. The existence of organic matter has been found to increase the survival. Other microorganisms decrease the survival time of the bacteria, maybe because of competition for nutrients in soil [*Gerba et al., 1984*].

Factors that may influence virus survival in soil are temperature, moisture content, sunlight, pH, cations, soil property, and biological factors. Temperature is probably the most detrimental factor affecting virus survival in soils: the survival is longer at lower temperature. Viruses persist longer in moist soil than dry soil. Sunlight inactivates viruses at the soil surface. The soil pH may affect virus survival indirectly by controlling adsorption onto soil particles, as viruses are known to survive better in the sorbed state. Certain cations (Ca, Mg) increase the adsorption of viruses onto soil, which results in longer survival. Clay minerals and humic substances in soil increase water retention by soil and have an impact on viruses subjected to desiccation. It is likely that biological factors may influence virus inactivation in soils, but no clear trend has been observed. Regarding the contribution of soil microflora to virus decline, some investigators did not observe any effect while others reported a greater virus decline in nonsterile soils [*Gerba et al., 1984*].

1.3 Transport Model

Equations for one-dimensional solute transport in porous media were applied to fit experimental breakthrough curves of viruses and bacteria. The units of concentration for viruses and bacteria are the plaque-forming unit (pfu) and colony-forming unit (cfu), respectively (see Section 2.2). Three different one-dimensional, advection-dispersion models (equilibrium, first-order kinetic, and two-site kinetic models) were used in order to estimate the magnitude of attachment and time scales for reaching equilibrium. As a general governing equation, the two-site kinetic, non-equilibrium adsorption model was applied. This model is based on the assumption that the sorption sites are divided into two fractions; adsorption on one fraction (type-1 sites) is assumed to be fast, while adsorption on the other fraction (type-2 sites) is thought to be kinetically limited [*van Genuchten, 1981*]. Governing equations have been given by various investigators [*Cameron, 1977, Rao et al., 1979*]. General equations for a unit volume are:

$$\theta \frac{\partial C}{\partial t} + \phi \frac{\partial S_1}{\partial t} + \phi \frac{\partial S_2}{\partial t} = \theta D \frac{\partial^2 C}{\partial z^2} - u \theta \frac{\partial C}{\partial z} \tag{1}$$

$$S_1 = K_{p1} C \tag{2}$$

$$\phi \frac{\partial S_2}{\partial t} = \theta k_1 C - \phi k_2 S_2 \tag{3}$$

where C is the virus or bacteria concentration (pfu cm^{-3} or cfu cm^{-3}) in the aqueous phase; t is time (s); S_1 and S_2 are the bound concentrations (pfu g^{-1} or cfu g^{-1}) for type-1 and type-2 sites, respectively; z is distance (cm); θ is porosity; ϕ is the dry bulk density (g cm^{-3}) of the solid material; D is the longitudinal dispersion coefficient (cm^2 s^{-1}); u is the average interstitial velocity (cm s^{-1}); K_{p1} is the equilibrium partition coefficient (cm^3 g^{-1}) for the type-1 sites; k_1 is a pseudo-first-order rate coefficient (s^{-1}) for attachment, which depends on the virus's or bacteria's diffusion coefficient and the sticking efficiency (i.e., net energy of interaction between virus and collector or bacteria and collector); and k_2 is a pseudo-first-order detachment rate coefficient (s^{-1}), which also depends on the energy of the interaction between virus and collector-surface or bacteria and collector-surface. These rate coefficients do not depend on the surface-site concentration, as only a small fraction of the surface was covered by attached virus or bacteria.

Total attachment S at equilibrium is expressed as

$$S = S_1 + S_2 = K_{p1}C + K_{p2}C = f\,K_p\,C + (1-f)K_p\,C = K_p C \tag{4}$$

where S_1 is the concentration of particles attached to the type-1 sites; S_2 is the amount of particles attached to the type-2 sites; K_{p2} is the equilibrium partition coefficient (cm^3 g^{-1}) for the type-2 sites; K_p is the equilibrium partition coefficient (cm^3 g^{-1}) for the total surface sites (type-1 and type-2 sites); and f is the fraction of type-1 sites on the total attachment sites. Since the time scales for attachment for type-1 sites and type-2 sites are different, the attachment process proceeds as follows. First, immediately after the contact of solution (concentration C) to the collector surface, type-1 sites reach equilibrium but type-2 sites have almost no attachment (S_2 = 0). Thus, $S = S_1 = K_{p1}C = f\,K_p\,C$. As time passes, type-2 sites become gradually occupied (S_2 increases), and $S > S_1$. After a sufficient time has passed (over the time scale of k_i), type-2 sites reach equilibrium and $S_2 = K_{p1}C = (1-f)K_p\,C$. Then, total attachment S becomes $S_1 + S_2 = K_p\,C$.

Equation (1) expresses the total change in concentration with time due to advection, dispersion, attachment, and detachment. This equation assumes that flow occurs under steady-state conditions, the medium is homogeneous and saturated with a constant soil-water content, immobile flow regions do not exist, and relationships between sorbed and aqueous solute concentrations do exist. Equation (2) expresses the linear attachment equilibrium for the fast (type-1, equilibrium) attachment sites. Type-1 sites could correspond to colloids held near the surface in a secondary minimum of the potential energy of interaction, with little or no energy barrier for detachment. Equation (3) shows that the change in virus or bacteria concentration bound to type-2 sites with time is the difference between the attachment and detachment rates.

In order to transform equations (1), (2), and (3) to the dimensionless equations for which the solutions are known, the following variables are substituted:

$$T = \frac{vt}{L} \tag{5}$$

$$Z = \frac{x}{L} \tag{6}$$

$$C_1 = \frac{C}{C_0} \tag{7}$$

$$C_2 = \frac{S_2}{(1-f)K_p C_0} \tag{8}$$

The substitution results in the following dimensionless equations:

$$\beta R \frac{\partial C_1}{\partial T} + (1-\beta) R \frac{\partial C_2}{\partial T} = \frac{1}{P} \frac{\partial^2 C_1}{\partial Z^2} - \frac{\partial C_1}{\partial Z} \tag{9}$$

$$(1-\beta) R \frac{\partial C_2}{\partial T} = \omega (C_1 - C_2) \tag{10}$$

where the model parameters are as follows:

The retardation factor:

$$R = 1 + \frac{\phi K_p}{\theta} = 1 + \frac{\phi f K_p + \phi(1-f)K_p}{\theta} = \frac{\theta + \phi K_p}{\theta} \tag{11}$$

The Peclet number:

$$P = \frac{L\,u}{D} = \frac{L^2/D}{L/u} = \frac{\textit{Time scale for dispersion}}{\textit{Residence time}} \tag{12}$$

The Damkohler number is a dimensionless mass-transfer coefficient:

$$\omega = \frac{L/u}{1/k_1} = \frac{k_1 L}{u} = \frac{\textit{Physical time scale}}{\textit{Chemical time scale}} \tag{13}$$

where L is the length of the column. When $\omega > 100$, local equilibrium applies, since the attachment and detachment become relatively fast (chemical time scale is much smaller relative to physical time scale). As ω drops below about 0.1–0.5 with $K_p = 0$, attachment is too slow to observe and the solute appears to be conservative. A fourth parameter related to the scaling factor of equilibrium to total attachment (f) and to the ratio of the attachment and detachment rate coefficient is given by

$$\beta = \frac{\theta + f\,\phi K_p}{\theta + \phi K_p} = 1 - \frac{k_1}{k_2 R} = 1 - \frac{\omega u}{k_2 L R} \tag{14}$$

For the estimation of these parameters, the curve-fitting routine of *van Genuchten* [*1981*] was used. The routine applies the initial conditions:

$$C_1(Z,0) = C_2(Z,0) = 0 \tag{15}$$

$$S_1(Z,0) = S_2(Z,0) = 0 \tag{16}$$

and the boundary conditions:

$$\left\{ -\frac{1}{P}\frac{\partial C_1}{\partial Z} + C_1 \right\}_{(0,T)} = 1 \tag{17}$$

$$\frac{\partial C_1}{\partial Z}_{(\infty,T)} = 0 \tag{18}$$

Equation (18) is strictly valid only for an infinite column, but the solutions should provide close approximations for a finite system, especially for not-too-short laboratory columns, because of the relatively small influence of the imposed mathematical boundary conditions.

The equilibrium model is obtained from no type-2 sites ($f = 0$ and $\omega \geq 100$), which is a two-parameter model of R and P since $\beta = R^{-1}$. The first-order model is derived from no type-1 sites ($f = 0$), which is a three-parameter model of R, P and ω since $\beta = R^{-1}$.

Physical and chemical factors influencing the magnitude of k_1 can be described separately following the single-collector model used to describe particle removal in water filtration [*O'Melia, 1980*]. The single-collector removal efficiency is:

$$\eta = \frac{\textit{Rate at which particles strike a collector}}{\textit{Rate at which particles approach a collector}} \tag{19}$$

and the sticking efficiency is:

$$\alpha = \frac{\textit{Rate at which particles stick to a collector}}{\textit{Rate at which particles strike a collector}} \tag{20}$$

Particles are removed from a unit volume of fluid at the rate k_1C , and thus are removed by (stick to) a single collector at the rate $k_1C\left[\frac{\pi\theta d^3}{6(1-\theta)}\right]$, where the quantity in parentheses is the volume of fluid associated with a single, spherical collector of diameter d. The rate at which particles approach this volume is $\theta u\ C\left[\frac{\pi d^2}{4}\right]$, giving [*Bales et al., 1990*]

$$\eta\alpha = \frac{2}{3}\frac{k_1 d}{u}\frac{1}{1-\theta} \tag{21}$$

where d is the diameter of the collector.

Some available solutions for η are the following [*O'Melia, 1980*]:

$$\eta_d = 4Pe^{-2/3} = 0.9\left[\frac{\bar{k}\,T}{\mu d_p\, d\, u}\right]^{2/3} \tag{22}$$

$$\eta_i = \frac{3}{2}\left[\frac{d_p}{d}\right]^2 \tag{23}$$

$$\eta_g = \frac{(\rho_p - \rho)g}{18\mu u}d_p{}^2 \tag{24}$$

where, η_d, η_i and η_g are the single-collector removal efficiencies for diffusion, interception, and gravity, respectively, considered separately as transport processes; Pe is a Peclet number; $\bar{k}$ is the Boltzmann constant; T is temperature; μ is fluid viscosity; d_p is the virus (bacteria) diameter; ρ_p is the density of fluid; ρ is the density of virus (bacteria); and g is the gravitational constant. Thus, total single-collector removal efficiency is $\eta = \eta_d + \eta_i + \eta_g$.

For the virus colloids, Brownian diffusion is the primary mechanism for particle transport to the collector. In the steady-state case, neglecting dispersion, detachment, and weak (equilibrium) binding sites, equations (1), (3), and (21) reduce to

$$\frac{dC}{dz} = -\frac{k_1C}{u} = -\frac{3}{2}\frac{1-\theta}{d}\eta\alpha C \tag{25}$$

Integrating equation (25), given $C=C_0$ at $z=0$, yields

$$\log\frac{C}{C_0} = -\frac{1}{2.303}\frac{3}{2}\frac{1-\theta}{d}\eta\alpha z \tag{26}$$

At the column outlet ($z = L$), rearranging equation (26) gives

$$\alpha = -\,2.303\,\frac{2}{3}\,\frac{d}{1-\theta}\,\frac{1}{\eta L}\log\frac{C}{C_0} \tag{27}$$

1.4 Research Objectives

Generally, virus and bacteria transport experiments have used specific soils or groundwater media, but few have used well-characterized surfaces. Hence, the available data base does not provide general information regarding attachment of viruses and bacteria under specific chemical conditions. In addition, the reversibility of virus adsorption has been studied for only a few cases. This results in the difficulty of validating existing mathematical models for virus, bacteria, and other colloid transport in groundwater [*Bales et al., 1990*].

The main objective of this study was to examine the role of pH and hydrophobicity on the attachment and detachment of viruses to soil and bacteria to silica-bead surfaces. A second objective was to contribute to model testing by developing quantitative data on the chemical conditions — pH and hydrophobicity — affecting virus and bacteria transport in groundwater.

2. *MATERIALS AND METHODS*

2.1 Column-Experiment Procedures

Continuous-flow column experiments were conducted to obtain breakthrough curves of bacteriophage PRD-1 and/or MS-2 through soil and bacteria through silica beads. Attachment and detachment were examined at several pH values. All experiments were done at 7°C in order to minimize viral inactivation and bacterial growth.

2.1.1 Experiment Conditions

A total of 17 column experiments were conducted (Table 1). Four kinds of media were used: 1) Borden, Ontario, Canada soil; 2) Cambridge, Ontario, Canada soil; 3) Cape-Cod, Massachusetts, U.S.A. soil; and 4) silica beads (1.0 mm and 0.5 mm in diameter). Applied viruses and bacteria were bacteriophage PRD-1 for Borden soil and Cambridge soil, MS-2 and PRD-1 for Cape Cod soil, and Pseudomonas fluorescens P17 or Bacillus subtilis TF-32 for silica beads. Calcium-phosphate buffer adjusted to pH 5.5 to 7.0 were used for attachment and 7.0 to 8.2 for detachment.

2.1.2 Apparatus

The column-experiment apparatus is illustrated in Figure 1. Stock solution of virus or bacteria and buffer solution were sent to the column through independent channels of a peristaltic pump. For the first six experiments (1, 2, 3, 10, 11, and 12 in Table 1), the type A tubing system in Figure 1 was used, in which stock solution was changed to virus (bacteria) free buffer by switching the ends of tubing at the column top. Later, the tubing system was changed to type B, in which solution flow was changed by clamping the tube. The latter has less chance to introduce air into the column.

Glass chromatography columns (Spectrum Medical Industries, Inc., Los Angeles, CA) were used. The dimensions of columns for bacteria experiments were 20.0 cm in length and 1.4 cm in inside-diameter. For soil experiments, 14.8 cm × 2.7 cm or 10.6 cm × 2.7 cm columns

Table 1. Experiment conditions

No.	Date	Media	Virus or Bacteria	pH of phosphate[a] buffer: 1st day attachment detachment	pH of phosphate[a] buffer: 2nd day detachment	Temp. (°C)
1	7/11/90	Borden		6.5	7.0(B.E.)[b]	
2	7/23/90	Ontario	PRD-1	7.0	7.0(B.E.)[b]	7.0
3	8/29/90	Soil		7.6	7.6(B.E.)[b]	
4	10/3/90	Cambridge Ontario Soil	PRD-1	7.0	7.0(B.E.)[b]	7.0
5	9/26/90			5.5[c]	-----	
6	11/14/90	Cape Cod	MS-2	5.7	8.2	7.0
7	11/28/90	Soil	&	5.7	8.2	
8	1/16/91		PRD-1	7.0	8.2	
9	1/29/91			5.7, 7.0, 8.2(att)[e] 8.2(det)[f]	-----	
10	8/3/90	1.0-mm silica beads	Pseudomonas fluorescens P17	7.0[d]	-----	7.0
11	8/14/90	0.5-mm	Pseudomonas	7.0[d]	7.0(B.E.)[b,d]	
12	9/10/90	silica	fluorescens	7.0	8.0	7.0
13	9/18/90	beads	P17	7.0	8.0	
14	10/10/90			5.5	8.2	
15	10/18/90	0.5-mm	Bacillus	7.0	8.0	
16	10/24/90	silica	subtilis	5.5	7.0	7.0
17	10/31/90	beads	TS-32	7.0	8.0	

[a] Ion concentrations: $Ca^{2+} = 10^{-4}$ M, $PO_4^{3-} = 2 \times 10^{-2}$ M,
$Na^{+} = 2 \times 10^{-2}$ M (pH ≤ 5.7), 3×10^{-2} M (pH ≥ 6.5)

[b] Beef extract was added.

[c] Ca^{2+} ($10^{-4.76}$) was added.

[d] NO Ca^{2+} added ($NaPO_4$ buffer).

[e] Attachment

[f] Detachment

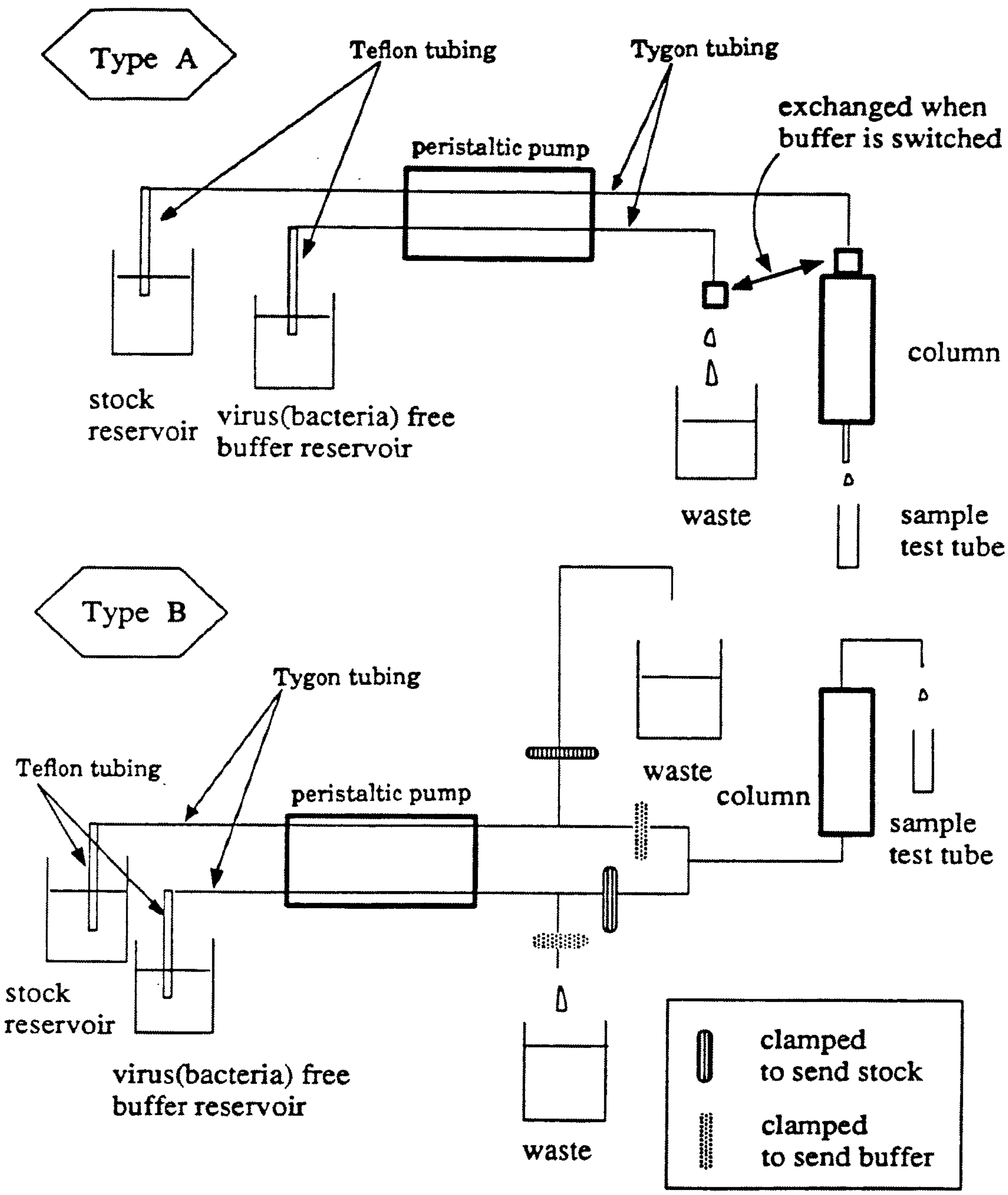

Figure 1 Column experiment apparatus

were used. Columns were packed by the tap and fill method of *Snyder and Kirkland* [1979] and the weight of media was recorded to estimate dry bulk density. The soils were collected from different depths at each site, then mixed well and oven-dried at about 105 °C overnight in the laboratory. The dried soils were kept in sealed plastic bags for later use. Columns were packed with new beads or soil for each experiment. Two different peristaltic pumps were used — an Ismatec peristaltic pump (Cole Parmer Instrument Co., Chicago, IL) and a Multistaltic pump (Buchler Instruments, Lenexa, KA). Teflon tubing was used from the input reservoir up to the peristaltic pump and Tygon tubing (Cole Parmer Instrument Co., 0.76 mm inner diameter) from the peristaltic pump to the column. Polypropylene fittings (Cole Parmer Instrument Co., 1.6 mm × 1.6 mm × 1.6 mm inner diameters) were used for the connection of tubings in system B.

2.1.3 Experimental Procedure

In order to standardize the time for the breakthrough curves, *pore volume* (PV) was used throughout this column study. The pore volume was calculated in terms of residence time of water in a column. The PV at a time t is

$$PV = \frac{t}{\bar{t}} = \frac{t}{L/u}$$

where $\bar{t}$ is the hydraulic residence time, L is the column length, and u is the average interstitial velocity. This leads to

$$PV = \frac{t}{L/u} = \frac{t}{\dfrac{L}{Q/A\theta}} = \frac{tQ}{LA\theta} = \frac{\textit{Volume of water that passed through a column}}{\textit{Volume of pore-space in a column}}$$

where A is the inner section of a column and θ is porosity. Hence, "one pore volume" means that a water molecule passed from one end of the column to the other and also the volume of water equivalent to the pore space has passed the column (water in the column was replaced once).

The column was flooded from the bottom at a low flow rate to minimize air entrapment. The silica-bead column for bacteria experiments was wrapped with aluminum foil and sterilized by steaming for about half an hour before flooding. Soil media have a higher possibility of leaving entrapped air in the flooding process ; therefore, for the Cape-Cod soil column, CO_2 gas was sent from the bottom of the column to replace the soil gases because CO_2 dissolves into solution in the flooding process, resulting in complete saturation. In system A (Figure 1), the pump was attached to the top of the column. Buffer at the same pH as the stock solution was run through the column for about five to eight pore volumes overnight prior to the experiment. It was found that effluent pH became the same as that of the buffer in the input reservoir after this process.

During an experiment, solution was sent at about 1 to 1.5 pore volumes per hour. Samples were collected for four min for the soil column and 5 min for the silica-bead column at least every hour. Sample-collection time was determined so that the sample amount was enough to perform two assays, i.e., an extra amount of sample was collected for re-assay. The number of pore volumes at a plotting point on a breakthrough curve represents the one at which the sampling started. Flow rate was monitored by measuring at the column outlet throughout the experiment. Due to an unstable pump, the flow rate during each experiment fluctuated about the nominal set-point value. The fluctuations in flow rates for experiments 10 through 13 were less than 24 percent, for experiments 5, 7, and 9 less than 12 percent, and for the other experiments less than 6 percent. Also, switching from one channel to the other caused a 32 percent increase in experiment 17, a 5–8 percent increase in experiments 6, 13, 15, and 16, and an 8 percent decrease in experiment 14, but only a slight change was observed in all the other experiments. Monitored flow rates were used to calculate the pore volumes of solution that had passed through the column. To verify the buffering system of soil, effluent pH from the soil column was checked occasionally.

Effective column pore volumes were calculated from conservative-tracer breakthrough curves by fitting equilibrium model parameters using a non-linear-least-squares algorithm [*van Genuchten, 1981*]. These pore volumes are theoretically the same as the ones derived from the time to $C / C_0 = 0.5$. Pore volume of a column was the average of two breakthrough-curve fits using 0.1-M and 0.2-M NaCl. A column was flooded with 0.1-M NaCl solution until the conductivity reading became stable. Then, a pulse flow of 0.2-M NaCl was sent for about 2 pore volumes, and then switched back to 0.1-M NaCl. The conductivity was monitored with a Wescan model 213a conductivity detector (Wescan Instruments, Inc., Santa Clara, CA) connected to a strip-chart recorder. A tracer experiment was done prior to each virus experiment with soil. The bacteria experiment with the silica-bead column was performed after the tracer experiment, since the steam-sterilizing process could cause unsaturation and chemical change on the surface of silica beads.

2.1.4 Buffer

Calcium-phosphate buffer was used for both stock solution and detachment buffer. A 0.02-M phosphate buffer solution (2.67 g of $NaH_2PO_4 \cdot H_2O$ and 0.09 g of Na_2HPO_4 in 1 L of deionized water) was used for pH 7.0. A 0.02-M phosphate buffer solution (1.30 g of $NaH_2PO_4 \cdot H_2O$ and 1.51 g of Na_2HPO_4 in 1 L of deionized water) was used for pH 5.5. One mL of a 10^{-3}-M $CaCl_2$ solution was added to 1 L of phosphate buffer to make 10^{-6}-M calcium phosphate buffer. Buffers of other pH were obtained by adjusting with 1-N HCl or 1-N NaOH.

Beef extract (2.5 percent in weight) was used for elution in five experiments. In order to make 1 L of beef extract solution, 2.5 g of beef extract (Becton Dickinson and Co., Cockeysville, MD) were added to 1 L of phosphate buffer and stirred while heated, and then filter sterilized with a 0.2-μm pore-size filter (Costar Co., Cambridge, MA). After it was cooled down to 7 °C, the pH was adjusted to the desired value with 1-N HCl or 1-N NaOH. The pH meter was calibrated with 7 °C standard buffers.

2.1.5 Viruses and Bacteria

The viruses and bacteria sent to column are listed in Table 1. PRD-1 was used for Borden and Cambridge soils, and MS-2 and PRD-1 were mixed together in the same buffer and sent to Cape-Cod soil columns. <u>Pseudomonas</u> <u>fluorescens</u> P17 and <u>Bacillus</u> <u>subtilis</u> TF-32 were used for silica-bead columns. Preparation methods will be described in Section 2.2.2.

Bacteriophage PRD-1 is an icosahedral (twenty triangular faces) lipid phage with an average diameter of 62 nm [*Olsen et al., 1974*]. Its isoelectric point in calcium-phosphate buffer (10^{-4}-M calcium) appears to be between pH 3 and 4 [*Hinkle, 1990*]. A virion is composed of a core of nucleic acid (DNA or RNA) surrounded by a icosahedral capsid (protein coat). They can be surrounded by an envelope that contains lipoproteins or lipids. Functional groups on the surface are $-COOH$ or $-NH_2$. Surface hydrophobicity varies, depending on the fraction and presence of lipids. Bacteriophage are known to infect a wide range of bacteria. The advantages of using bacteriophage are the following: 1) the phage is nonpathogenic to man and domestic animals, 2) it is specific for its host bacteria, 3) assay is simple and rapid, and 4) it has good survival characteristics [*Keswick et al., 1982*].

Bacteriophage MS-2 is an icosahedral phage with an average diameter of 26 nm. The isoelectric point is near pH 4 [*Zerda, 1982*]. Functional groups on the surface are $-COOH$, $-OH$, and $-NH_2$. MS-2 is less hydrophobic than PRD-1, since it does not have lipids.

Bacillus subtilis TF-32 are gram-positive, rod-shaped bacteria. According to *Buchanan and Gibbons* [*1974*], they are motile, they produce heat-resistant endospores (0.8 by 1.5-1.8 μm), and their metabolism is respiratory.

Gram-positive bacteria have a thick cell wall of polymeric composition , which has various functional groups such as $-COOH$, $-CH_3$ (aliphatic), $-NH_2$. These functional groups are significant in the adsorption of bacteria to surfaces.

Pseudomonas fluorescens P17 are gram-negative bacteria. They are also rods, 0.7-0.8 by 2.3-2.8 μm during exponential growth and may be shorter and thinner in old cultures; motile with polar multitrichous flagellation, and occasionally non-motile; and obligately aerobic. Optimal temperature for growth ranges from 25-30 °C, with growth at 4 °C or below and no growth at 41 °C [*Buchanan and Gibbons, 1974*].

Gram-negative bacteria have more complex walls than gram-positive bacteria. The walls have an outer membrane over the gram-positive bacterial cell. An outer membrane is also composed of various functional groups.

The actual bacterial-cell surface has, particularly in gram-positive bacteria, cell-wall-associated components that are not covalently bonded to other cell-wall components [*Wicken, 1985*]. Moreover, the existence of surface appendages, such as flagella, fimbriae, and pili, increases the difficulty of characterizing bacterial surfaces.

2.1.6 Silica Beads

Spheriglass silica beads nominally 0.5 mm in diameter (Potters Industries Inc., Hasbrouck Heights, NJ, stock no. A-100, solid glass spheres with 0.600 mm–0.425 mm diameter range) were used for bacteria column experiments. Also, nominal 1.0 mm diameter silica beads (Potters Potters Industries Inc., stock no. A-050 with 0.850 mm–1.180 mm diameter range) were used in experiment 10.

In order to avoid soluble oxides of calcium and sodium that affect surface characteristics, the beads were washed to remove these compounds on their surfaces. The beads were washed by the following steps: 1) approximately 200 mL of beads were wetted with deionized water, rinsed in 1000 mL of 1-M NH_4OH, and rinsed to below pH 11 with deionized water; 2) beads were refluxed in 1000 mL of 2-M HCl for 4 hr, HCl was drained, and the beads were rinsed in deionized water; 3) beads were refluxed in fresh 2-M HCl for 2 more hr and drained; 4) process of 3) was repeated; 5) the beads were rinsed in deionized water until the rinse-water pH rose above pH 4; 6) the beads were refluxed in deionized water for one hour in order to remove excess hydrogen ions from the surfaces; and 7) beads were rinsed in deionized water and then oven-dried overnight at approximately 105°C.

2.1.7 Soil

Soil media were collected at three locations. Properties of three aquifers and background groundwater characteristics are presented in Table 2 and Table 3, respectively.

The Borden site is located within the confines of the Canadian Forces Base, Borden, about 80 km northwest of Toronto, Ontario, Canada. A sanitary landfill posed groundwater contamination and the site has been under intense investigation. The unconfined Borden

Table 2. Properties of 3 aquifers

Properties	Borden Ontario[a]	Cambridge Ontario[c]	Cape Cod MA
Groundwater Velocity ($m\,dy^{-1}$)	0.05-0.10 (0.09)	0.05-0.11	0.24-0.69[d,h]
Hydraulic Conductivity ($m\,dy^{-1}$)	0.043-17.3 (6.22)	4.3,25.9[g]	60-90[d]
Dry Bulk Density ($g\,cm^{-3}$)	1.81[b]	NR	1.72[e]
Solid Densityg cm^{-3})	2.71[b]	NR	NR
Porosity	0.33-0.38(0.33)	NR	0.35[e]
Organic Carbon Content (percent)	0.01-0.09(0.028)	0.05	<0.01[f]
Specific Surface Area (m^2g^{-1})	0.6-1.6(0.8)	NR	1.09-1.13[f,i]
Cation Exchange capacity ($meq\,(100g)^{-1}$)	0.52(0.52)	5.0	NR
Clay Size Fraction (percent)	0-15(0)	0	<1[f]
Grain Size (wt.%)	median = 0.07-0.69 mm[b]		median = 0.59 mm[e]
sand (2-0.053mm)		95	
silt (0.053-0.002mm)		5	
Mineralogy(percent)[b]		NR	
Quartz	58		50[f,i]
Feldspars	19		40[f,i]
Carbonates	14		
Amphiboles	7		
Chlorite	2		
Others			10[f,i]

[a] Lemon et al. [1989], ( ) : Estimated mean
[b] Mackay et al. [1986]
[c] Robertson et al. [1990]
[d] LeBlanc [1984]
[e] Harvey et al. [1991]
[f] Barger [1990]
[g] Two different areas
[h] Through sand and gravel
[i] Measurement made with particles from the 0.125-0.250 mm diameter size fraction of Cape-Cod soil.
[j] Measurement made with particles from the 0.250-1.000 mm diameter size fraction of Cape-Cod soil.

Table 3. Background groundwater characteristics (mgL^{-1})

Constituents and Properties	Borden Ontario	Cambridge Ontario	Cape Cod MA
Ca	50-110	88	1.8
Mg	2.4-6.1	16	1.7
Na	0.9-2.0	4	5.5
K	0.1-1.2	2	0.6
Cl	1-3	17	8.1
SO_4	10-30	59	5.2
PO_4 (as P)	NR	<0.01	<0.01
NO_3 (as N)	<0.6	27	0.42
NO_2 (as N)	NR	NR	<0.1
NH_4 (as N)	NR	<0.1	0.01
Organic Nitrogen (as N)	NR	NR	<0.1
Bicarbonate (as HCO_3)	NR	NR	7
F	NR	NR	<0.1
B (μg/L)	NR	NR	7
SiO_2	NR	NR	9.1
Alk (as $CaCO_3$)	100-250	204	6
TDS	380-500	NR	39
DOC (as C)	<0.7	3	2.1
DO	0-8.5	NR	NR
Temp. (°C)	6-15	NR	11.0
pH	7.3-7.9	7.3	5.8

Sources
Borden : Lemon et al. [1989]
Cambridge: Robertson et al. [1990]
Cape Cod : LeBlanc [1984]

aquifer is comprised of glacio-fluvial sand, which is common in the glaciated region of North America. The aquifer is locally very heterogeneous due to complex distributions of beds and lenses of fine-, medium-, and coarse-grained sand. Thickness of the aquifer varies from 15 to 30 m, underlain by a clayey silt bed [*MacFarlane et al., 1983*].

The hydraulic conductivity (K) was studied by several techniques. The value varies over a range of more than 2 orders of magnitude (Table 2) [*Lemon et al., 1989*].

The results of chemical analysis on uncontaminated background groundwater shows that organic-carbon content, clay-size fraction, specific-surface area, the cation-exchange capacity, and dissolved-organic carbon (DOC) are all low. Several measurements showed that dissolved oxygen (DO) was quite variable over the field of study. The total-dissolved solids (TDS) is relatively low, although the water would be considered moderately hard based on the calcium and magnesium contents [*Mackay et al., 1986*].

The Cambridge site is located near Cambridge, Ontario, Canada, at an agricultural research station. The septic system on this site has been producing large-scale contaminant plumes in the aquifer. The aquifer consists of glacio-lacustrine and outwash sand to a depth of 4-8 m and is overlain by a silt till of low permeability [*Robertson et al., 1990*]. Near the ground surface, the soil horizons exhibit slight variations in permeability, but otherwise the aquifer is relatively homogeneous [*Shutter et al., 1990*].

In the area north of a piezometer bundle, about 30 m north of the septic system, the aquifer is comprised of clean medium-to-coarse sand having an average K of 3×10^{-2} cm s^{-1} (2.6 m dy^{-1}). In the south of the bundle including the septic system area the most saturated portion of the aquifer material is less permeable, fine to medium-grained sand, and has an average K of 5×10^{-3} (0.43 m dy^{-1}). The lower-K zone is, however, underlain at all locations along the bottom of the aquifer by a high K layer of coarse sand approximately 0.3 m thick [*Robertson et al., 1990*]. The aquifer materials are larger than clay size and organic-carbon content is low (Table 2).

Acidity produced by NH_4^+ nitrification depressed pH levels in the plumes, but the depression was minor compared to background pH (7.0 versus 7.3) due to carbonate buffering [*Robertson et al., 1990*].

At the Cape Cod, Massachusetts site, discharge from a sewage treatment facility at Otis Air Force Base resulted in a large plume of contaminated groundwater [*LeBlanc, 1984*]. The top 30 to 50 m of sediment are a glacial outwash composed of stratified, well-sorted, medium-to-coarse sand with some gravel. In the northern part of the study area, the sand and gravel overlie fine sand and silt. To the south, the outwash overlies fine sand, silt, and dense sandy till. The till contains lenses of silt and clay, and sand and gravel. These unconsolidated sediments overlie a crystalline (granodiorite) bedrock surface, which generally slopes from west to east through the study area [*Garabedian et al., 1989*].

The hydraulic conductivity was estimated by comparison with measured values of the K of similar sediments at other locations on Cape Cod and from general relationships between grain-size distribution of sediments and K. The estimated K of the sand and gravel outwash is 60 to 90 m dy^{-1}. The K of the fine to very fine sand and the sandy till is lower than the K of the sand and gravel. The crystalline bedrock with very low K is assumed to be the bottom of the groundwater flow system [*LeBlanc, 1984*]. *Garabedian [1987]* reported that the results of an aquifer test conducted in the study area in 1984 indicated the horizontal K of the sand and gravel was about 120 m dy^{-1} [*Garabedian, 1989*].

The TDS is low because the aquifer is sand and gravel, composed predominantly of quartz and some feldspar derived from crystalline bedrock. The alkalinity is also low because of the absence of carbonate minerals in the aquifer. The pH of uncontaminated groundwater in the study area typically is less than 6.0 [*LeBlanc, 1984*].

Compared to the other two aquifers, groundwater is significantly lower in hardness, and also SO_4^{2-} concentration is much less than the others.

2.2 Assay Procedures

Viruses were enumerated by counting infected zones (plaques) of host cells that were confluently grown in a medium solidified by overlay agar on a Trypticase Soy Agar (TSA) layer. The assay method is essentially the method of *Adams [1959]*.

Bacteria were detected by colonies grown on R2A plates. This spread-plate method was adopted from that outlined in Standard Methods for the Examination of Water and Wastewater [*American Public Health Association, 1985*].

2.2.1 Media

Tris-buffered saline solution (TRIS) was used for dilution of water samples. First, 63.2 g of Trisma Hydrochloride (Sigma Chemical Co., St.Louis, MO), 163.6 g NaCl, 7.46 g KCl, and 1.13 g Na_2HPO_4 were dissolved in 1600 mL of distilled water. The pH of the solution was adjusted to between pH 7.2 and 7.4 with 12-N HCl. Then, 160 mL of this solution were diluted by adding 1840 mL of distilled water. Of this diluted solution, 2.7 mL were dispensed into glass test tubes and capped. Finally, these tubes were autoclaved for 15 min at 121°C and 15 psi, then stored at 7°C until needed.

Three kinds of media were prepared for virus assay. These were Trypticase soy broth (TSB) for host bacteria growth, Trypticase soy agar (TSA) mixed with Bactoagar for overlay medium, and TSA for bottom agar plates.

Trypticase soy broth (TSB) was prepared by dissolving 30 g of Trypric soy broth powder (Difco, Detroit, MI) in 1 L of distilled water. The solution was heated to boiling while mixing with a magnetic stir bar. One hundred mL of TSB were dispensed into plastic bottles and autoclaved for 15 min at 121°C and 15 psi.

Overlay medium consisted of 30 g of TSB powder and 10 g of Bactoagar (Difco) and 1.0 L of distilled water. The solution was heated to boiling while mixing with a magnetic stir bar. Three mL of this medium were dispensed into glass test tubes, capped, and autoclaved for 15 min at 121°C and 15 psi, then stored at 7°C.

TSA for bottom agar plates was prepared by dissolving 40 g of Tryptic soy agar (Difco, Detroit, MI) in 1 L of distilled water. This solution was then autoclaved for 15 min at 121°C and 15 psi, cooled to 50°C in a water bath, and dispensed in 10-mL aliquots into sterile 100-mm by 15-mm plastic petri dishes (Becton Dickinson Co., Lincoln Park, NJ). After the agar solidified, the dishes (TSA plates) were inverted and stored at 7°C.

For bacteria assay, R2A Agar was prepared. The agar was made by dissolving 18.2 g of Bacto R2A agar dehydrated (Difco) in 1 L of distilled water. The solution was heated to boiling while mixing with a magnetic stir bar. Ten mL of agar were dispensed into plastic petri dishes. After the agar solidified, the dishes (R2A plates) were inverted and stored at 7°C.

2.2.2 Virus Assays

MS-2 and PRD-1 viruses were used. They were prepared by placement of one mL of overnight culture of MS-2 host bacteria, Escherichia coli E (E. coli) in TSB, in 100 mL of fresh TSB and continuous shaking for 3 – 6 hr at 37°C. Stock MS-2 (ATCC, 15587B) was diluted in TRIS to an approximate concentration of 10^5 pfu mL^{-1}. One mL of E. coli and 0.1 mL of MS-2 dilution were added to molten overlay agar, vortexed, and poured onto TSA plates. After plates were incubated overnight at 37°C, 5 mL of TRIS were dispensed onto plates and left at room temperature for a maximum of 2 hr to allow the phage to diffuse into the overlying TRIS. The liquid fraction was recovered from the plates and centrifuged at 10,000 rpm and 10°C for 10 min in a Beckman J2-21 centrifuge (Beckman Instruments, Irvine, CA). The resulting supernatent was centrifuged again at 23,000 rpm and 10°C for 3 hr. The stock solution was made by resuspending the pellet in sterile, filtered well water and stored at 7°C.

PRD-1 was prepared in the same procedure as MS-2 using Salmonella typhimurium LT2 as a host bacteria in place of E. coli.

Column-outlet samples were assayed on the same day that samples were collected. The assay procedure was as follows. One day before an assay, the host bacteria culture (see Section 2.2.3) was prepared by adding 0.3 mL of culture into 100 mL of TSB bottle and incubating at 37°C overnight. If more culture was necessary on the day of an assay, 1 mL of overnight grown culture was transferred to another 100 mL of TSB bottle and placed on a shaker table in a 37°C incubator for 3–6 hr. TSA plates were warmed to room temperature to permit easier spreading of medium on plates. Overlay media was melted in a steamer and kept in a 45°C water bath.

Samples were serially diluted until the estimated concentration range was covered. Each dilution step reduced the concentration by one order of magnitude: pipetting 0.3 mL of diluent into 2.7 mL of TRIS or peptone and vortexing the mixture. One mL of host culture and 0.1 mL of diluted sample were added to the overlay tube. Then the tube was vortexed, the contents were poured onto a TSA plate, swirled, and the plate was covered with a lid. After the overlay agar solidified, plates were inverted and placed in a 37°C incubator overnight.

Plaques were counted the next day. An attempt was made to use plaque counts between 10 and 300 for the result of each sample. Plaque counts less than 10 are statistically unreliable and ones more than 300 are difficult to count.

2.2.3 Host Bacteria

The host bacteria for MS-2 was Escherichia coli B and for PRD-1 Salmonella typhimurium LT2 was used.

MS-2 host bacteria Escherichia coli B (E. coli) was obtained from American Type Culture Collection (ATCC, stock # 15597). The E. coli culture was spread on TSA plates with a sterile loop and incubated overnight. From the spread plate, a test tube with 10 mL of TSB was inoculated with an isolated bacteria colony and incubated at 37°C overnight. A few drops of glycerol were then added to this test tube and stored at 7°C for future use. The host culture for phage growth or assay was prepared by inoculating bottles containing 50 - 100 mL of TSB with glycerol stock culture and incubating at 37°C overnight.

PRD-1 host bacteria Salmonella typhimurium LT2 was obtained from University of Arizona, Department of Microbiology and Immunology stock cultures or existing plate cultures. The stock culture was prepared in the same manner as E. coli.

2.2.4 Bacteria Assays

Pseudomonas fluorescens P17 was obtained from the Metropolitan Water District (Los Angeles, CA). One loopful of stock culture solution was suspended in 9 mL of Standard Method Phosphate Buffer (SMPB). The solution was vortexed and serially diluted with SMPB to 3 orders of magnitude lower concentration. Four mL of this dilution were added to 36 mL of SMPB in a flask (– 4 dilution). Fifty mL of the 1 μgL^{-1} sodium acetate solution and 40 mL of the P17 solution were mixed in a sterile 125 mL screw-top Erlenmeyer flask. The solution was incubated at room temperature for 4 days.

Bacillus subtilis TF-32 was isolated from Tumamoc Hill, Tucson, AZ, in 1987 by K. Duncan (University of Arizona, Department of Ecology and Evolutionary Biology). The culture was spread on R2A plates and incubated at 37°C overnight. An isolated bacteria colony was transferred to a bottle containing 50 - 100 mL of TSB and incubated for 3 hr at 37°C with continuous shaking. The TSB culture solution was centrifuged at 8,000 g (10,000 rpm) and 10°C for 15 min. The resulting pellet was resuspended in filtered well water and centrifuged again at the same condition. Again, the pellet was resuspended in filtered well water and stored at 7°C.

For bacteria assay, sample dilution was made by the same manner as described in Section 2.2.2. Diluent was plated onto the R2A plate on a turntable, spreading with a flamed, L-shaped glass stick. Glass sticks were sterilized by flaming with methanol immediately after use and placed in a covered, sterilized plastic petri dish. Three sticks were used in succession. Pseudomonas fluorescens P17 plates were incubated at room temperature for three days before counting. Bacillus plates were incubated at 37°C overnight.

2.3 Microelectrophoresis

The surface charges of silica beads and bacteria in various pH's were evaluated by electrophoretic-mobility measurement. Rank Brothers Mark II particle-electrophoresis apparatus (Rank Brothers, Ltd., Cambridge, England) was used to determine the mobility. A flat cell was set up for this purpose.

For each value of mobility, 20 particles were timed under constant voltage: 5 times for both polarity at one stationary level, and the same at the other stationary level. Mean mobility (u_m) was calculated by (particle velocity)/(gradient of potential) using the average travel time of the particles:

$$u_m = \frac{D/t}{V/L}$$

where D is the travel distance (μm), t is travel time (sec), L is cell length (cm), and V is applied voltage (v).

For silica mobility, silica beads nominally 5 μm in diameter (Pennsylvania Glass Sand Co., Berkeley Springs, WV, Min-U-Sil) were used. The size of the beads is close to that of bacteria, which are 3–4 μm in length (see Section 2.1.5). Prior to the measurement, the beads were washed. Approximately 1 mL of beads were rinsed in 50 mL of 1 N HCl and rinsed in deionized water until the rinse-water became a neutral pH, then oven-dried overnight at 100 °C.

A small amount of beads was placed in 200 mL of 0.02 M pH 7-phosphate buffer (see Section 2.1.4). Buffer pH was reduced with 1 M HCl from about 7 to 3 in order to obtain pH vs. mobility curves.

Bacteria were purified by the procedure described in Section 2.2.4. An arbitrary amount of bacteria stock solution was placed in 200 mL of the buffer until the bacteria became visible under the microscope. The pH of the buffer was reduced by the same manner.

All the measurements were done at room temperature.

3. *RESULTS*

3.1 Microelectrophoresis

Electrophoretic mobilities of silica beads and Bacillus as a function of pH in 0.02-M phosphate buffer are shown in Figure 2. Apparent isoelectric points (pH_{iep}) of silica beads and Bacillus are lower than pH 3. Although the estimated pH_{iep} of silica beads in this measurement is lower than the reported value of pH 2.0±0.2 [*Parks, 1965*], it is clear that silica beads are negatively charged at natural-water pH values as well as bacteria.

It can be assumed the surface potential of the beads measured in this mobility experiment was equal to that of the silica beads in the column experiments due to their uniform surface. However, the surface potential of bacteria could be different, since the surface composition of bacteria is complex and differs among individual bacteria as well as different species. Also, it is difficult to have bacteria with pure surfaces. In the measurement of Bacillus mobility, turbidity in the buffer was observed. It could be a biological matter, such as metabolites of bacteria, which was not separated by the two centrifugations. Those substances present in the buffer possibly affected the mobility either physically or chemically. For mobility measurement, it is suggested to wash bacteria with at least three successive cycles of centrifugation. Regarding the purpose of this measurement, identifying the isoelectric points of the bacteria in the column experiments, two centrifugations can better simulate the surface condition in the experiments, since the bacteria were processed by two centrifugations for the column experiments. Also, too many centrifugations may result in different surface conditions, since purifying by washing may remove capsular material from the bacteria [*Richmond et al., 1973*].

It is also important to note that these measurements were done at room temperature. The viscosity of fluids varies a great deal according to the temperature [*de Marsily, 1981*]. The sensitivity of the mobility measurement to these effects and other factors such as

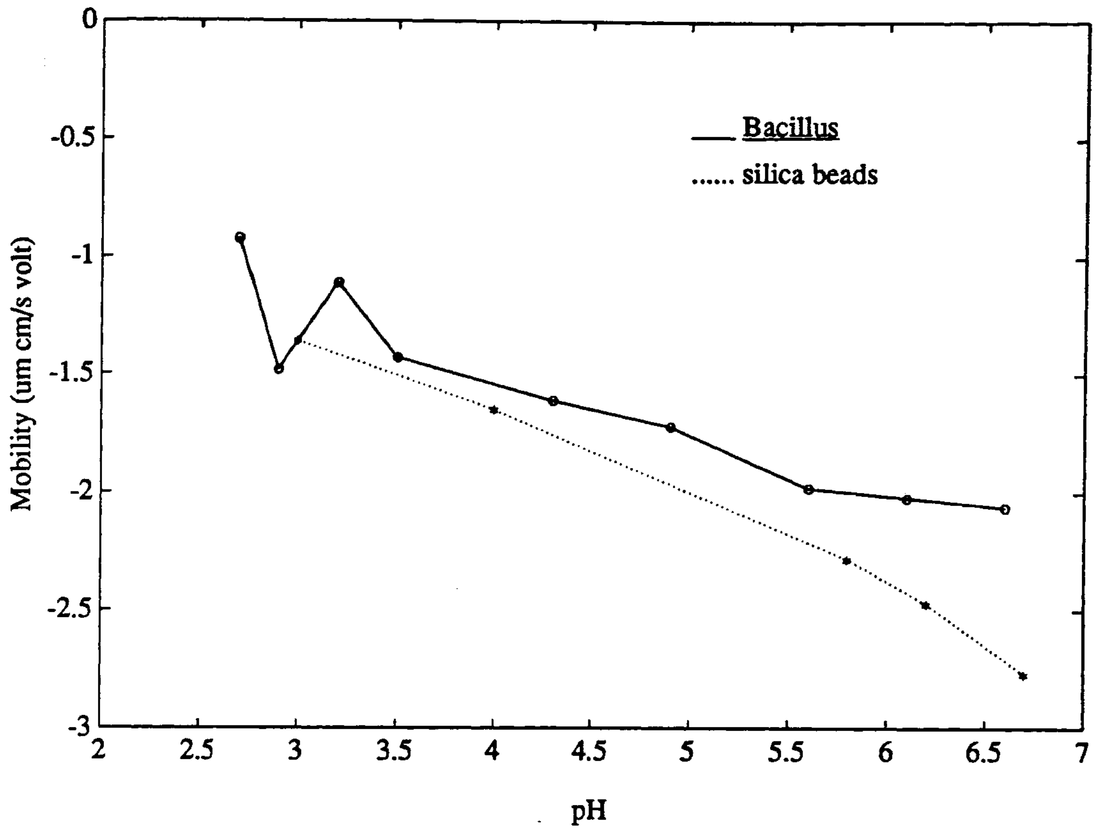

Figure 2. Mobility of silica beads and bacteria as a function of pH in 0.02 M phosphate buffer.

motility, the nature of the growth medium, and the age of the culture [*Richmond et al., 1973*] needs to be investigated.

3.2 Breakthrough Curves

The breakthrough curves of the column experiments are shown in Figures 3 through 10. Log C/C_0 versus pore volume and C/C_0 versus pore volume were plotted. In the figures, att, det, and B.E. represent attachment, detachment, and beef extract, respectively. The numbers in parentheses are pH's of the buffer. The points on the lower horizontal dashed line in the figure of log C/C_0 mean below detection limit. The detection limit of the assay was about 10 pfu mL^{-1} (10 cfu mL^{-1}). The first vertical dotted line is at the value of pore volume (PV) at which stock solution of virus (bacteria) was switched to a phage-free (bacteria-free) buffer. The second vertical dotted line is at the value of PV at which the buffer was switched to the one of higher pH with or without beef extract.

3.2.1 Borden Soil — PRD-1

Breakthrough curves of Borden soils are presented in experiments 1 to 3, as shown in Figure 3. Buffer solution was sent at 100–150 minutes per pore volume, which is about 140–200 cm dy^{-1}. This velocity was about 13–24 times faster than that in the field (vs. mean velocity 9 cm dy^{-1} at Borden site in Table 2). The dry bulk densities of the soil packed in the column were 1.69–1.70 g cm^{-3}, which is lower than the reported value of core samples by *Mackay et al.* [*1986*]. The dry bulk density of volume-weighted arithmetic mean of then 36 samples was 1.81 g cm^{-3} (Table 2). The standard deviation of the spatial distribution was 0.045 g cm^{-3}. The breakthrough curves for all the cases showed a steep rise in virus concentration after about one pore volume of virus-containing solution had passed through the column, followed by a steady-state value until the eluent was switched to a virus-free solution. The C/C_0 showed less steep or no declines about one pore volume after the feed was switched. Addition of the beef extract raised the pulse to higher than stock titer in all cases. The experiment was not run long enough to get complete recovery of attached phage, but

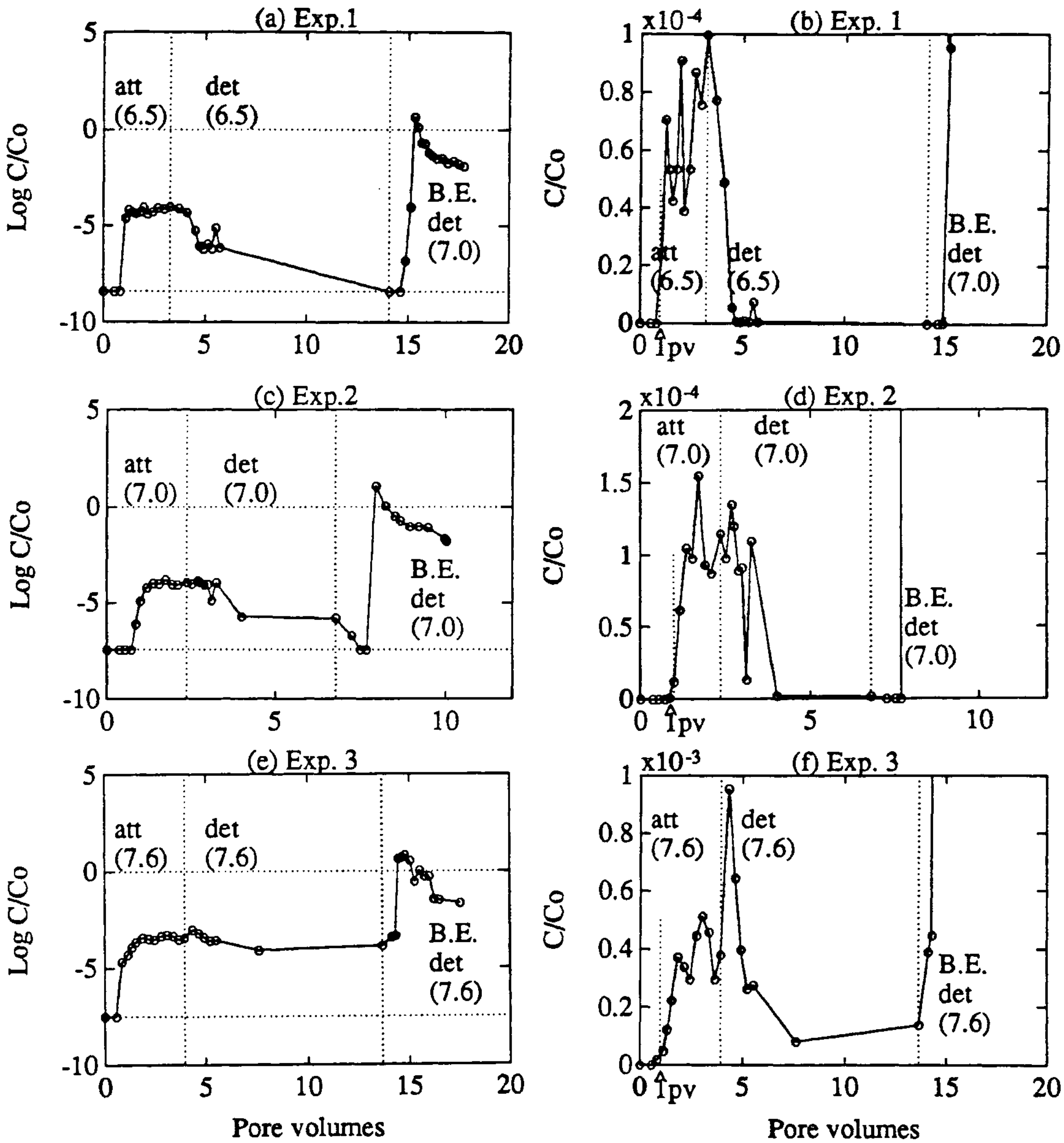

Figure 3. **Breakthrough curves of column experiment for PRD-1 through Borden soil plotted as Log (C/C_0) and C/C_0 vs. pore volume: a) and b) pH 6.5 during attachment and first detachment steps of experiment 1; c) and d) pH 7.0 during attachment and first detachment steps of experiment 2; e) and f) pH 7.6 during attachment and first detachment steps of experiment 3.**

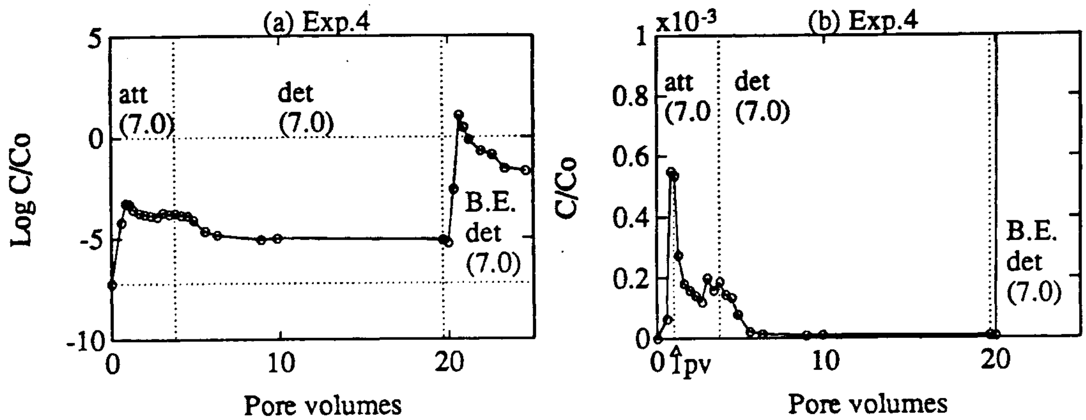

Figure 4. **Breakthrough curves of column experiment for PRD-1 through Cambridge soil plotted as Log (C/C_0) and C/C_0 vs. pore volume: a) and b) pH 7.0 during attachment and first detachment steps of experiment 4.**

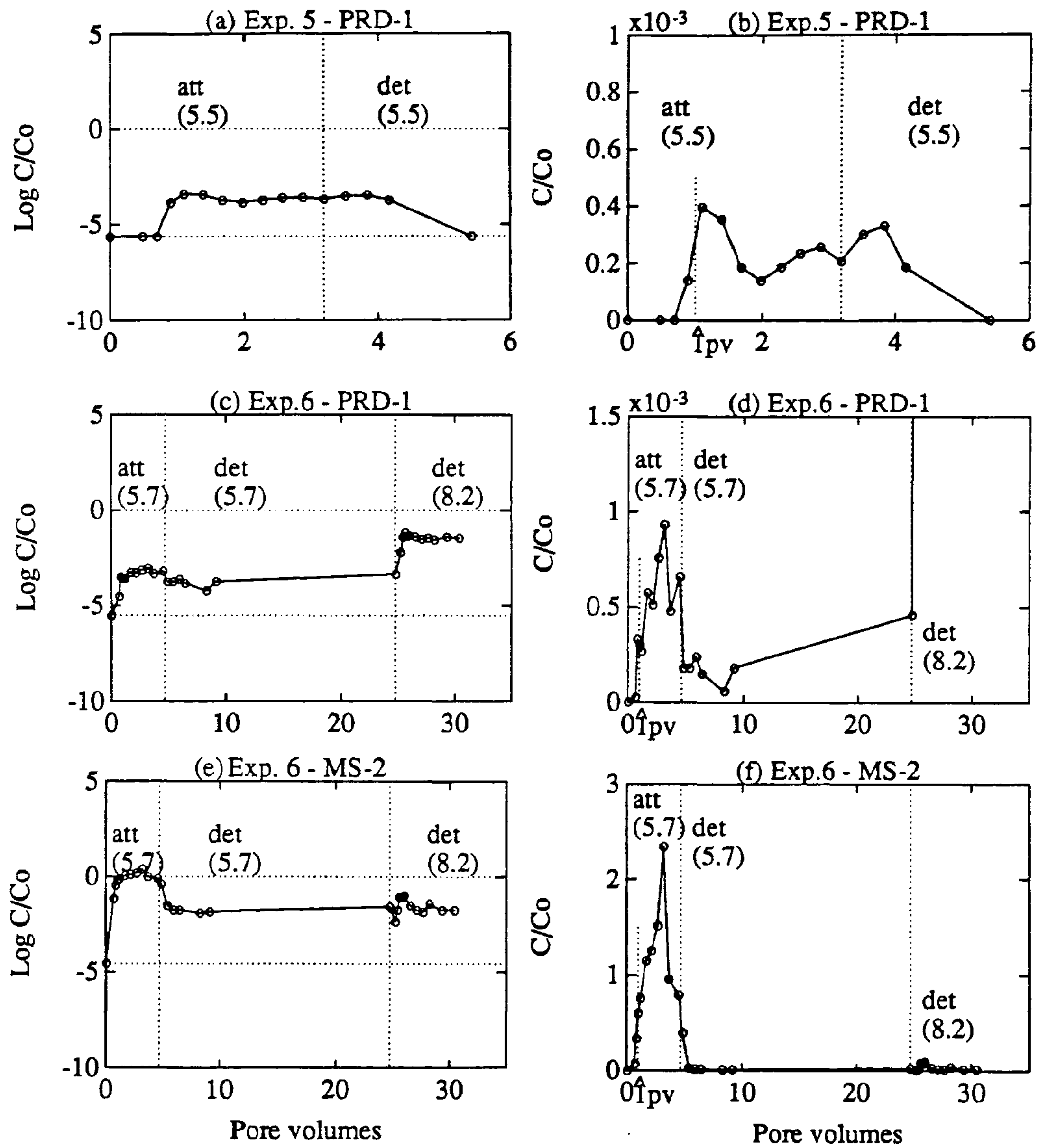

Figure 5. Breakthrough curves of column experiment for PRD-1 and MS-2 through Cape-Cod soil plotted as Log (C/C_0) and C/C_0 vs. pore volume: a) and b) pH 5.5 during attachment and detachment steps of experiment 5 (PRD-1); c) and d) pH 5.7 during attachment and first detachment steps of experiment 6 (PRD-1); e) and f) pH 5.7 during attachment and first detachment steps of experiment 6 (MS-2). Breakthrough curve for MS-2 in experiment 5 was not plotted, since no phage was detected throughout the experiment.

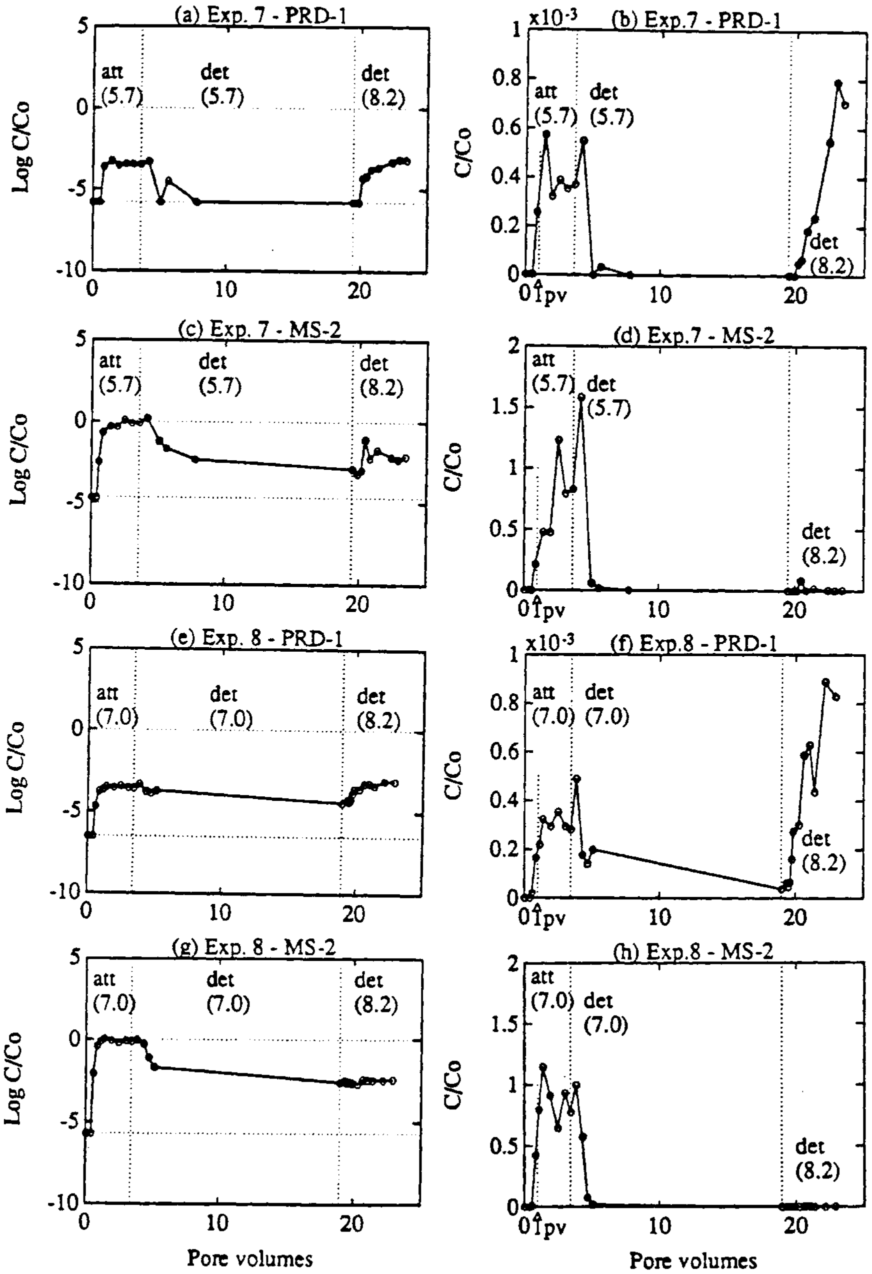

Figure 6. Breakthrough curves of column experiment for PRD-1 and MS-2 through Cape-Cod soil plotted as Log (C/C_0) and C/C_0 vs. pore volume: a) and b) pH 5.7 during attachment and first detachment steps of experiment 7 (PRD-1); c) and d) pH 5.7 during attachment and first detachment steps of experiment 7 (MS-2); e) and f) pH 7.0 during attachment and first detachment steps of experiment 8 (PRD-1); g) and h) pH 7.0 during attachment and first detachment steps of experiment 8 (MS-2).

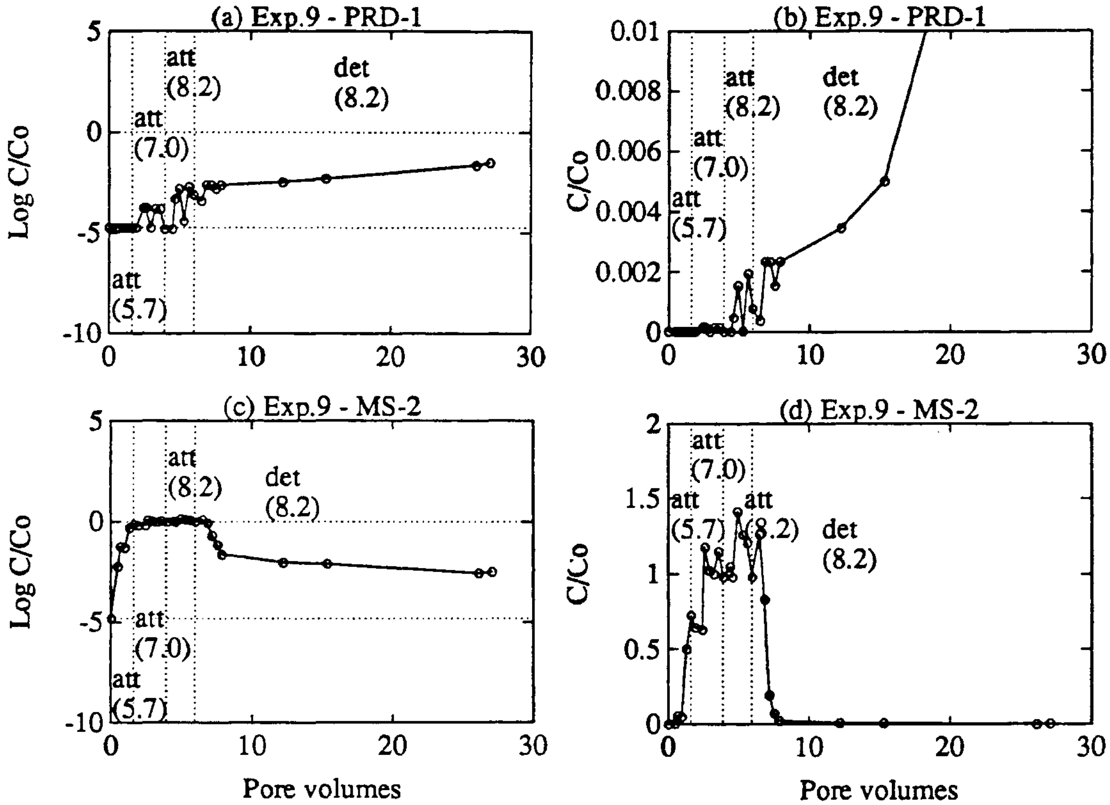

Figure 7. Breakthrough curves of column experiment for PRD-1 and MS-2 through Cape-Cod soil plotted as Log (C/C_0) and C/C_0 vs. pore volume: a) and b) pH 5.7, 7.0 and 8.2 during attachment and detachment steps of experiment 9 (PRD-1); c) and d) pH 5.7, 7.0 and 8.2 during attachment and detachment steps of experiment 9 (MS-2).

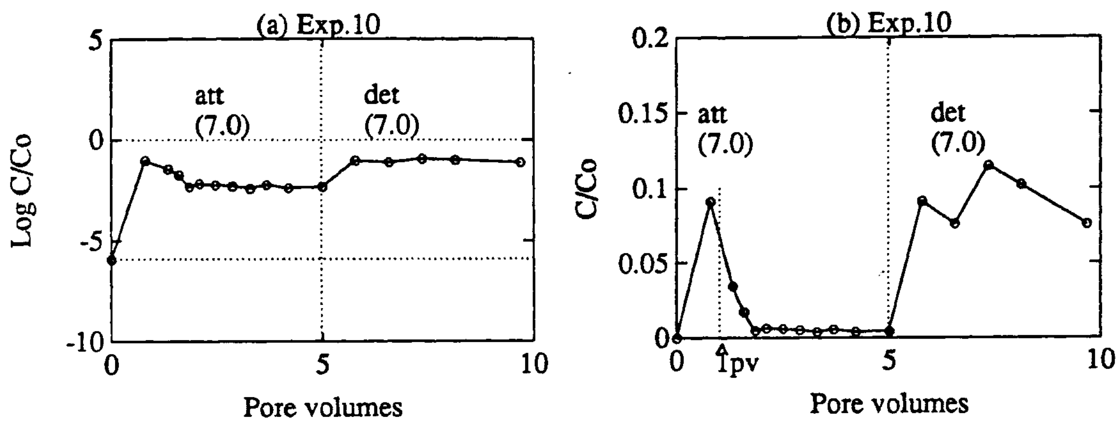

Figure 8. Breakthrough curves of column experiment for Pseudomonas fluorescens P17 through 1.0-mm silica beads plotted as Log (C/C_0) and C/C_0 vs. pore volume: a) and b) pH 7.0 during attachment and detachment steps of experiment 10.

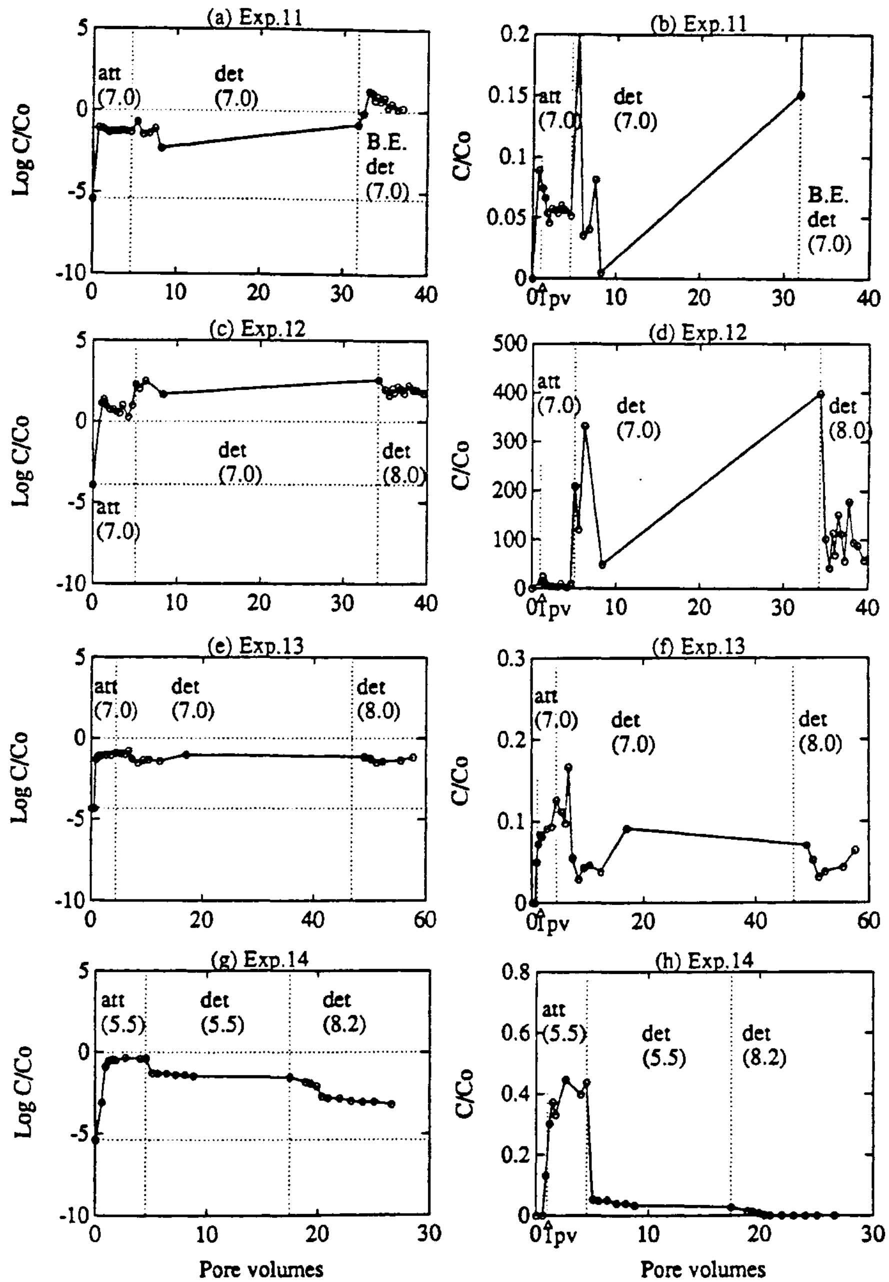

Figure 9. Breakthrough curves of column experiment for Pseudomonas fluorescens P17 through 0.5-mm silica beads plotted as Log (C/C_0) and C/C_0 vs. pore volume: a) and b) pH 7.0 during attachment and first detachment steps of experiment 11; c) and d) pH 7.0 during attachment and first detachment steps of experiment 12; e) and f) pH 7.0 during attachment and first detachment steps of experiment 13; g) and h) pH 5.5 during attachment and first detachment steps of experiment 14.

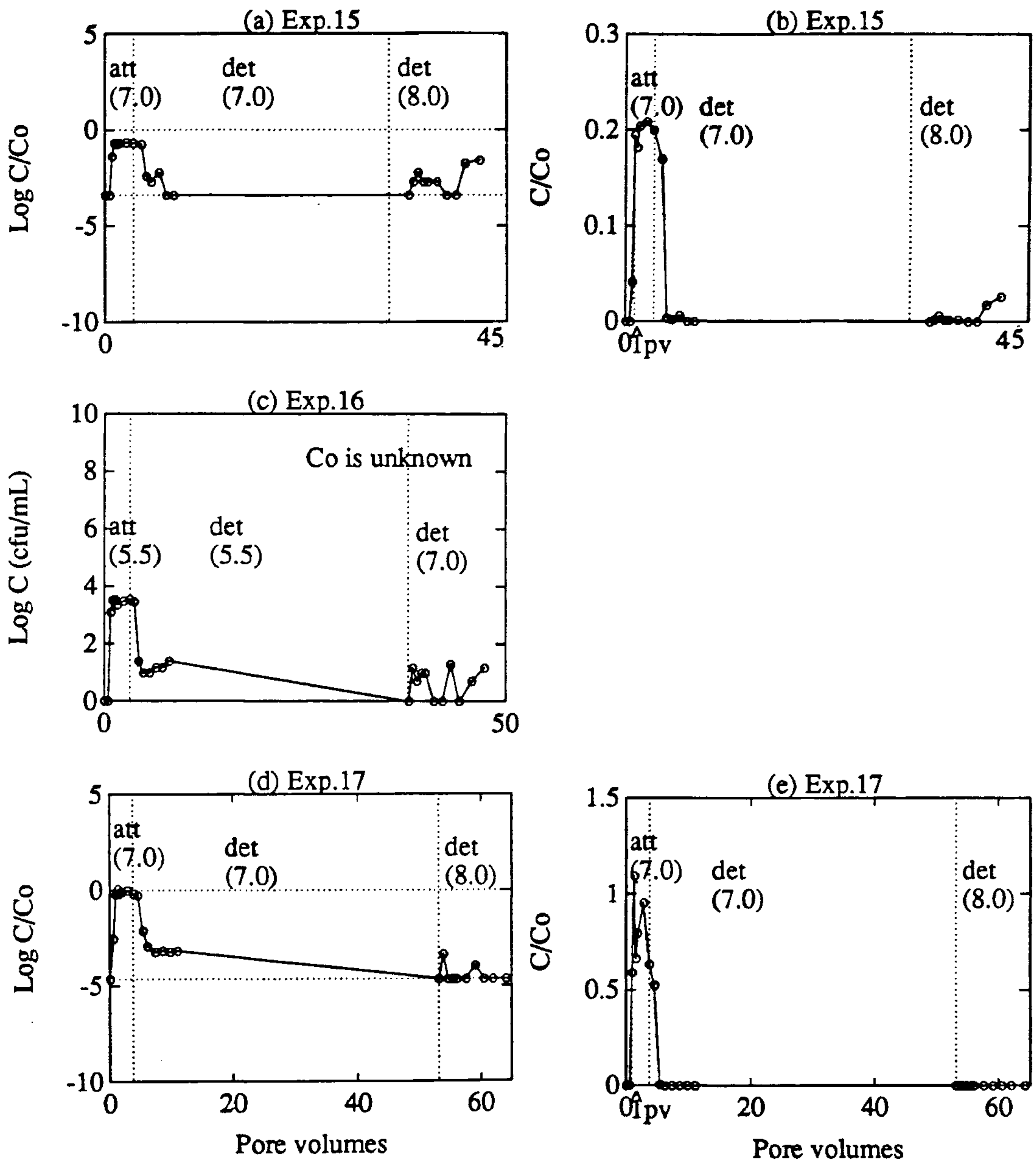

Figure 10. Breakthrough curves of column experiment for Bacillus subtilis TF-32 through 0.5-mm silica beads plotted as Log (C / C_0) and C / C_0 vs. pore volume: a) and b) pH 7.0 during attachment and first detachment steps of experiment 15; c) pH 5.5 during attachment and first detachment steps of experiment 16. C / C_0 vs. pore volume was not plotted, since the titer was unknown.; d) and e) pH 7.0 during attachment and first detachment steps of experiment 17.

Hinkle [1990] reported about 80 percent recovery in his silica-bead column experiments. Since the soil consisted of fine to coarse sand and the virus size was small, removal by straining should be negligible.

In experiment 1 at pH 6.5, C/C_0 of the steady-state attachment was about 0.7×10^{-4}. The phage were first detected after about 1.1 pore volume of water had passed through the column. Upon switching the inlet feed to a phage-free buffer, the column-outlet concentration dropped by more than 100-fold — log C/C_0 dropped from -4 to slightly lower than -6. The attachment was slowly reversible with non-zero phage concentrations in the column outlet after switching to the phage-free buffer. The detachment rate decreased to zero (below the detection limit) by the time about ten pore volumes of phage-free buffer had passed (at 14 pore volumes). Addition of a pH-7.0 buffer containing beef extract resulted in a column-outlet pulse to above the stock titer.

In experiment 2 at pH 7.0, C/C_0 of the steady-state attachment was about 1.1×10^{-4} — higher than at pH 6.5. The phage were first detected after about 0.9 pore volume of water had passed. The column-outlet concentration dropped by less than 100-fold (the drop of log C/C_0 was -4 to slightly higher than -6) upon switching to a phage-free buffer. After the detachment rate dropped at four pore volumes, it appeared to be maintained until the buffer was switched at seven pore volumes. However, the plaque counts for this period were less than ten and statistically unreliable (see Section 2.2.2). Addition of a pH-7.0 buffer containing beef extract resulted in a column-outlet pulse to higher than the stock titer. The C/C_0 dropped immediately after the switching, but the plaque counts for these samples were less than ten.

In experiment 3 at pH 7.6, C/C_0 of the steady-state attachment was about 0.5×10^{-3} — higher than at pH 6.5 and 7.0. The phage were first detected after about 0.9 pore volume of water had passed. The column-outlet concentration did not drop upon switching to a phage-free buffer, indicating that the detachment was faster relative to pH 6.5 and 7.0. Again, addition of beef extract to the pH-7.6 buffer resulted in a column-outlet pulse to above stock titer.

The large amount of attachment at these higher pH's and the relative insensitivity to pH suggests that hydrophobic effects can be important. The three results showed a weak trend of decreasing attachment rate with higher pH, which is consistent with the theory of Derjaguin, Landau, Verwey and Overbeek (the DLVO theory). Approximate C/C_0's of the steady-state attachment were 0.7×10^{-4} at pH 6.5, 1.1×10^{-4} at pH 7.0, and 5.0×10^{-4} at pH 7.6. There is a weak trend of decreasing concentration drop (increasing detachment rate) at higher pH upon switching to a phage-free buffer: about 2 orders of magnitude drop for pH lower than 7.0 and a slight drop for pH 7.6. This is also consistent with the DLVO theory. In order to conclude these trends, replicates are necessary. The results suggest that once the phage is loaded, the soil will be a source of phage for a considerable time.

3.2.2 Cambridge Soil — PRD-1

The breakthrough curves for the Cambridge soil column at pH 7.0 are presented in experiment 4, as shown in Figure 4. Since the medium was sandy soil and the virus was small, removal by straining should be negligible. The dry bulk density of the soil packed in the column was 1.68 $g\,cm^{-3}$. Flow velocity was 250 $cm\,dy^{-1}$, which is about 30-fold faster than that in the field (vs. average 8 $cm\,dy^{-1}$ at the Cambridge site in Table 2).

The sharp peak of attachment limb was caused by a misfeeding of a higher concentration of phage solution at the beginning of the experiment. The breakthrough curve showed a steep attachment limb and a moderate detachment limb. Ignoring the effect of the misfeeding, C/C_0 of the steady-state attachment was about $2.0 \times \times 10^{-4}$. This attachment rate is close to that of Borden soil (vs. $C/C^0 = 1.1 \times 10^{-4}$). The phage were first detected after about 0.6 pore volume of water had passed. The column-outlet concentration dropped upon switching to a phage-free buffer about 10-fold — $\log C/C_0$ dropped from slightly higher than -4 to -5. At this pH, the elution effect of a phage-free buffer appeared to be less sensitive than Borden soil (vs. 100-fold drop). The pH-7.0 beef-extract buffer raised the effluent phage concentration to one order of magnitude higher than the titer of the stock solution. The large amount of attachment at this high pH suggests that hydrophobic effects can be important. Additional experiments would be necessary to verify this observation.

3.2.3 Cape-Cod Soil — PRD-1 and MS-2

The results for the Cape-Cod soil column are shown in Figures 5 through 7. Experiment 7 is a replication of Experiment 6. Since the medium was sandy soil and the viruses were small, removal by straining should be negligible. The dry bulk densities of the soil packed in the column were 1.68–1.71 $g\,cm^{-3}$, close to the reported value 1.72 $g\,cm^{-3}$ (Table 2). Flow velocity was 200–260 $cm\,dy^{-1}$, which is about 5-fold faster than that in the field (vs. an average 47 $cm\,dy^{-1}$ at the Cape-Cod site in Table 2). The breakthrough curves showed a steep rise after about one pore volume of water had passed. When switched to a virus-free solution, the steady-state attachment was followed by a slight (PRD-1) or steep (MS-2) decline of the detachment limb. The increase of pH caused a rapid detachment, but to different degrees for PRD-1 and MS-2. PRD-1 was attached to soil in large amounts as opposed to MS-2. The results of the each experiment are as follows.

Experiment 5 at pH 5.5 had a problem of calcium precipitation and the experiment was stopped after a short period. In this experiment, 0.7 ppm ($10^{-4.76}$ M) of calcium (calcium content of the effluent of the column in the tracer experiment) was added to the phosphate buffer. This addition of calcium resulted in calcium phosphate precipitation. Only the result of PRD-1 is presented in the figure, since MS-2 from the column-outlet was not detected.

In experiment 6 at pH 5.7, PRD-1 was more attached to the soil than MS-2 (approximate C/C_0 of the steady-state attachment was 0.7×10^{-3} for PRD-1 and 1.5 for MS-2). The reason that C/C_0 of MS-2 was over one may be due to an assay error of the stock concentration. Another possible reason is that the aggregated viruses were caught in the soil medium, resulting in a high pulse by a sudden release of virus aggregates. This reason is unlikely since the soil medium has large pore space relative to the size of virus. Both PRD-1 and MS-2 were first detected after about 0.7 pore volume of water had passed. MS-2 concentration dropped more upon switching to a phage-free buffer than PRD-1: about 2 orders of magnitude drop for MS-2 (log C/C_0 dropped from 0 to − 2) vs. a slight drop for PRD-1. Since MS-2 was not significantly attached to the soil (C/C_0 was over one), this detachment limb is nearly that of a conservative particle. More PRD-1 was eluted upon increasing the pH than MS-2: about 2 orders of magnitude increase in pulse concentration for PRD-1 (log C/C_0 increased from − 3 to − 1) vs. a slight rise for MS-2. MS-2 did not respond to the increase of the pH from 5.7 to 8.2, because most of the MS-2 was eluted by this time. These results suggest that the major mechanism of attachment of MS-2 to this soil was electrostatic attraction and above the isoelectric point of MS-2 (about pH 4) attachment did not occur significantly, i.e., MS-2 was a conservative particle in this medium. Since MS-2 is relatively hydrophilic, the hydrophobicity may be a minor effect.

Experiment 7, a replication of experiment 6, exhibited basically the same trend as experiment 6. The C/C_0 of PRD-1 and MS-2 of the steady-state attachment was about 0.4×10^{-3} and 1.0, respectively. The differences between experiments 6 and 7 may be due in part to the inconsistent accuracy of the assay of the stock solutions. PRD-1 were first detected after about 0.8 pore volume of water had passed, and 0.6 for MS-2. The column-outlet concentration of PRD-1 upon switching to a phage-free buffer appeared to have dropped more than in experiment 6. However, the plaque counts of these points on the detachment limb are less than ten.

In experiment 8 at pH 7.0, C/C_0 of PRD-1 and MS-2 of the steady-state attachment were about 0.3×10^{-3} and 0.8, respectively. The trends of breakthrough curves for both PRD-1 and MS-2 were the same as those in experiment 6. Both PRD-1 and MS-2 were first detected after about 0.6 pore volume of water had passed. Regarding the large amount of attachment at this high pH and the relative insensitivity to pH (C/C_0 of the steady-state attachment were $0.4 - 0.7 \times 10^{-3}$ at pH 5.7 and 0.3×10^{-3} at pH 7.0), these results suggest that the hydrophobic effect is important for PRD-1 attachment to this soil. However, the elution by pH 8.2-buffer showed that pH also affects the attachment.

In experiment 9, three different pH's of phage stock (pH 5.7, 7.0, and 8.2) were sent to the column serially and switched to pH-8.2 phage-free buffer. The result confirmed the previous results. The steady-state attachment of PRD-1 was insensitive to the pH change, and a phage-free buffer at pH 8.2 eluted the phage slowly. MS-2 was conservative in this range of pH's. A large amount of PRD-1 was attached to the soil in this pH range, as opposed to no attachment of MS-2.

The results exhibited the sharp contrast of attachment mechanism for PRD-1, hydrophobic effect, and MS-2, electrostatic attraction, in this soil medium. However, there was no clear trend of pH effect.

3.2.4 Silica Beads — P17

The results for P17 in silica beads are shown in Figures 8 and 9. Only experiment 10 used 1.0-mm silica beads for the medium, and experiments 11 through 17 used 0.5-mm beads. Experiments 10 through 12 had entrapped air in the column and can be examined by comparison to experiment 13, which was at the same pH and better controlled. The results were not reliable as will be explained below. Experiments 13 and 14 need repeating. The solution was sent at 30–43 minutes per pore volume, which is 28–32 cm per hour. As for the viruses, the breakthrough curves showed a steep rise and a steady-state attachment plateau. Comparing experiments 13 and 14, the drop of C/C_0 upon switching to a bacteria-free buffer was smaller in higher pH. The C/C_0 increased gradually after each drop at higher pH, but decreased slowly at lower pH. Since the beads were very large compared to the bacteria, straining should be negligible.

Experiment 10 at pH 7.0 (1.0-mm beads) had entrapped air and showed an anomaly in the breakthrough curve compared with experiment 13, which was at the same pH and better controlled. The column was accidentally drained before the experiment and it was not completely saturated again. The attachment limb had a sharp peak to $C/C_0 = 0.09$, then dropped to 0.005 and maintained a steady-state for the rest of the attachment period. The C/C_0 of the first peak is close to the one of the steady-state attachment in experiment 13 (about 0.1), but the steady-state value following is too low. This may be due to the effects of air in the unsaturated column. P17 in the buffer might be excluded to the less polar, air-water interface and kept in the column with the air, since P17 is relatively hydrophobic as will be discussed later. The C/C_0's dropped after switching to a bacteria-free buffer in experiment 13 and all the other cases, but it increased in this case. P17 may have started to be released with air when the stock solution was switched. It may also have involved assay error such as dilution mistake or contamination. Therefore, this breakthrough curve will be omitted from the model parameter analysis.

In experiment 11 at pH 7.0, C/C_0 of the steady-state attachment was about 0.06. This experiment also had entrapped air. Attachment limbs showed a sharp peak of C/C_0 to 0.09 followed by a drop to 0.06. Upon switching to a bacteria-free buffer, C/C_0 dropped about 10-fold (log C/C_0 dropped from -1 to -2). At 32 pore volumes, after about 27 pore volumes of a bacteria-free buffer had passed, C/C_0 increased to 0.15. The pH-7.0 beef-extract buffer raised the effluent concentration, showing that beef extract is a elution agent for P17. Since air in the column may be affecting the results and there are too few data points on both the attachment and detachment limbs, this result will be omitted from the model-parameter analysis.

The breakthrough curve of experiment 12 at pH 7.0 clearly broke the mass conservation. Therefore, this breakthrough curve will be omitted from the model parameter analysis. Also, C/C_0 of the steady state showed a sudden shift of the curve (about one order of magnitude increase) in spite of no change of input and other conditions. This may be due to the effects of entrapped air.

In experiment 13 at pH 7.0, C/C_0 of the steady-state attachment was about 0.1. The bacteria were first detected after 0.9 pore volumes of water had passed through the column. Upon switching to bacteria-free buffer, C/C_0 dropped 3-fold from 0.12 to 0.04. Then it gradually increased to about the same level as before the drop and was maintained until pH was raised to pH 8.0. This steady-state detachment was about 0.09 in C/C_0. The detachment rate appeared to have increased slowly, responding to the bacteria-free condition and reaching a steady state (the detachment rate is time dependent). After raising the pH of the buffer to 8.0, column-outlet concentration dropped and gradually increased. This is distinctive from the other results, since raising the pH resulted in a higher pulse in the cases of the viruses. A biological reaction (die-off due to a sudden change of pH, etc.) may be the cause of this phenomenon.

In experiment 14 at pH 5.5, C/C_0 of the steady-state attachment was about 0.4. This value is higher than at pH 7.0 (vs. 0.1 in experiment 13) and contrary to the DLVO theory. The bacteria were first detected after 0.6 pore volume of water had passed through the column. Upon switching to a bacteria-free buffer, C/C_0 dropped 8-fold from 0.4 to 0.05. From this point, the detachment rate was maintained until pH was raised to pH 8.2. This steady-state detachment was about 0.03 in C/C_0. The pH increase to 8.2 caused another drop of C/C_0 (about one order of magnitude) and further continuous decrease.

The steady-state attachment was larger at higher pH ($C/C_0 = 0.12$ at pH 7.0 vs. 0.4 at pH 5.5) and a relatively large amount was attached at high pH. On the other hand, steady-state detachment rate in a bacteria-free buffer was larger at higher pH (C/C_0 is about 0.09 at pH 7.0 and 0.03 at pH 5.5). Attachment and detachment of P17 are not consistently correlated with pH as predicted by the DLVO theory: strong attachment at lower pH and a lack of attachment at higher pH. This indicates that the major mechanism of attachment for P17 to silica beads would not be electrostatic attraction, but hydrophobic effect. Since bacteria surfaces in general have hydrophobic substances such as lipids, they are likely to exhibit hydrophobic interaction. The larger steady-state detachment at higher pH may be due in part to the flow-rate change. During the attachment, velocity for both pH cases were about 6.5×10^{-3}cm s^{-1}, upon switching to a bacteria-free buffer, velocity increased to 7.1×10^{-3}cm s^{-1} in the pH-7.0 experiment but decreased to 6.5×10^{-3}cm s^{-1} in the pH-5.5 experiment. Higher velocity could elute more bacteria from the silica surface. The hydrodynamic lift force acting on attached particles is roughly proportional to the third power of the dimension of the particle, and sizes > 1 μm can readily be sheared off surfaces under the action of only small velocity gradients [*Lips et al., 1979*]. Motility may have affected the attachment of bacteria, and it may possibly have been influenced by pH. Insoluble polysaccharides produced by microorganisms are often involved in attachment as a glue [*Rogers, 1979*]. Surface appendages might be involved in the attachment process. Activity of bacteria might be affected by their population in the buffer (it might be different in stock solution and in a bacteria-free buffer). It is important to study the biological phenomena involved in these attachment-detachment processes. Additional work would be necessary to study these factors.

3.2.5 Silica Beads — Bacillus

The breakthrough curves for Bacillus subtillis TF-32 silica beads are presented in Figure 10. Experiment 15 and 17 are replications. The solution was sent at 28–38 minutes per pore volume, which is 32–43 cm per hour. It was found that the results of the detachment of the second day were not reliable, since inactivation of the bacteria was significant, as will be explained in experiment 17. Therefore, only the breakthrough curves of the first day will be focused upon. The breakthrough curves also showed a rapid rise, steady-state plateau, and a steep drop upon switching to a bacteria-free buffer. A higher-pH buffer caused some elution of the bacteria. Since the beads were very large compared to the bacteria, straining should be negligible.

In experiment 15 at pH 7.0, C/C_0 of the steady-state attachment was about 0.2. The bacteria were first detected after 0.8 pore volume of water had passed through the column. The column-outlet concentration dropped to zero detection upon switching to a bacteria-free buffer.

In experiment 16 at pH 5.5, the titer of the bacterial stock solution was not obtained, so only the pore volume vs. log C/C_0 breakthrough curve is presented. The bacteria were first detected after 0.8 pore volume of water had passed through the column. Upon switching to a bacteria-free buffer, the column-outlet concentration dropped rapidly by more than 2 orders of magnitude.

In experiment 17 at pH 7.0, C/C_0 of the steady-state attachment was about 0.8. The bacteria were first detected after 0.6 pore volume of water had passed through the column.

The column-outlet concentration dropped by more than 2 orders of magnitude upon switching to a bacteria-free buffer. Titer of stock solution changed 2 orders of magnitude: 4.63 cfu mL^{-1} at 9:30 a.m., and 4.45 cfu mL^{-1} at 2:45 p.m. on the first day, and 2.62 cfu mL^{-1} the next day (titer of stock solution in experiment 15 was not monitored). This was a replication of experiment 15 , but C/C_0 values were quite different (0.2 in experiment 15 vs. 0.8 in experiment 17). Regarding the stable titer of the stock solution (but only the first day) monitored in experiment 17, the results may be more reliable.

Although the results of the second day were not reliable, they indicated that raising pH could elute attached bacteria from silica beads. Since C/C_0 at pH 5.6 was not obtained, the pH effect on the steady-state attachment rates cannot be compared. Due to the large amount of bacteria attached at high pH, hydrophobicity can be an attachment mechanism. As observed for P17, biological effects may be involved in attachment-detachment of Bacillus.

4. DISCUSSION

4.1 pH and Hydrophobic Effects

As shown in the results of mobility measurements, silica beads and bacteria used in the column experiments are negatively charged at natural-water pH values. Soil material, PRD-1, and MS-2 are also negatively charged at this pH range. Therefore, the attachment phenomenon is expected to be consistent with the theory of Derjaguin, Landau, Verwey, and Overbeek (the DLVO theory): strong attachment at lower pH and a lack of attachment at higher pH.

PRD-1 in Borden soil showed a weak trend consistent with the DLVO theory. *Hinkle* [*1990*] demonstrated the attachment of PRD-1 to silica beads was consistent with the DLVO theory. However, the large amount of attachment at high pH's and the relative insensitivity to pH suggest that the magnitude of hydrophobic interaction was much larger. This is confirmed by the fact that the surface of PRD-1 has lipids and is hydrophobic. On the other hand, the organic carbon content of the soil, which gives hydrophobicity to the soil materials, is very low (0.028 percent, see Table 2). Hydrophobicity of this soil could be caused by some other materials. For example, *Hinkle* [*1990*] suggested that the attachment of PRD-1 to silica beads without organic material can be attributed to hydrophobic effects. Since the soil is about 60 percent quartz (SiO_2), the SiO_2 present in the soil may be responsible for the observed hydrophobic effect. Another possibility is that although the organic carbon content is low it exhibits enough hydrophobicity to attract PRD-1. As will be explained below, PRD-1 showed hydrophobic interaction in all the other soils with low organic carbon content. The following rough estimation implies a physical availability of organic carbon on the surface as (possible) hydrophobic sites. From Table 2, dry bulk density = 1.7 $\mathrm{g\,cm^{-3}}$, specific surface area = 0.8 $\mathrm{m^2 g^{-1}}$, and organic carbon content = 0.03 percent. Assuming approximately 0.03 percent of the surface area is covered with organic materials:

$$\textit{Organic surface area} = 1.7\frac{\mathrm{g}}{\mathrm{cm^3}}\times 0.8\frac{\mathrm{m^2}}{\mathrm{g}}\times 0.03\frac{1}{100}\frac{\mathrm{m^2}}{\mathrm{m^2}} = 4.08\times10^{-4}\frac{\mathrm{m^2}}{\mathrm{cm^3}} = 4.08\times10^{14}\frac{\mathrm{nm^2}}{\mathrm{cm^3}}$$

$$\textit{Cross sectional area of PRD1} = \frac{\pi}{4}62^2\text{nm}^2 = 3.0\times10^3\text{nm}^2$$

Hence, the number of surface sites of organic material physically available to PRD-1 is:

$$4.08\times10^{14}\frac{\text{nm}^2}{\text{cm}^3}\times(3.0\times10^3\frac{\text{nm}^2}{\text{site}})^{-1} = 1.36\times10^{11}\frac{\text{site}}{\text{cm}^3}$$

This number of sites available is far larger than the stock solution concentrations (about 10^5 pfu mL^{-1}). The deviation in the composition of the soil used from the one examined in the previous study can also explain this discrepancy.

The large attachment of PRD-1 in Cambridge soil at pH 7.0 implies that the hydrophobic interaction is dominant in this soil material. Again, the organic-carbon content of the soil is low (0.05 percent).

PRD-1 in Cape-Cod soil also showed strong hydrophobic interactions, though the organic carbon content is low (<0.01 percent). In this soil the attachment of PRD-1 was almost independent of pH. PRD-1 was attached more in Borden soil than in Cape-Cod soil (C/C_0 of the steady state at pH 7.0 was 1.14 vs. 0.3×10^{-3}). Since Borden soil has a higher clay-size fraction (0–15 vs. <1 percent), it can be postulated that PRD-1 was affected by double-layer repulsion forces more than in Cape-Cod soil. This is confirmed by the pH effects in Borden soil consistent with the DLVO theory. MS-2 in Cape-Cod soil was apparently conservative, even at low pH. Double-layer repulsion forces were dominant for MS-2 in this medium. However, *Bales et al.* [*1991*] reported the hydrophobic attachment of MS-2 to hydrophobic silica beads. Their results showed that C/C_0 at the attachment plateau in five percent hydrophobic beads dropped 10^{-4}-fold. Therefore, it is expected that hydrophobic interaction on MS-2 will prevail if the organic carbon content or other hydrophobic material increased.

P17 in silica beads showed hydrophobic interaction, since it was strongly attached at high pH. The pH effect was not evident in the results of this column study. Replication of the experiments is necessary to examine these effects. As suggested in Chapter 3, it is important to study the biological effects such as die-off, bacterial motility, etc..

Attachment of Bacillus in silica beads implies hydrophobic effects for the same reason. In fact, *Doyle et al.* [*1984*] showed the hydrophobicity of spores of Bacillus subtillis. They demonstrated the strong adherence of the spores to (hydrophobic) hexadecane. Regarding the elution by raising pH from 7 to 8, pH effects consistent with the DLVO theory are expected. Since the two experiments at pH 7.0 are inconsistent, it is necessary to repeat the experiments in order to identify the attachment-detachment interactions.

4.2 Conservative-Tracer Dispersion

In order to estimate Peclet numbers for the parameter estimation in the following sections, D's of NaCl in each medium were calculated. The results are presented in Table 4. Breakthrough curves for Borden soil and 0.5-mm silica beads were adopted from the tracer tests done prior to this study. For Cambridge and Cape-Cod soils, the breakthrough curves of the tracer tests conducted to estimate the effective pore volume before each virus experiment (see Section 2.1.3) were used. The D's were calculated from Peclet numbers (equation (12)) obtained by the equilibrium-model fits. Both attachment and detachment limbs were fitted. The D values are in the order of 10^{-4}. The data were plotted in Figure 11 as log (D/D_0) vs. log (ud/D_0), where D is the equilibrium-model dispersion coefficient (cm^2 s^{-1}), D_0 is the molecular-diffusion coefficient (cm^2 s^{-1}), u is the average interstitial velocity (cm s^{-1}), and d is the mean particle diameter of the medium (cm). The unique linear relation between D/D_0 and ud/D_0 was discussed by *Rose* [*1977*]. The molecular diffusion coefficient for NaCl at 25°C, the temperature at which the experiments were conducted, is 1.5×10^{-5} cm^2 s^{-1}. The mean particle diameters of the medium are 0.038, 0.103, 0.059, and 0.05 cm for Borden, Cambridge, and Cape-Cod soils and silica beads, respectively. The data of the MS-2 column experiments using the soil of Tanque Verde Wash in Arizona [*Bales et al., 1989*] were also plotted in the figure. The points for Borden soil, Cambridge soil, and 0.5-mm silica beads were close to the 1:1 line of log (D/D_0) = log (ud/D_0). This reduces to a simple relation between D, u, and d:

Table 4. Equilibrium-model fits to data (conservative tracer NaCl)

No.	Media	u 10^{-3} cm s^{-1}	P	ssq[a]	D cm^2 s^{-1}	ϕ g cm^{-3}	θ[b]
1[c]	Borden	0.47	237.6	0.032	2.93×10^{-5}	1.70	0.322
2[c]	Borden	1.04	272.0	0.035	5.66×10^{-5}	1.70	0.306
3[c]	Borden	2.65	317.0	0.064	1.24×10^{-4}	1.70	0.309
4[c]	Borden	3.50	102.2	0.179	5.07×10^{-4}	1.70	0.344
5[d]	Cambridge	2.07	93.7	0.021	3.27×10^{-4}	1.68	0.298
6[d]	Cambridge	3.24	71.3	0.010	6.73×10^{-4}	1.68	0.307
7[e]	Cape Cod	1.67	30.6	0.132	5.79×10^{-4}	1.70	0.345
8[e]	Cape Cod	2.95	31.3	0.105	9.98×10^{-4}	1.70	0.345
9[f]	Cape Cod	2.01	53.5	0.207	3.98×10^{-4}	1.68	0.356
10[f]	Cape Cod	2.37	53.3	0.119	4.72×10^{-4}	1.68	0.357
11[c]	Si (0.5-mm)	5.42	145.6	0.294	7.45×10^{-4}	1.72	0.461
12[c]	Si (0.5-mm)	6.95	343.8	0.088	4.04×10^{-4}	1.72	0.419
13[c]	Si (0.5-mm)	10.30	326.0	0.040	6.32×10^{-4}	1.72	0.432

[a] Sum of squared errors.

[b] Values of porosity were derived from the values of pore volume determined by curve fitting.

[c] Results from the NaCl tracer test conducted prior to this study.

[d] Results from the NaCl tracer test conducted to obtain an effective pore volume of the column for experiment 4 (see Section 2.1.3).

[e] Results from the NaCl tracer test conducted to obtain an effective pore volume of the column for experiment 6 (see Section 2.1.3).

[f] Results from the NaCl tracer test conducted to obtain an effective pore volume of the column for experiment 7 (see Section 2.1.3).

[g] R was fixed as a unity.

[h] The curve was fitted to both adsorption and desorption.

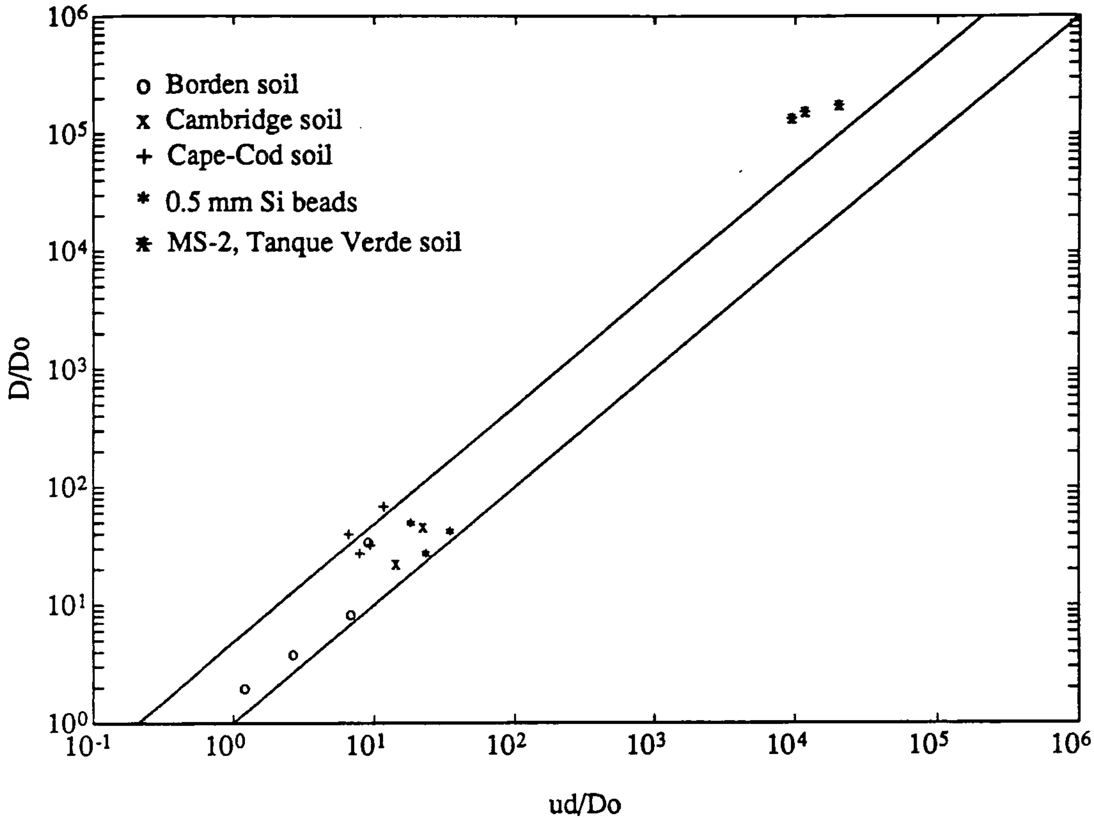

Figure 11. **Plot of log (D/D_0) vs. log (ud/D_0) for equilibrium-model fits of NaCl and MS-2 column experiments.**

$$D = ud \tag{28}$$

Since the points for Cape-Cod soil deviated from the points of the other media, a linear regression line was derived for this soil. The regression line is log (D/D_0) = 1.015 × log (ud/D_0)+ 0.6312 , r^2=0.38 (the upper line in Figure 11). This leads to the relation, given d = 0.059 cm:

$$D = 0.286u \tag{29}$$

Stocking [*1989*] found the following relation in her NaCl tests using silica beads of 45-90 µm in diameter:

$$D = 0.0303u + 1.92\times10^{-6} \; (r^2 = 0.99) \tag{30}$$

Calculation by equation (30) at $u = 2.5\times10^{-3}$ cm s^{-1} (average velocity of soil column experiments in this study) gives 7.77×10^{-5}. On the other hand, equations (28) and (29) give 9.5×10^{-5}, 2.58×10^{-4}, 7.15×10^{-4}, and 1.25×10^{-6} for Borden, Cambridge, and Cape-Cod soils and 0.5-mm silica beads, respectively. These values are 1.2, 3.4, 9.3, and 0.02-fold of those estimated by equation (30). The D's calculated by equations (28) and (29) will be used for the Peclet number in the parameter estimation for viruses and bacteria.

4.3 Equilibrium-Model Parameter Estimation

The C/C_0 of a breakthrough curve at steady-state attachment (plateau during attachment period) reaches one with the equilibrium model (no slow attachment-detachment site), since there is no apparent attachment-detachment during this period. The equilibrium model can adjust the shape of the breakthrough curve only by R and P. The value of R shifts the time for ascent of the attachment limb and P changes the slope of the attachment limb, but cannot lower the steady-state C/C_0 to less than one. In order to obtain a steady-state C/C_0 less than one, slow attachment sites (type-2 sites) need to be incorporated, which are in the first-order and two-site models. Most of the breakthrough curves in this study, except the ones of MS-2 in Cape-Cod soil, have steady-state C/C_0 less than one. Therefore, only the parameters for MS-2 in Cape-Cod soil were estimated with the equilibrium model.

Table 5 shows u, ϕ, and θ used for the derivation of K_p from R. The u of experiment 1 was not recorded but 1.99×10^{-3} cm s^{-1}, an average u of experiments 2 and 3, was used for the later analyses. The estimated values of experiment 1 should be only for reference. The results are shown in Table 6. Standard errors are presented for P and R. Attachment and detachment limbs of breakthrough curves were modeled separately because of poor performance of the fitting algorithm when modeling both limbs as a unit. Data were separated into the two limbs at the point where stock solution was switched to a phage-free (bacteria-free) buffer. R's were fixed for fitting the detachment limb and are not listed in the table, since R depends on the pulse value used. Therefore, K_p derived from R are not listed for the limb. R's ranged from 0.9 to 1.4. R can be less than one if there is colloid exclusion from a part of the pore volume. *Bales et al. [1989]* reported R values less than one from the soil column experiment of MS-2. The scattered data points also could cause this result. D's varied from 10^{-5} to 10^{-2}. However, the values of D, which were calculated using P, are not statistically significant, since P values have large standard errors. This is approximately in the same range as that of the conservative tracer (Table 4). The fitted curves are shown in Figure 12. Data points with C/C_0 over one cannot be fitted with this model. The curves represent the average value of the breakthrough.

4.4 First-Order-Model and Two-Site-Model Parameter Estimation

Model parameter values of the first-order model and two-site model were estimated for the breakthrough curves. D values calculated from P incorporate the effects of slow attachment, detachment, and dispersion. In order to separate the effects of slow attachment and detachment from that of dispersion, P was fixed for the later analyses. The P values were derived by the D/D_0 vs. ud/D_0 relation for salt tracer described in Section 4.2. It can be assumed that D values derived from these relations are close to the true values, since the points of MS-2 in Tanque-Verde soil are close to those derived lines. Molecular diffusion coefficients for each virus and bacteria were calculated by the Stokes-Einstein relation:

$$D_0 = \frac{\bar{k}\,T}{3\pi\mu d_p} \tag{31}$$

Table 5. Data for parameter estimation

Exp.	Column length(cm)	u 10^{-3}cm s^{-1}	ϕ g cm^{-3}	θ
1	14.8	–[a]	1.69	0.277
2	14.8	1.64	1.70	0.280
3	14.8	2.28	1.69	0.282
4	14.8	2.84	1.68	0.299
6	10.6	3.05	1.70	0.344
7	10.6	2.42	1.68	0.357
8	10.6	2.36	1.68	0.344
13	20.0	11.11	1.72	0.416
14	20.0	9.01	1.72	0.432
15	20.0	8.77	1.72	0.438
17	20.0	11.90	1.72	0.438

[a] Flow rate was not recorded; the arithmetic average of the values of u from experiments 2 and 3 was used as an estimate – 1.99×10^{-3} cm s^{-1}.

Table 6. Equilibrium-model fits to data

Exp.[a]		P	R	ssq[b]	K_p $cm^3 g^{-1}$	D $cm^2 s^{-1}$
6	attachment	31±84	0.9±0.2	2.2104	<0	1.1×10^{-3}
6	detachment	92±5000	–	0.0011	0.25	3.5×10^{-4}
7	attachment	5.5±4.8	1.4±0.2	0.2371	0.09	4.6×10^{-3}
7	detachment	2000±num[c]	–	0.3426	0.54	1.3×10^{-5}
8	attachment	39±46	0.9±0.1	0.2200	<0	6.4×10^{-4}
8	detachment	0.53±37	–	0.0501	<0	4.7×10^{-2}

[a] Attachment and detachment parts of breakthrough curves listed separately.

[b] Sum of squared errors.

[c] Larger than 9999.

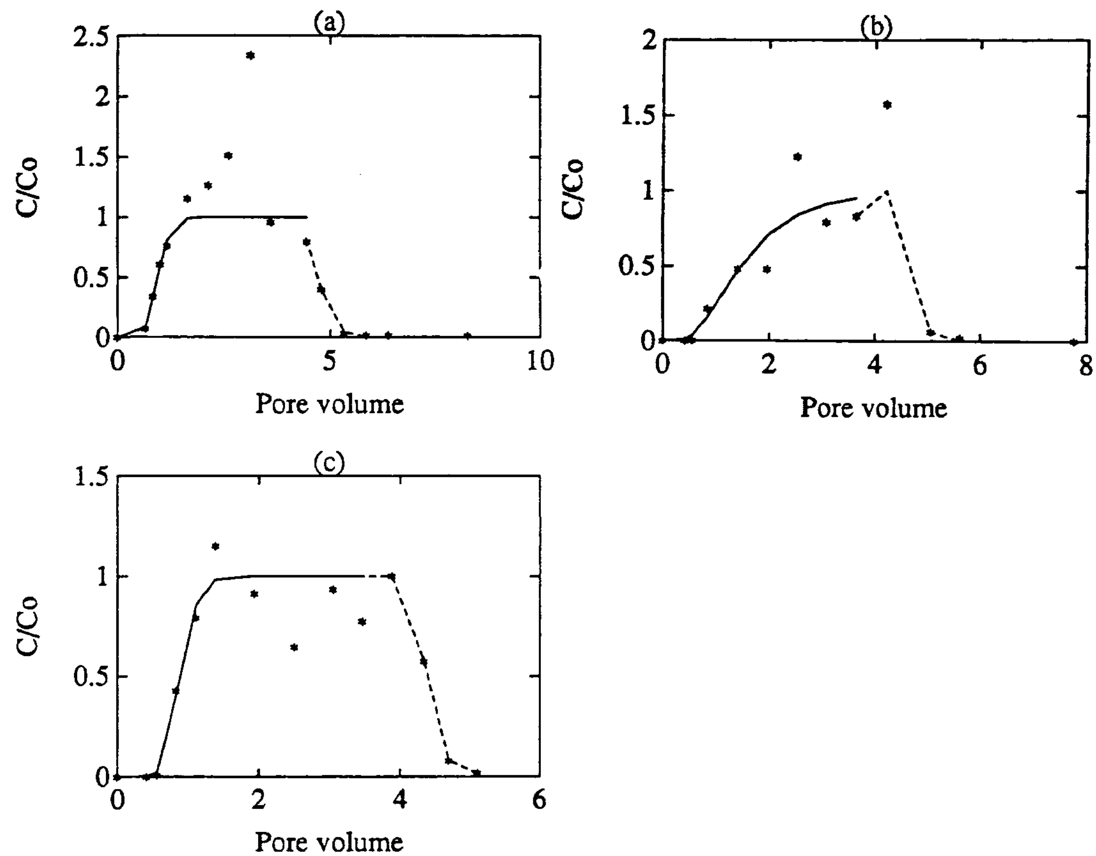

Figure 12. **Equilibrium-model fits to the breakthrough curve of MS-2 through Cape-Cod soil: a) experiment 6 at pH 5.7; b) experiment 7 at pH 5.7; c) experiment 8 at pH 7.0.**

where $\bar{k}$ is the Boltzman constant, T is the temperature, d_p is the virus or bacteria diameter, and μ is fluid viscosity. The following values were used: T = 280 K (7 °C); d_p = 6.2×10^{-6} cm (PRD-1), 2.6×10^{-6} cm (MS-2), 2.5×10^{-4} cm (P17 and Bacillus); and μ = 0.01428 g/cm s^{-1} (at 7 °C). From the calculated value, 389, 143, 37, and 400 were given to P of Borden soil, Cambridge soil, Cape-Cod soil, and silica beads, respectively.

Estimated parameter values of the first-order model are shown in Table 7 and those of the two-site model are in Table 8. R's were fixed for fitting the detachment limb and are not listed in the table, since R depends on the pulse value used. Therefore, K_p and k_2 derived from R are not listed for the limb. Fitted curves are presented in Figures 13 through 18. As a whole, the two models provided the same order of values. Since the β values estimated by the two-site model were all low (no type 1 site), the two-site model was basically the same as the first-order model. The calculations of the two-site model were less stable than the first-order model. The two-site model had more cases in which convergence criteria were not met and was forced to stop the iteration step (see Tables 7 and 8). The scattered data points and low C/C_0 values may decrease the stability. Also, converging many parameters may cause the calculation to be unstable. However, the values which did not converge were relatively stable at the end of calculation for both models. Exceptions are attachment of PRD-1 in experiment 7 for the first-order model and detachment of PRD-1 in experiment 1 for the two-site model: they diverged. There are many R's and ω's that have standard errors larger than their own values. In the subsequent analyses, these values (R and ω) and the other parameters (K_p, k_1, and k_2) which used them for calculation will be disregarded.

Fitted curves for PRD-1 in Borden soil are shown in Figure 13. Attachment limbs were well fitted in both models. In the detachment-limb fit, the two-site model shows less stable results. Calculation diverged in the detachment fit line of the two-site model for experiment 1 (b). In the two-site model fitting, three cases did not converge and one case diverged as opposed to only one non-converged case in the first-order model. Parameter values are approximately in the same range in both models. R was about 200 for this column. The large R value (3 att) of the two-site model is not reliable relative to the others, since the

Table 7. First-order-model fits to data

Exp.[a]	R	ω	ssq[b]	K_p $cm^3 g^{-1}$	k_1 s^{-1}	k_2 s^{-1}
1 att	230±90	10.3±0.2	3.12×10^{-9}	38	1.4×10^{-3}	6.0×10^{-6}
1 det[d]	–	1.2±30	1.14×10^{-8}	–	1.7×10^{-4}	–
2 att	210±140	9.8±0.3	6.37×10^{-9}	34	1.1×10^{-3}	5.3×10^{-6}
2 det	–	9.6±0.3	8.87×10^{-9}	–	1.1×10^{-3}	–
3 att	180±80	8.8±0.3	1.09×10^{-7}	30	1.4×10^{-3}	7.5×10^{-6}
3 det	–	7.7±0.3	1.83×10^{-7}	–	1.2×10^{-3}	–
4 att	–	–	–	–	–	–
4 det	–	9.3±0.1	1.75×10^{-9}	–	1.8×10^{-3}	–
6 att PRD1	280±150	9.2±0.3	2.39×10^{-7}	56	2.7×10^{-3}	9.7×10^{-6}
6 det PRD1	–	1.8±25	1.73×10^{-8}	–	5.2×10^{-4}	–
6 att MS2[d]	0.9±0.1	0.001±4	0.0970	–	3.2×10^{-7}	–
6 det MS2	–	0.2±0.01	6.05×10^{-5}	–	6.0×10^{-5}	–
7 att PRD1[c]	–	–	–	–	–	–
7 det PRD1[d]	–	1.5±72	2.34×10^{-7}	–	3.3×10^{-4}	–
7 att MS2	1.7±0.3	1.4±1.5	0.2480	0.14	3.2×10^{-4}	4.8×10^{-4}
7 det MS2[d]	–	0.004±0.008	0.3823	–	9.1×10^{-7}	–
8 att PRD1	440±230	9.9±0.2	9.36×10^{-9}	89	2.2×10^{-3}	5.1×10^{-6}
8 det PRD1[d]	–	0.9±45	1.15×10^{-7}	–	2.1×10^{-4}	–
8 att MS2[d]	0.9±0.3	0.2±1800	0.2201	–	4.7×10^{-5}	–
8 det MS2	–	0.1±0.05	0.0283	–	2.2×10^{-5}	–
13 att	50±23	2.6±0.2	0.0027	12	1.4×10^{-3}	3.0×10^{-5}
13 det	–	2.5±0.4	0.0069	–	1.4×10^{-3}	–
14 att	12±9	1.1±0.1	0.0218	3.0	5.0×10^{-4}	4.4×10^{-5}
14 det	–	1.0±0.03	0.0007	–	4.4×10^{-4}	–
15 att[c]	–	–	–	–	–	–
15 det	–	1.7± 0.1	0.0008	–	7.3×10^{-4}	–
17 att	1.0±0.5	0.004±9.3	0.4314	0.0	2.4×10^{-6}	–
17 det	–	0.4±0.1	0.0110	–	2.6×10^{-4}	–

[a] Attachment (att) and detachment (det) parts of breakthrough curves listed separately.

[b] Sum of squared errors.

[c] Calculation diverged.

[d] Convergence criteria for parameter estimation were not met.

Table 8. Two-site-model fits to data

Exp.[a]	R	β	ω	ssq[b]	K_p $cm^3 g^{-1}$	k_1 s^{-1}	k_2 s^{-1}
1 att	290±150	0.0038±0.0018	10.18±0.22	2.97×10^{-9}	48	1.4×10^{-3}	4.7×10^{-6}
1 det[c]	–	–	–	–	–	–	–
2 att[d]	200±85	0.0049±0.0033	9.66±0.31	6.82×10^{-9}	33	1.1×10^{-3}	5.2×10^{-6}
2 det[d]	–	0.0045±0.0243	1.50±84	2.73×10^{-8}	–	1.7×10^{-4}	–
3 att[d]	720±800	0.0021±0.0024	8.14±0.17	5.54×10^{-8}	120	1.3×10^{-3}	1.8×10^{-6}
3 det	–	0.0020±0.0050	7.73±0.38	1.83×10^{-7}	–	1.2×10^{-3}	–
4 att[d]	–	–	–	–	–	–	–
4 det	–	0.4015±0.0074	0.89±0.28	2.43×10^{-9}	–	1.7×10^{-4}	–
6 PRD1 att	390±350	0.0030±0.0025	8.99±0.40	2.22×10^{-7}	79	2.6×10^{-3}	6.6×10^{-6}
6 PRD1 det[d]	–	$<10^{-5}$±2.2278	9.17±28	0.3444	–	2.6×10^{-3}	–
6 MS2 att[d]	8.4±0	0.0951±$<10^{-4}$	$<10^{-5}$±0.20	2.3637	1.5	–	–
6 MS2 det	–	0.0894±0.0041	0.23±0.004	1.90×10^{-5}	–	6.6×10^{-5}	–
7 PRD1 att[d]	5300±$>10^4$	0.0002±0.0021	9.23±0.32	4.20×10^{-8}	1100	2.1×10^{-3}	4.0×10^{-7}
7 PRD1 det[d]	–	0.0002±0.003	9.08±0.34	1.84×10^{-8}	–	2.1×10^{-3}	–
7 MS2 att	1.6±0.3	0.4231±0.6383	2.80±7.55	0.2354	0.13	6.4×10^{-4}	2.8×10^{-4}
7 MS2 det[d]	–	$<10^{-5}$±100	9.44±$>10^4$	3.1996	–	2.2×10^{-3}	–
8 PRD1 att	840±900	0.0014±0.0014	9.73±0.17	6.82×10^{-9}	170	2.2×10^{-3}	2.6×10^{-6}
8 PRD1 det	–	0.0052±0.0017	9.04±1.56	4.18×10^{-8}	–	2.0×10^{-3}	–
8 MS2 att[d]	2.2±26	0.3775±4.52	0.09±0.18	0.1368	0.25	2.0×10^{-5}	6.5×10^{-6}
8 MS2 det	–	0.0083±0.0042	0.10±0.05	0.0267	–	2.2×10^{-5}	–
13 att	48±9	0.0174±0.0031	2.63±0.07	0.0004	11	1.5×10^{-3}	3.0×10^{-5}
13 det	–	0.0707±0.0209	2.33±0.17	0.0023	–	1.3×10^{-3}	–
14 att	12±5	0.0747±0.0324	1.13±0.09	0.0070	2.7	5.1×10^{-4}	4.0×10^{-5}
14 det	–	0.0357±0.0201	0.97±0.03	0.0007	–	4.4×10^{-4}	–
15 att[d]	620±3900	0.0014±0.0084	1.63±0.03	0.0004	160	7.2×10^{-4}	1.2×10^{-6}
15 det	–	0.0257±0.0080	1.62±0.06	0.0003	–	7.1×10^{-4}	–
17 att[d]	280±$>10^4$	0.0033±3	0.19±0.17	0.1563	72	1.1×10^{-4}	4.0×10^{-7}
17 det	–	0.0167±0.0641	0.42±0.10	0.0139	–	2.5×10^{-4}	–

[a] Attachment (att) and detachment (det) parts of breakthrough curves listed separately.

[b] Sum of squared errors.

[c] Calculation diverged.

[d] Convergence criteria for parameter estimation were not met.

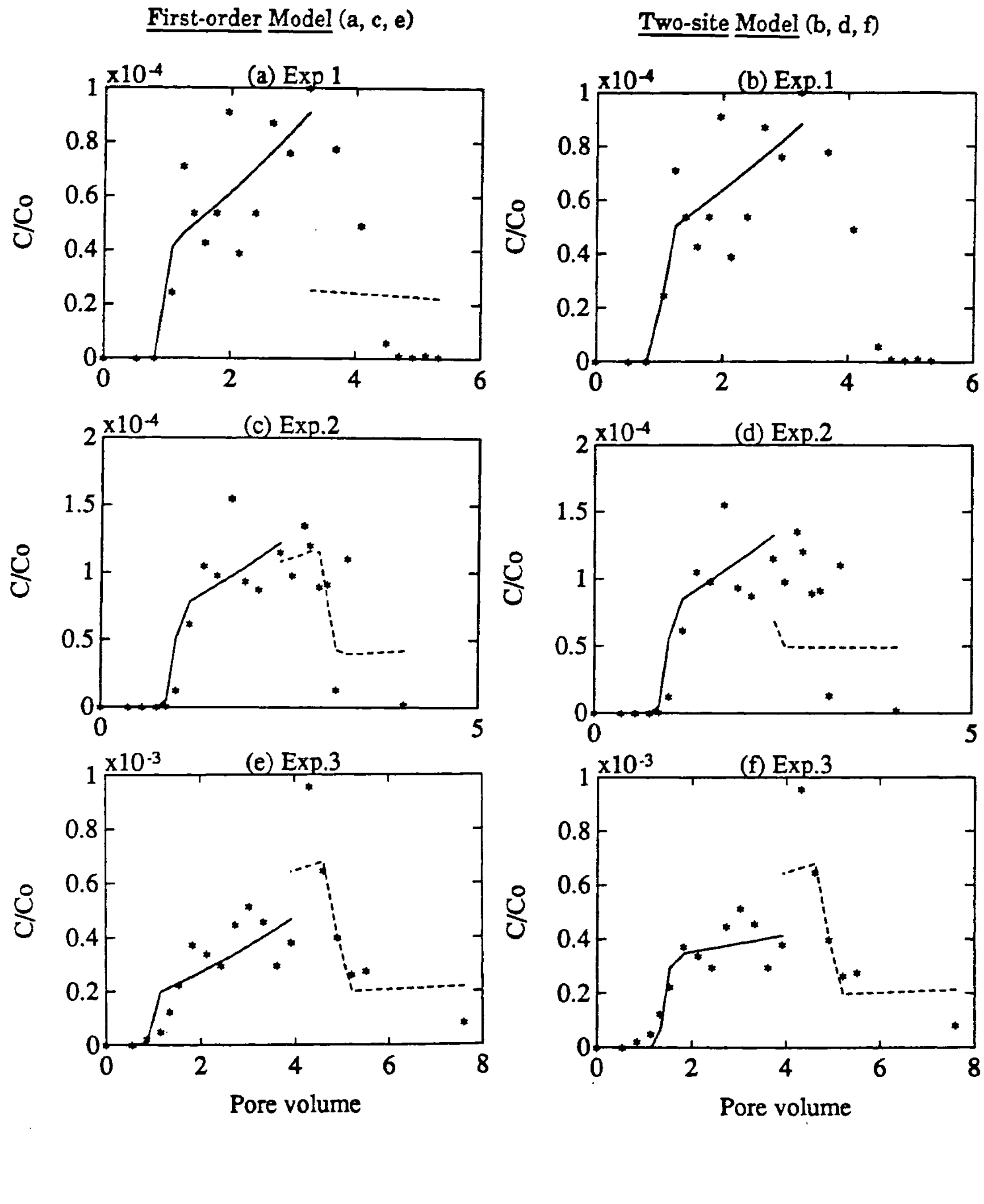

Figure 13. First-order and two-site model fits to the breakthrough curves of PRD-1 through Borden soil: a) First-order model fit to experiment 1; b) Two-site model fit to experiment 1; c) First-order model fit to experiment 2; d) Two-site model fit to experiment 2; e) First-order model fit to experiment 3; f) Two-site model fit to experiment 3.

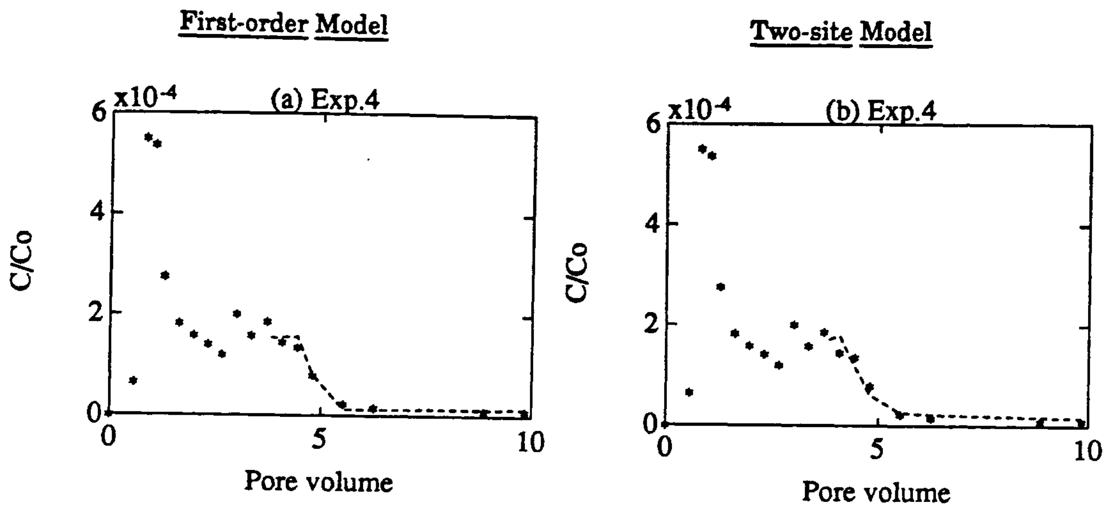

Figure 14. First-order and two-site model fits to the breakthrough curves of PRD-1 through Cambridge soil: a) First-order model fit to experiment 4; b) Two-site model fit to experiment 4.

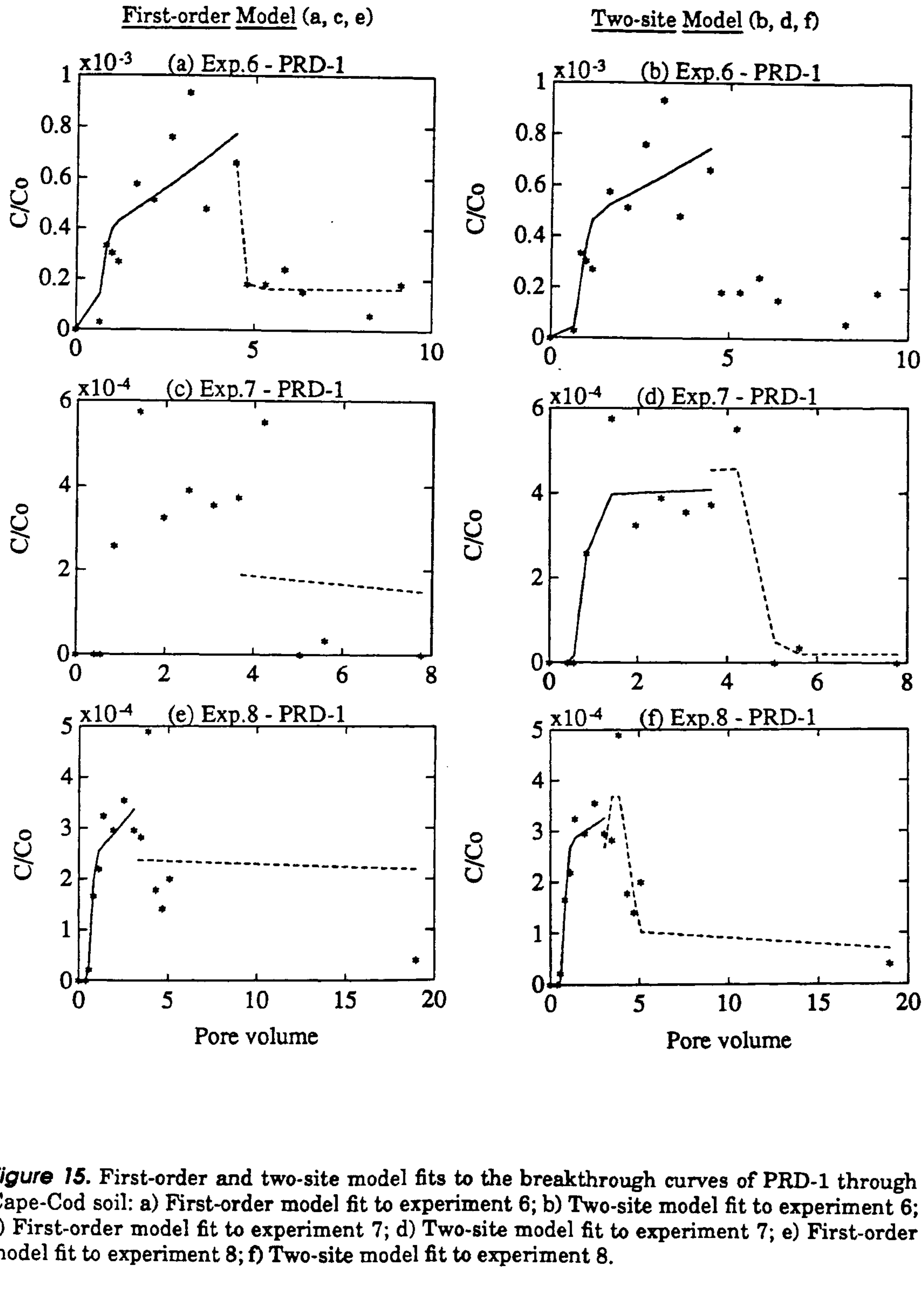

Figure 15. First-order and two-site model fits to the breakthrough curves of PRD-1 through Cape-Cod soil: a) First-order model fit to experiment 6; b) Two-site model fit to experiment 6; c) First-order model fit to experiment 7; d) Two-site model fit to experiment 7; e) First-order model fit to experiment 8; f) Two-site model fit to experiment 8.

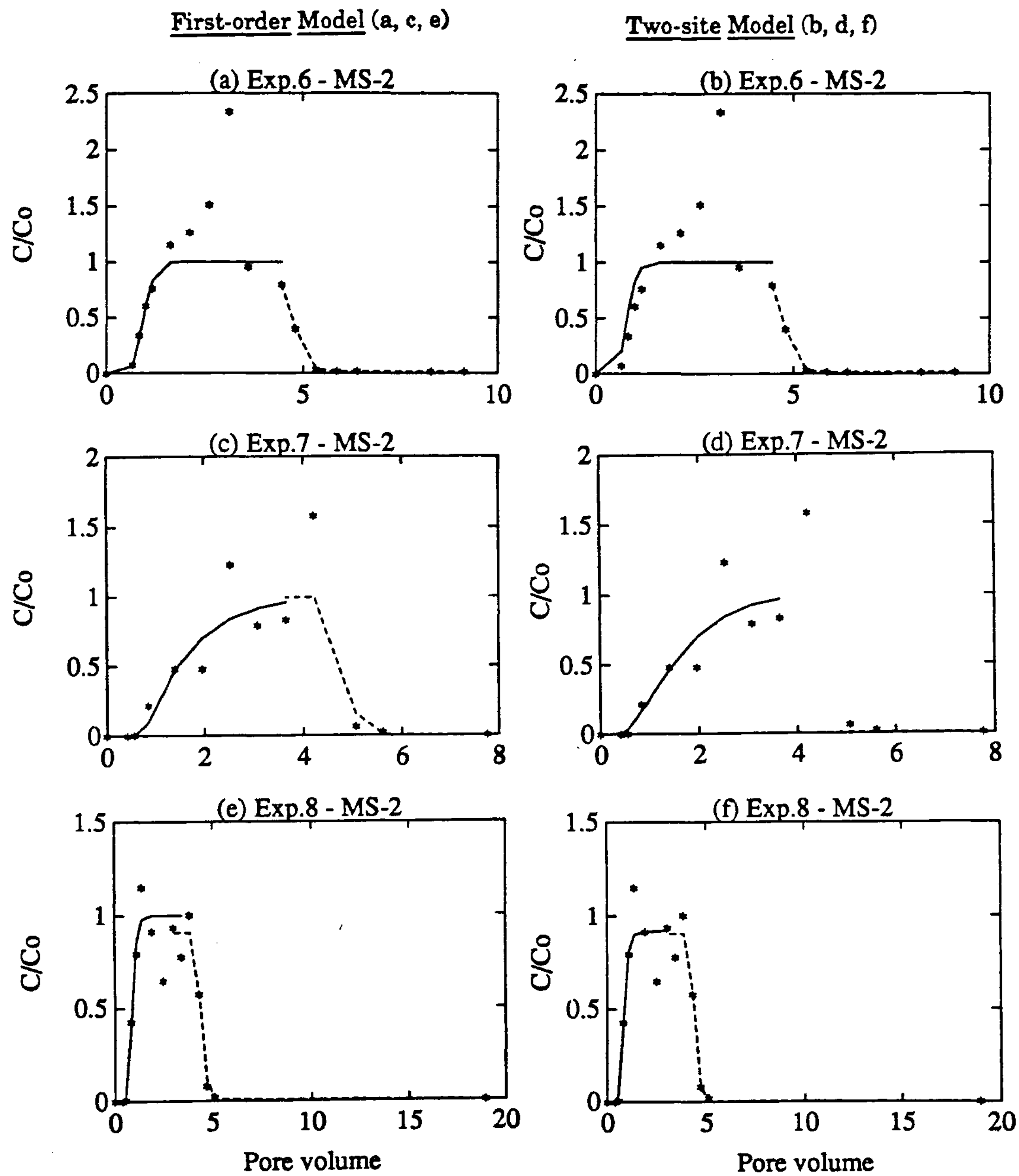

Figure 16. First-order and two-site model fits to the breakthrough curves of MS-2 through Cape-Cod soil: a) First-order model fit to experiment 6; b) Two-site model fit to experiment 6; c) First-order model fit to experiment 7; d) Two-site model fit to experiment 7; e) First-order model fit to experiment 8; f) Two-site model fit to experiment 8.

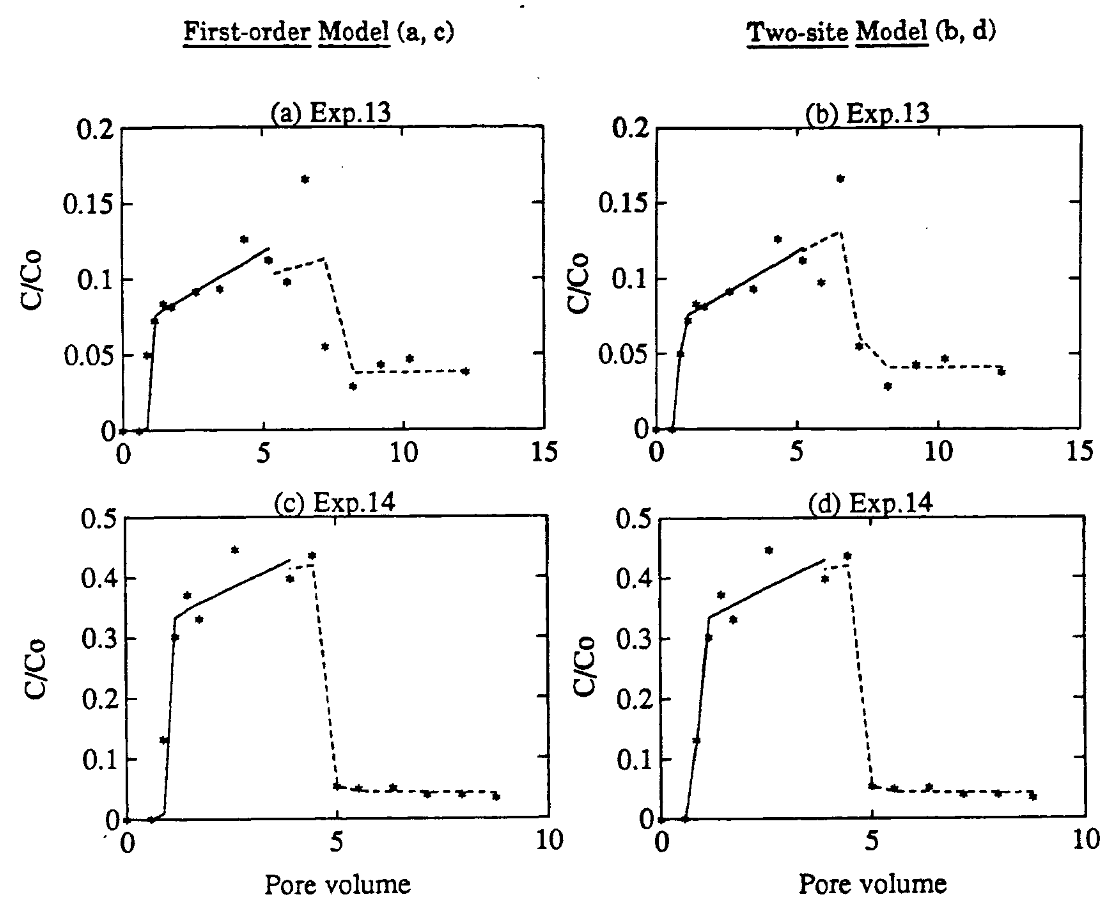

Figure 17. First-order and two-site model fits to the breakthrough curves of P 17 through 0.5-mm silica beads: a) First-order model fit to experiment 13; b) Two-site model fit to experiment 13; c) First-order model fit to experiment 14; d) Two-site model fit to experiment 14.

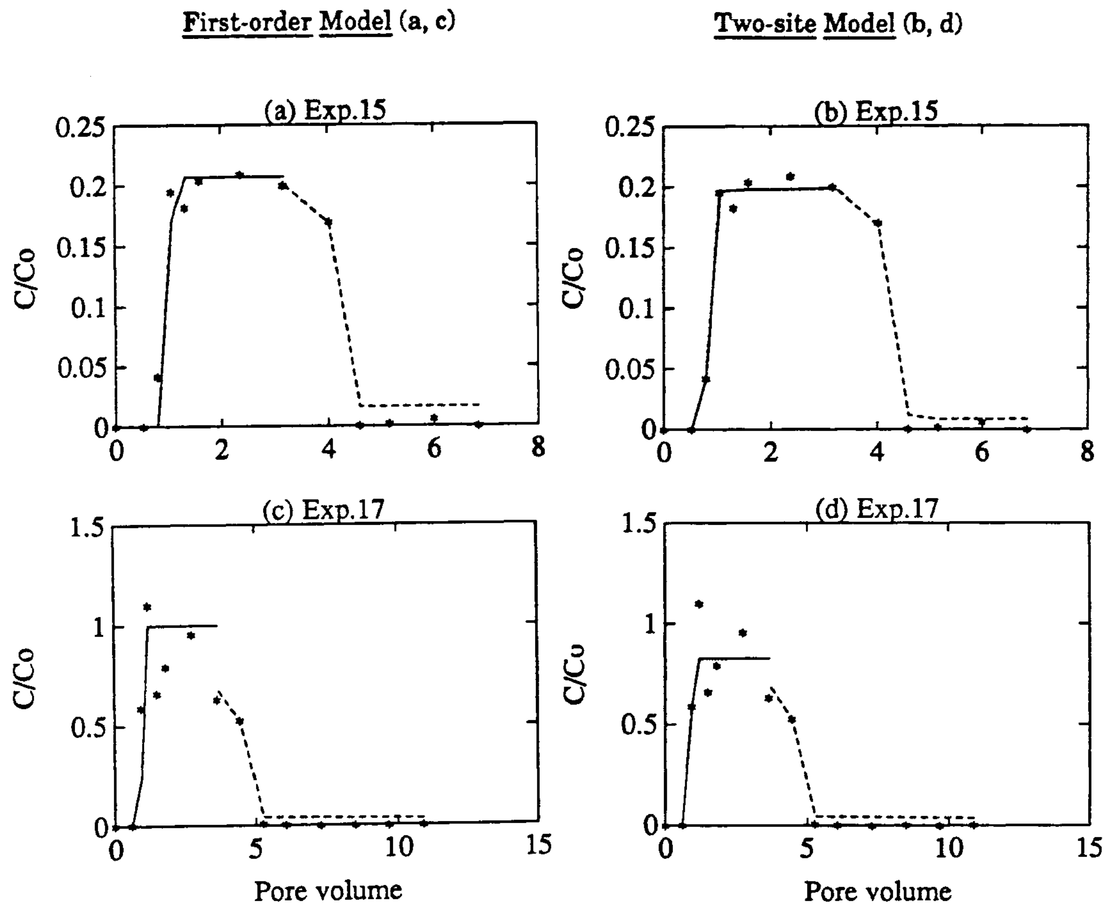

Figure 18. First-order and two-site model fits to the breakthrough curves of Bacillus through 0.5-mm silica beads: a) First-order model fit to experiment 15; b) Two-site model fit to experiment 15; c) First-order model fit to experiment 17; d) Two-site model fit to experiment 17.

standard error is too large (larger than its value). R values show a weak trend of decrease with higher pH. At higher pH, PRD-1 was less adsorbed and R would decrease. The low values of ω indicate non-equilibrium conditions (see equation (13)). Ignoring the values derived from the ω or R with a large error range, k_1's are $1.1–1.4\times10^{-3}$ s^{-1} and k_2's are $4.7–7.5\times10^{-6}$ s^{-1}: attachment is 3 orders of magnitude faster than detachment. There is no significant difference among these values at different pH's. The low value of β indicates type-1 (fast) sites contribute little to the total attachment. K_p values are 30 - 50 cm^3g^{-1}. This is consistent with the value *Hinkle* [*1990*] reported (41 - 520 cm^3g^{-1}) for PRD-1 in silica beads. Since his pH of the buffer was lower (5.5 vs. 6.5 in experiment 1), more PRD-1 would be attached (consistent with the DLVO theory). This is supported by the increasing K_p with lower pH (30 cm^3g^{-1} at pH 7.6, 34 cm^3g^{-1} at pH 7.0, and 38 cm^3g^{-1} at pH 6.5 by the first-order model).

Fitted curves for PRD-1 in Cambridge soil are shown in Figure 14. The attachment limb was not fitted, since it was affected by a misfeeding of stock solution. The detachment limb was fitted well. The low ω suggests non-equilibrium conditions and the low β value implies that a small fraction of the surface consisted of type-1 (fast) sites. The values of k_1 are one order of magnitude different between the two models. More data are necessary to obtain reliable values.

Fitted curves for PRD-1 in Cape-Cod soil are shown in Figure 15. The calculations were unstable in both models. The calculation for the attachment limb by the first-order model in experiment 7 (c) diverged. The detachment line for experiment 6 of the two-site model in experiment 6 (b) was beyond 1×10^{-3}. All R values by the two-site model have too large a standard error. R's are larger than those in Borden soil (276–436 vs. 182–232) according to the first-order model. Again, low β and ω imply few type-1 sites and thus non-equilibrium conditions. Due to the large standard error value, reliable K_p's were not obtained from the two-site model, but the values from the first-order model (56–89 cm^3g^{-1}) are consistent with those of *Hinkle* [*1990*]. Relatively reliable k_1 values are $2.0–2.7\times10^{-3}$ s^{-1} by both models.

The k_2's are on the order of 10^{-6} by the first-order model, suggesting that k_2 is about 3 orders of magnitude slower than k_1.

Fitted curves for MS-2 in Cape-Cod soil are shown in Figure 16. The calculations were unstable in both models. Both models did not converge in three cases out of six. The detachment curve of the two-site model in experiment 7 (Figure 16d) lies close to the base line. The fitted curves also demonstrated the unstable results for the detachment limb by the two-site model. R values of the first-order model (0.9–1.7) are similar to those of the equilibrium model, but the two-site model gave slightly larger values (1.6–8.4). Regarding the conservative behavior of MS-2 in this soil, an R value close to one is more reasonable. K_p's were very small: 0.13-1.5 $cm^3 g^{-1}$. This value range is close to that reported by *Stocking* [*1989*]. Her K_p of MS-2 in silica beads was 0.37–0.6 $cm^3 g^{-1}$. The values of β and ω are low. The k_1's are 2.2 – 6.6×10^{-5} s^{-1}; k_2 has no reliable estimate.

Fitted curves for P17 in 0.5-mm silica beads are shown in Figure 17. Apparently curve fitting is stable for P17 transport in silica beads. The two-site model followed the detachment limb data of experiment 13 slightly better than the first-order model, but both models fitted relatively well. All the calculations converged and the estimated values for each parameter are approximately the same in both models. However, R values have relatively large standard error. R's are 50 in experiment 13 at pH 7.0 and 12 in experiment 14 at pH 5.5. As in the previous cases, ω and β values are all low. K_p's are approximately 12 $cm^3 g^{-1}$ at pH 7.0 and 3 $cm^3 g^{-1}$ at pH 5.5, which is contrary to the DLVO theory. Estimated k_1's are 1.3 – 1.5×10^{-3} s^{-1} at pH 7.0 and 4.4 – 5.1×10^{-4} s^{-1} at pH 5.5. The values of k_2 are 3.0×10^{-5} s^{-1} at pH 7.0 and 4.0 – 4.4×10^{-5} s^{-1}. There is no significant difference between the two pH's. However, as suggested in Section 3.2.4, k_2 at pH 7.0 is expected to increase to reach equilibrium. The values of k_1 are about 3-fold larger at higher pH, which suggests a slightly steeper attachment limb at higher pH. The values of k_2 are lower than k_1: about 2 orders of magnitude lower in pH 7.0 and one order of magnitude lower in pH 5.5. At steady state, this is consistent with the relation of K_p's at pH 7.0 and 5.5. Equation (3) at steady state becomes $S_2 = \frac{\theta k_1}{\phi k_2} C$. Since (k_1/k_2) at pH 7.0 is larger than (k_1/k_2) at pH 5.5, K_p at pH 7.0 is larger than K_p at pH 5.5. This is supported by the fact that P17 was more strongly attached at pH 7.0 than at 5.5.

Fitted curves for Bacillus in 0.5-mm silica beads are shown in Figure 18. There is no clear difference of fitted curves between the two models. R's of the two-site model have large standard errors and are not appropriate for analysis; subsequently, K_p and k_2 calculated using R are not reliable. For R, 1.0 of experiment 17 obtained by the first-order model is relatively reasonable judging from the attachment limb similar to the conservative break-through curve. The values of ω and β are also low. The values of k_1 are 7.1 – 7.3$\times10^{-4}$ s^{-1} in experiment 15 and 2.5 – 2.6$\times10^{-4}$ s^{-1} in experiment 17. The only k_2 value which can be valid is 4.4$\times10^{-4}$ s^{-1} in experiment 15. As discussed in the previous chapter, these values cannot be validated, since the two experiment were not consistent.

4.5 Sticking Efficiency

A filtration model using single-collector removal efficiency η and sticking efficiency α was successfully applied to a modeling of bacterial movement through Cape-Code soil by *Harvey et al.* [*1991*]. It is important to note that η represents physical processes depending only on the physical properties of collectors, suspended particles, and fluid. These are relatively easy to measure and the mechanisms of removal are well-known as described in equations (22), (23), and (24). On the other hand, α represents chemical interaction between the surfaces. Sticking efficiency α depends on the chemical conditions, and there are uncertainties in its evaluation. Therefore, the chemical conditions for the values obtained in this study, as well as reported values, should be well specified.

Estimated removal efficiencies for diffusion (η_d), interception (η_i), gravity (η_g), total (η), and α's for each experiment are shown in Table 9. The following values were used: $\bar{k}$ = 1.4×10^{-16} g cm^2 s^{-2} K^{-1}; T = 280 K; and μ = 0.014 g cm^{-1} s^{-1}(7 °C). The viral and bacterial diameters d_p are 6.2×10^{-6} cm (PRD-1), 2.6×10^{-6} cm (MS-2), and 2.5×10^{-4} cm (P17 and Bacillus). The diameters of media are 0.038 cm (Borden soil), 0.103 cm (Cambridge soil), 0.059 cm (Cape-Cod soil), and 0.05 cm (silica beads). The η_g was calculated with 1.000 g cm^{-3}

Table 9. Estimates of α from breakthrough curves

Exp.	pH	$\log C/C_0$	η_d[a]	η_i[b]	η_g[c]	η[d]	η_d/η (percent)	α[e]
1	6.5	-4.2	3.0×10^{-2}	4.0×10^{-8}	7.5×10^{-10}	3.0×10^{-2}	100	0.77
2	7.0	-4.0	3.4×10^{-2}	4.0×10^{-8}	9.1×10^{-10}	3.4×10^{-2}	100	0.65
3	7.6	-3.3	2.7×10^{-2}	4.0×10^{-8}	6.6×10^{-10}	2.7×10^{-2}	100	0.67
4	7.0	-3.7	1.2×10^{-2}	5.4×10^{-9}	5.3×10^{-10}	1.2×10^{-2}	100	4.69
6 PRD1	5.7	-3.2	1.7×10^{-2}	1.7×10^{-8}	4.9×10^{-10}	1.7×10^{-2}	100	2.51
6 MS2	5.7	0.2	3.0×10^{-2}	2.9×10^{-9}	8.6×10^{-11}	3.0×10^{-2}	100	-0.09
7 PRD1	5.7	-3.4	1.9×10^{-2}	1.7×10^{-8}	6.2×10^{-10}	1.9×10^{-2}	100	2.33
7 MS2	5.7	0.0	3.5×10^{-2}	2.9×10^{-9}	1.1×10^{-10}	3.5×10^{-2}	100	0.00
8 PRD1	7.0	-3.5	2.0×10^{-2}	1.7×10^{-8}	6.3×10^{-10}	2.0×10^{-2}	100	2.31
8 MS2	7.0	-0.1	3.5×10^{-2}	2.9×10^{-9}	1.1×10^{-10}	3.5×10^{-2}	100	0.04
13	7.0	-1.0	6.7×10^{-4}	3.8×10^{-5}	2.2×10^{-7}	7.0×10^{-4}	95	9.33
14	5.5	-0.4	7.7×10^{-4}	3.8×10^{-5}	2.7×10^{-7}	8.0×10^{-4}	95	3.36
15	7.0	-0.7	7.8×10^{-4}	3.8×10^{-5}	2.8×10^{-7}	8.2×10^{-4}	95	5.84
17	7.0	-0.1	6.4×10^{-4}	3.8×10^{-5}	2.0×10^{-7}	6.8×10^{-4}	94	1.01

[a] Removal efficiency for diffusion.

[b] Removal efficiency for interception.

[c] Removal efficiency for gravity.

[d] $\eta_d + \eta_i + \eta_g$.

[e] Estimated using η.

as the density of water and 1.001 $g\,cm^{-3}$ as the density of bacteria. The average interstitial velocities are listed in Table 5. The density of bacteria was not measured, but *Harvey et al.* [*1991*] assumed 1.001 $g\,cm^{-3}$ based on their slow sinking velocities. The same density was assumed in this study judging from their slow sinking velocities observed in microelectrophoresis work. According to the results in Table 9, η's are mostly determined by diffusion in all cases. For viruses in soil, η_i and η_g are 6–8 orders of magnitude smaller than η_d. For bacteria in silica beads, diameters of bacteria are about two orders of magnitude larger than the viruses. As a result, the denominator of equation (22) is larger and η_d's are smaller than the ones for viruses (Brownian diffusion is less significant for larger suspended particles). The η_i and η_g become about three orders of magnitude larger than those for viruses, due to a larger diameter of bacteria (equations (23) and (24)). However, they are still determined by η_d (95 percent of η).

Harvey et al. [*1991*] reported 5×10^{-3}–1×10^{-2} of α's for bacteria (0.2–1.4μm) in the Cape-Cod field site. These α values are about two orders of magnitude lower than the ones of the bacteria column experiments in this study. Regarding equations (22) through (27), there are two physical factors which have the largest differences in magnitude between the analyses. One is flow velocity (u) and the other is the distance from inlet to outlet (L). First, the u value in this study (approximately 1×10^{-2} $cm\,s^{-1}$) was about 26-fold faster than that of *Harvey et al.* [*1991*] (vs. 0.33 $m\,dy^{-1} = 3.82\times10^{-4}$ $cm\,s^{-1}$), resulting in one order of magnitude smaller η_d's (equation (22)) than their values. Brownian diffusion is inversely related to u. Since laboratory column experiments tend to have higher velocities than field experiments, this lower diffusion effect should be recognized for the interpretation of column-experiment results. Secondly, the column length was only 20 cm, while the distance from the injection well to the monitoring well was 6.8 m (about 34-fold longer). The C/C_0 decreased to 0.1–0.8 over 20 cm in the column and to 0.1–0.04 over 6.8 m in the field. The retention of bacteria was much stronger in the silica-bead column than in the Cape-Cod field site. Equation (27) indicates that the smaller η and L in the denominator make larger α's. There are many factors which made this large difference in α's. Hydrophobicity of their bacteria might be lower than that of the column experiments, while soil from the Cape-Cod site appears to have relatively large hydrophobicity (see Section 3.2.3). Also, *Harvey et al. [1991]* point out the uncertainties due to bacterial motility, chemotaxis (movement in response to chemical gradients), buoyant densities, and microbial and grain size morphology. These may have affected the chemical attachment.

5. CONCLUSIONS

The results of PRD-1 transport through several kinds of soil columns showed strong hydrophobic attachments to soil surfaces. Although a large amount of phage was attached to the soils at high pH, the attachment was relatively insensitive to pH change. This suggests that the magnitude of hydrophobic interaction far exceeds the double-layer repulsion for this virus in these media. On the other hand, MS-2 in Cape-Cod soil showed conservative behavior. Since PRD-1 with lipid on its surface is relatively more hydrophobic than MS-2, these results were expected. Bacteria in silica beads also showed hydrophobic behavior. However, the results are not consistent and need to be replicated to be confirmed. Bacteria experiments indicated biological effects such as die-off. Surface complexity of bacteria also increases the difficulties in characterizing bacterial behavior. The study of surface characterization of virus, bacteria, and soil will contribute to the understanding of microbial attachment to soil.

The model parameter estimation by the first-order and two-site models suggests that both models can provide approximately the same values due to the small type-1 (fast) sites in these media. However, the calculations of the two-site model were less stable with incomplete convergence or divergence. The scattered data points, low C / C_0, and convergence of many parameters may cause this problem. Well-controlled assay may give stable data points for the solution of this problem. Estimated ω values were low for all cases, indicating non-equilibrium conditions. The attachment rate constants k_1 were on the order of 10^{-5} to 10^{-3} s^{-1}, and the detachment rate constants k_2 were 10^{-6} to 10^{-5} s^{-1}. Time scales for equilibration are thus on the order of one to ten days. For a typical groundwater velocity of about one m dy^{-1}, this time scale indicates that microbial movement could be confined by retention in a small area, within a range of ten meters from the source, provided K_p is large enough to capture viruses or bacteria. This time scale also suggests that once soil is loaded with microorganisms, it will continue to release them on the order of ten days. Typical groundwater pH's would enhance transport of viruses or bacteria rather than retention. However, acidic-contaminated water or rain water would result in a large amount of attachment, creating a later source of contamination. Hydrophobic interaction would be an important attachment process for viruses or bacteria in natural groundwater systems, even with low organic-carbon content (less than one percent), as observed in the soil-column experiments. In the column experiments, virus-particle interaction was predictable as a colloid particle by the DLVO theory and hydrophobic interaction. For both virus and bacteria, hydrophobic forces appeared to be dominant, and viruses showed stronger attachment (higher R, K_p) and slower detachment (lower k_2) than bacteria. This indicates that virus contamination would spread slower but need longer time to clean, compared to bacteria. However, this comparison may be affected by the differences of the media, including surface components and geometry.

From these soil column studies, viruses or bacteria can attach to soil surfaces and the soil will be a source of phage for a considerable time. Therefore, the assessment of virus and bacteria contamination in the subsurface environment must take this interaction into account. Further study of quantitative information and modeling efforts will contribute to solution of microbial environmental problems. Moreover, the discrepancies between laboratory column studies and field results have been reported. For the solution of this problem, well-designed field studies are necessary as well as column studies.

APPENDIX A

Results of Virus and Bacteria Column Experiments

Experiment 1

PRD-1
Borden soil
Column length = 14.8 cm
Average interstitial velocity was not recorded
Dry bulk density = 1.69 $g\,cm^{-3}$
Porosity = 0.277
Input pH = 6.5 (No.1 - 13, PRD-1)
Input pH = 6.5 (No.14 - 23, phage-free)
Input pH = 7.0 (No.24 - 39, beef extract)
Titer = 8.41 pfu mL^{-1}

No.	PV	C/Co	log C pfu/cm3
1	0.00	0.000E+00	0.00
2	0.53	0.000E+00	0.00
3	0.80	0.000E+00	0.00
4	1.07	0.245E-04	3.80
5	1.25	0.708E-04	4.26
6	1.42	0.537E-04	4.14
7	1.60	0.427E-04	4.04
8	1.78	0.537E-04	4.14
9	1.96	0.912E-04	4.37
10	2.14	0.389E-04	4.00
11	2.40	0.537E-04	4.14
12	2.67	0.871E-04	4.35
13	2.94	0.759E-04	4.29
14	3.25	0.100E-03	4.41
15	3.67	0.776E-04	4.30
16	4.09	0.490E-04	4.10
17	4.50	0.575E-05	3.17
18	4.71	0.871E-06	2.35
19	4.92	0.617E-06	2.20
20	5.13	0.112E-05	2.46
21	5.34	0.617E-06	2.20
22	5.54	0.741E-05	3.28
23	5.75	0.724E-06	2.27
24	14.09	0.000E+00	0.00
25	14.61	0.000E+00	0.00
26	14.87	0.155E-06	1.60
27	15.13	0.955E-04	4.39
28	15.31	0.457E+01	9.07
29	15.48	0.138E+01	8.55
30	15.65	0.219E+00	7.75
31	15.83	0.182E+00	7.67
32	16.00	0.603E-01	7.19
33	16.17	0.457E-01	7.07
34	16.43	0.316E-01	6.91
35	16.69	0.331E-01	6.93
36	16.95	0.186E-01	6.68
37	17.22	0.234E-01	6.78
38	17.48	0.162E-01	6.62
39	17.74	0.126E-01	6.51

Experiment 2

PRD-1
Borden soil
Column length = 14.8 cm
Average interstitial velocity = 1.64×10^{-3} cm s^{-1}
Dry bulk density = 1.70 $g\,cm^{-3}$
Porosity = 0.280
Input pH = 7.0 (No.1 - 12, PRD-1)
Input pH = 7.0 (No.13 - 21, phage-free)
Input pH = 7.0 (No.22 - 34, beef extract)
Titer = 7.42 pfu mL^{-1}

No.	PV	C/Co	log C pfu/cm3
1	0.00	0.000E+00	0.00
2	0.37	0.000E+00	0.00
3	0.55	0.000E+00	0.00
4	0.74	0.000E+00	0.00
5	0.86	0.759E-06	1.30
6	0.99	0.123E-04	2.51
7	1.17	0.617E-04	3.21
8	1.36	0.105E-03	3.44
9	1.54	0.977E-04	3.41
10	1.72	0.155E-03	3.61
11	1.91	0.933E-04	3.39
12	2.09	0.871E-04	3.36
13	2.37	0.115E-03	3.48
14	2.53	0.977E-04	3.41
15	2.69	0.135E-03	3.55
16	2.77	0.120E-03	3.50
17	2.89	0.891E-04	3.37
18	3.00	0.912E-04	3.38
19	3.12	0.132E-04	2.54
20	3.27	0.110E-03	3.46
21	4.02	0.191E-05	1.70
22	6.78	0.151E-05	1.60
23	7.23	0.191E-06	0.70
24	7.50	0.000E+00	0.00
25	7.68	0.000E+00	0.00
26	7.95	0.120E+02	8.50
27	8.22	0.110E+01	7.46
28	8.50	0.316E+00	6.92
29	8.68	0.182E+00	6.68
30	8.95	0.912E-01	6.38
31	9.22	0.933E-01	6.39
32	9.49	0.794E-01	6.32
33	9.97	0.224E-01	5.77
34	10.03	0.162E-01	5.63

Experiment 3

PRD-1
Borden soil
Column length = 14.8 cm
Average interstitial velocity = 2.28×10^{-3} cm s^{-1}
Dry bulk density = 1.69 g cm^{-3}
Porosity = 0.282
Input pH = 7.6 (No.1 - 13, PRD-1)
Input pH = 7.6 (No.14 - 20, phage-free)
Input pH = 7.6 (No.21 - 34, beef extract)
Titer = 7.50 pfu mL^{-1}

No.	PV	C/Co	log C pfu/cm3
1	0.00	0.000E+00	0.00
2	0.55	0.000E+00	0.00
3	0.85	0.214E-04	2.83
4	1.14	0.490E-04	3.19
5	1.34	0.123E-03	3.59
6	1.54	0.224E-03	3.85
7	1.84	0.372E-03	4.07
8	2.14	0.339E-03	4.03
9	2.44	0.295E-03	3.97
10	2.74	0.447E-03	4.15
11	3.04	0.513E-03	4.21
12	3.34	0.457E-03	4.16
13	3.63	0.295E-03	3.97
14	3.93	0.380E-03	4.08
15	4.32	0.955E-03	4.48
16	4.62	0.646E-03	4.31
17	4.92	0.398E-03	4.10
18	5.22	0.263E-03	3.92
19	5.52	0.275E-03	3.94
20	7.61	0.813E-04	3.41
21	13.66	0.138E-03	3.64
22	14.14	0.389E-03	4.09
23	14.30	0.447E-03	4.15
24	14.46	0.417E+01	8.12
25	14.62	0.501E+01	8.20
26	14.78	0.661E+01	8.32
27	15.03	0.347E+01	8.04
28	15.27	0.282E+00	6.95
29	15.51	0.102E+01	7.51
30	15.75	0.513E+00	7.21
31	15.99	0.513E+00	7.21
32	16.23	0.355E-01	6.05
33	16.47	0.324E-01	6.01
34	17.52	0.224E-01	5.85

Experiment 4

PRD-1
Cambridge soil
Column length = 14.8 cm
Average interstitial velocity = 2.84×10^{-3} cm s^{-1}
Dry bulk density = 1.68 g cm^{-3}
Porosity = 0.299
Input pH = 7.0 (No.1 - 11, PRD-1)
Input pH = 7.0 (No.12 - 19, phage-free)
Input pH = 7.0 (No.20 - 29, beef extract)
Titer = 7.23 pfu mL^{-1}

No.	PV	C/Co	log C pfu/cm3
1	0.00	0.000E+00	0.00
2	0.58	0.646E-04	3.04
3	0.83	0.550E-03	3.97
4	1.05	0.537E-03	3.96
5	1.28	0.275E-03	3.67
6	1.63	0.182E-03	3.49
7	1.98	0.158E-03	3.43
8	2.32	0.141E-03	3.38
9	2.67	0.120E-03	3.31
10	3.02	0.200E-03	3.53
11	3.37	0.158E-03	3.43
12	3.72	0.186E-03	3.50
13	4.08	0.145E-03	3.39
14	4.45	0.135E-03	3.36
15	4.81	0.794E-04	3.13
16	5.53	0.229E-04	2.59
17	6.26	0.148E-04	2.40
18	8.87	0.891E-05	2.18
19	9.85	0.102E-04	2.24
20	19.66	0.832E-05	2.15
21	19.99	0.589E-05	2.00
22	20.33	0.257E-02	4.64
23	20.66	0.117E+02	8.30
24	20.89	0.288E+01	7.69
25	21.22	0.741E+00	7.10
26	21.89	0.204E+00	6.54
27	22.56	0.129E+00	6.34
28	23.33	0.275E-01	5.67
29	24.56	0.204E-01	5.54

Experiment 5

PRD-1
Cape-Cod soil
Column length = 14.8 cm
Average interstitial velocity = 2.52×10^{-3} cm s^{-1}
Dry bulk density = 1.71 g cm^{-3}
Porosity = 0.358
Input pH = 5.5 (No.1 - 11, PRD-1)
Input pH = 5.5 (No.12 - 16, phage-free)
Titer = 5.63 pfu mL^{-1}

No.	PV	C/Co	log C pfu/cm3
1	0.00	0.000E+00	0.00
2	0.49	0.000E+00	0.00
3	0.69	0.000E+00	0.00
4	0.89	0.141E-03	1.78
5	1.09	0.398E-03	2.23
6	1.39	0.355E-03	2.18
7	1.68	0.186E-03	1.90
8	1.98	0.141E-03	1.78
9	2.28	0.186E-03	1.90
10	2.57	0.245E-05	0.02
11	2.87	0.257E-03	2.04
12	3.18	0.209E-03	1.95
13	3.51	0.302E-03	2.11
14	3.83	0.331E-03	2.15
15	4.15	0.186E-03	1.90
16	5.42	0.000E+00	0.00

Experiment 6

PRD-1
Cape-Cod soil
Column length = 10.6 cm
Average interstitial velocity = 3.05×10^{-3} cm s^{-1}
Dry bulk density = 1.70 g cm^{-3}
Porosity = 0.344
Input pH = 5.7 (No.1 - 10, PRD-1)
Input pH = 5.7 (No.11 - 17, phage-free)
Input pH = 8.2 (No.18 - 29, phage-free)
Titer = 5.52 pfu mL^{-1}

No.	PV	C/Co	log C pfu/cm3
1	0.00	0.000E+00	0.00
2	0.66	0.302E-04	1.00
3	0.83	0.331E-03	2.04
4	0.99	0.302E-03	2.00
5	1.16	0.269E-03	1.95
6	1.65	0.575E-03	2.28
7	2.15	0.513E-03	2.23
8	2.64	0.759E-03	2.40
9	3.14	0.933E-03	2.49
10	3.63	0.479E-03	2.20
11	4.46	0.661E-03	2.34
12	4.81	0.182E-03	1.78
13	5.33	0.182E-03	1.78
14	5.86	0.240E-03	1.90
15	6.38	0.151E-03	1.70
16	8.28	0.603E-04	1.30
17	9.14	0.182E-03	1.78
18	24.72	0.457E-03	2.18
19	25.21	0.646E-02	3.33
20	25.40	0.372E-01	4.09
21	25.58	0.661E-01	4.34
22	25.77	0.447E-01	4.17
23	25.95	0.479E-01	4.20
24	26.51	0.417E-01	4.14
25	27.06	0.302E-01	4.00
26	27.62	0.355E-01	4.07
27	28.18	0.282E-01	3.97
28	29.29	0.398E-01	4.12
29	30.40	0.347E-01	4.06

Experiment 6

MS-2
Cape-Cod soil
Column length = 10.6 cm
Average interstitial velocity = 3.05×10^{-3} cm s^{-1}
Dry bulk density = 1.70 g cm^{-3}
Porosity = 0.344
Input pH = 5.7 (No.1 - 10, MS-2)
Input pH = 5.7 (No.11 - 17, phage-free)
Input pH = 8.2 (No.18 - 29, phage-free)
Titer = 4.54 pfu mL^{-1}

No.	PV	C/Co	log C pfu/cm3
1	0.00	0.000E+00	0.00
2	0.66	0.724E-01	3.40
3	0.83	0.339E+00	4.07
4	0.99	0.603E+00	4.32
5	1.16	0.759E+00	4.42
6	1.65	0.115E+01	4.60
7	2.15	0.126E+01	4.64
8	2.64	0.151E+01	4.72
9	3.14	0.234E+01	4.91
10	3.63	0.955E+00	4.52
11	4.46	0.794E+00	4.44
12	4.81	0.398E+00	4.14
13	5.33	0.316E-01	3.04
14	5.86	0.178E-01	2.79
15	6.38	0.182E-01	2.80
16	8.28	0.123E-01	2.63
17	9.14	0.145E-01	2.70
18	24.72	0.263E-01	2.96
19	25.21	0.457E-02	2.20
20	25.40	0.174E-01	2.78
21	25.58	0.871E-01	3.48
22	25.77	0.813E-01	3.45
23	25.95	0.977E-01	3.53
24	26.51	0.316E-01	3.04
25	27.06	0.174E-01	2.78
26	27.62	0.145E-01	2.70
27	28.18	0.372E-01	3.11
28	29.29	0.174E-01	2.78
29	30.40	0.174E-01	2.78

Experiment 7

PRD-1
Cape-Cod soil
Column length = 10.6 cm
Average interstitial velocity = 2.42×10^{-3} cm s^{-1}
Dry bulk density = 1.68 g cm^{-3}
Porosity = 0.357
Input pH = 5.7 (No.1 - 8, PRD-1)
Input pH = 5.7 (No.9 - 13, phage-free)
Input pH = 8.2 (No.14 - 22, phage-free)
Titer = 5.77 pfu mL^{-1}

No.	PV	C/Co	log C pfu/cm3
1	0.00	0.000E+00	0.00
2	0.42	0.000E+00	0.00
3	0.56	0.000E+00	0.00
4	0.84	0.257E-03	2.18
5	1.41	0.575E-03	2.53
6	1.97	0.324E-03	2.28
7	2.53	0.389E-03	2.36
8	3.09	0.355E-03	2.32
9	3.65	0.372E-03	2.34
10	4.22	0.550E-03	2.51
11	5.06	0.000E+00	0.00
12	5.62	0.339E-04	1.30
13	7.77	0.000E+00	0.00
14	19.49	0.000E+00	0.00
15	19.88	0.000E+00	0.00
16	20.15	0.513E-04	1.48
17	20.41	0.676E-04	1.60
18	20.80	0.186E-03	2.04
19	21.33	0.240E-03	2.15
20	22.38	0.550E-03	2.51
21	22.90	0.794E-03	2.67
22	23.43	0.708E-03	2.62

Experiment 7

MS-2
Cape-Cod soil
Column length = 10.6 cm
Average interstitial velocity = 2.42×10^{-3} cm s^{-1}
Dry bulk density = 1.68 g cm^{-3}
Porosity = 0.357
Input pH = 5.7 (No.1 - 8, MS-2)
Input pH = 5.7 (No.9 - 13, phage-free)
Input pH = 8.2 (No.14 - 22, phage-free)
Titer = 4.66 pfu mL^{-1}

No.	PV	C/Co	log C pfu/cm3
1	0.00	0.000E+00	0.00
2	0.42	0.000E+00	0.00
3	0.56	0.331E-02	2.18
4	0.84	0.214E+00	3.99
5	1.41	0.479E+00	4.34
6	1.97	0.479E+00	4.34
7	2.53	0.123E+01	4.75
8	3.09	0.794E+00	4.56
9	3.65	0.832E+00	4.58
10	4.22	0.158E+01	4.86
11	5.06	0.631E-01	3.46
12	5.62	0.224E-01	3.01
13	7.77	0.501E-02	2.36
14	19.49	0.132E-02	1.78
15	19.88	0.661E-03	1.48
16	20.15	0.110E-02	1.70
17	20.41	0.871E-01	3.60
18	20.80	0.617E-02	2.45
19	21.33	0.200E-01	2.96
20	22.38	0.759E-02	2.54
21	22.90	0.525E-02	2.38
22	23.43	0.813E-02	2.57

Experiment 8

PRD-1
Cape-Cod soil
Column length = 10.6 cm
Average interstitial velocity = 2.36×10^{-3} cm s^{-1}
Dry bulk density = 1.68 g cm^{-3}
Porosity = 0.344
Input pH = 7.0 (No.1 - 9, PRD-1)
Input pH = 7.0 (No.10 - 14, phage-free)
Input pH = 8.2 (No.15 - 26, phage-free)
Titer = 6.51 pfu mL^{-1}

No.	PV	C/Co	log C pfu/cm3
1	0.00	0.000E+00	0.00
2	0.41	0.000E+00	0.00
3	0.56	0.219E-04	1.85
4	0.83	0.166E-03	2.73
5	1.11	0.219E-03	2.85
6	1.39	0.324E-03	3.02
7	1.94	0.295E-03	2.98
8	2.50	0.355E-03	3.06
9	3.05	0.295E-03	2.98
10	3.47	0.282E-03	2.96
11	3.88	0.490E-03	3.20
12	4.34	0.178E-03	2.76
13	4.70	0.141E-03	2.66
14	5.11	0.200E-03	2.81
15	18.97	0.398E-04	2.11
16	19.35	0.646E-04	2.32
17	19.47	0.490E-04	2.20
18	19.60	0.676E-04	2.34
19	19.72	0.162E-03	2.72
20	19.85	0.275E-03	2.95
21	20.23	0.302E-03	2.99
22	20.60	0.589E-03	3.28
23	20.98	0.631E-03	3.31
24	21.36	0.437E-03	3.15
25	22.11	0.891E-03	3.46
26	22.86	0.832E-03	3.43

Experiment 8

MS-2
Cape-Cod soil
Column length = 10.6 cm
Average interstitial velocity = 2.36×10^{-3} cm s^{-1}
Dry bulk density = 1.68 g cm^{-3}
Porosity = 0.344
Input pH = 7.0 (No.1 - 9, MS-2)
Input pH = 7.0 (No.10 - 14, phage-free)
Input pH = 8.2 (No.15 - 26, phage-free)
Titer = 5.70 pfu mL^{-1}

No.	PV	C/Co	log C pfu/cm3
1	0.00	0.000E+00	0.00
2	0.41	0.000E+00	0.00
3	0.56	0.891E-02	3.65
4	0.83	0.427E+00	5.33
5	1.11	0.794E+00	5.60
6	1.39	0.115E+01	5.76
7	1.94	0.912E+00	5.66
8	2.50	0.646E+00	5.51
9	3.05	0.933E+00	5.67
10	3.47	0.776E+00	5.59
11	3.88	0.100E+01	5.70
12	4.34	0.575E+00	5.46
13	4.70	0.794E-01	4.60
14	5.11	0.209E-01	4.02
15	18.97	0.269E-02	3.13
16	19.35	0.339E-02	3.23
17	19.47	0.257E-02	3.11
18	19.60	0.257E-02	3.11
19	19.72	0.295E-02	3.17
20	19.85	0.251E-02	3.10
21	20.23	0.224E-02	3.05
22	20.60	0.372E-02	3.27
23	20.98	0.389E-02	3.29
24	21.36	0.363E-02	3.26
25	22.11	0.355E-02	3.25
26	22.86	0.372E-02	3.27

Experiment 9

PRD-1
Cape-Cod soil
Column length = 10.6 cm
Average interstitial velocity = 2.94×10^{-3} cm s^{-1}
Dry bulk density = 1.71 gcm^{-3}
Porosity = 0.334
Input pH = 5.7 (No.1 - 6, PRD-1)
Input pH = 7.0 (No.7 - 12, PRD-1)
Input pH = 8.2 (No.13 - 18, PRD-1)
Input pH = 8.2 (No.19 - 28, phage-free)
Titer = 4.73 pfu mL^{-1} (No.1 - 6)
Titer = 4.79 pfu mL^{-1} (No.7 - 12)
Titer = 4.41 pfu mL^{-1} (No.13 - 28)

No.	PV	C/Co	log C pfu/cm3
1	0.00	0.000E+00	0.00
2	0.49	0.000E+00	0.00
3	0.65	0.000E+00	0.00
4	0.98	0.000E+00	0.00
5	1.30	0.000E+00	0.00
6	1.63	0.000E+00	0.00
7	1.93	0.000E+00	0.00
8	2.44	0.191E-04	0.01
9	2.60	0.191E-04	0.01
10	2.93	0.000E+00	0.00
11	3.25	0.166E-04	0.01
12	3.58	0.166E-04	0.01
13	3.90	0.000E+00	0.00
14	4.41	0.000E+00	0.00
15	4.58	0.490E-03	1.48
16	4.92	0.155E-02	1.60
17	5.26	0.000E+00	0.00
18	5.60	0.195E-02	1.70
19	5.94	0.776E-03	1.30
20	6.46	0.398E-04	0.01
21	6.81	0.234E-02	1.78
22	7.16	0.234E-02	1.78
23	7.51	0.155E-02	1.60
24	7.86	0.234E-02	1.78
25	12.22	0.347E-02	1.95
26	15.30	0.501E-02	2.11
27	26.12	0.234E-01	2.78
28	27.08	0.309E-01	2.90

Experiment 9

MS-2
Cape-Cod soil
Column length = 10.6 cm
Average interstitial velocity = 2.94×10^{-3} cm s^{-1}
Dry bulk density = 1.71 gcm^{-3}
Porosity = 0.334
Input pH = 5.7 (No.1 - 6, MS-2)
Input pH = 7.0 (No.7 - 12, MS-2)
Input pH = 8.2 (No.13 - 18, MS-2)
Input pH = 8.2 (No.19 - 28, phage-free)
Titer = 4.82 pfu mL^{-1} (No.1 - 6)
Titer = 4.73 pfu mL^{-1} (No.7 - 12)
Titer = 4.57 pfu mL^{-1} (No.13 - 28)

No.	PV	C/Co	log C pfu/cm3
1	0.00	0.000E+00	0.00
2	0.49	0.603E-02	2.60
3	0.65	0.562E-01	3.57
4	0.98	0.490E-01	3.51
5	1.30	0.501E+00	4.52
6	1.63	0.724E+00	4.68
7	1.93	0.646E+00	4.63
8	2.44	0.631E+00	4.62
9	2.60	0.117E+01	4.89
10	2.93	0.102E+01	4.83
11	3.25	0.100E+01	4.73
12	3.58	0.115E+01	4.79
13	3.90	0.977E+00	4.72
14	4.41	0.105E+01	4.75
15	4.58	0.977E+00	4.72
16	4.92	0.141E+01	4.72
17	5.26	0.126E+01	4.67
18	5.60	0.120E+01	4.65
19	5.94	0.977E+00	4.56
20	6.46	0.126E+01	4.67
21	6.81	0.832E+00	4.49
22	7.16	0.195E+00	3.86
23	7.51	0.724E-01	3.43
24	7.86	0.240E-01	2.95
25	12.22	0.977E-02	2.56
26	15.30	0.813E-02	2.48
27	26.12	0.282E-04	0.02
28	27.08	0.324E-02	2.08

Experiment 10

P17
1.0-mm silica beads
Column length = 20.0 cm
Average interstitial velocity = 8.77×10^{-3} cm s^{-1}
Dry bulk density = 1.72 g cm^{-3}
Porosity = 0.419
Input pH = 7.0 (No.1 - 11, P17)
Input pH = 7.0 (No.12 - 17, bacteria-free)
Titer = 5.92 cfu mL^{-1}

No.	PV	C/Co	log C cfu/cm3
1	0.00	0.000E+00	0.00
2	0.79	0.912E-01	4.88
3	1.31	0.347E-01	4.46
4	1.57	0.174E-01	4.16
5	1.83	0.479E-02	3.60
6	2.10	0.661E-02	3.74
7	2.49	0.589E-02	3.69
8	2.88	0.525E-02	3.64
9	3.28	0.398E-02	3.52
10	3.67	0.575E-02	3.68
11	4.19	0.407E-02	3.53
12	4.98	0.468E-02	3.59
13	5.76	0.912E-01	4.88
14	6.55	0.759E-01	4.80
15	7.34	0.115E+00	4.98
16	8.12	0.102E+00	4.93
17	9.69	0.759E-01	4.80

Experiment 11

P17
0.5-mm silica beads
Column length = 20.0 cm
Average interstitial velocity = 7.75×10^{-3} cm s^{-1}
Dry bulk density = 1.72 g cm^{-3}
Porosity = 0.425
Input pH = 7.0 (No.1 - 11, P17)
Input pH = 7.0 (No.12 - 17, bacteria-free)
Input pH = 7.0 (No.18 - 29, beef extract)
Titer = 5.39 cfu mL^{-1}

No.	PV	C/Co	log C cfu/cm3
1	0.00	0.000E+00	0.00
2	0.72	0.891E-01	4.34
3	1.20	0.741E-01	4.26
4	1.44	0.661E-01	4.21
5	1.68	0.537E-01	4.12
6	1.92	0.457E-01	4.05
7	2.28	0.575E-01	4.15
8	2.64	0.562E-01	4.14
9	3.00	0.537E-01	4.12
10	3.36	0.603E-01	4.17
11	3.84	0.562E-01	4.14
12	4.55	0.513E-01	4.10
13	5.27	0.204E+00	4.70
14	5.99	0.355E-01	3.94
15	6.71	0.407E-01	4.00
16	7.43	0.813E-01	4.30
17	8.15	0.501E-02	3.09
18	31.74	0.151E+00	4.57
19	32.41	0.759E+00	5.27
20	33.08	0.162E+02	6.60
21	33.41	0.132E+02	6.51
22	33.75	0.490E+01	6.08
23	34.08	0.851E+01	6.32
24	34.41	0.407E+01	6.00
25	34.86	0.692E+01	6.23
26	35.31	0.178E+01	5.64
27	35.75	0.295E+01	5.86
28	36.42	0.135E+01	5.52
29	37.09	0.158E+01	5.59

Experiment 12

P17
0.5-mm silica beads
Column length = 20.0 cm
Average interstitial velocity = 10.10×10^{-3} cm s^{-1}
Dry bulk density = 1.72 g cm^{-3}
Porosity = 0.442
Input pH = 7.0 (No.1 - 10, P17)
Input pH = 7.0 (No.11 - 16, bacteria-free)
Input pH = 8.0 (No.17 - 31, bacteria-free)
Titer = 3.90 cfu mL^{-1}

No.	PV	C/Co	log C cfu/cm3
1	0.00	0.000E+00	0.00
2	1.06	0.138E+02	5.04
3	1.29	0.245E+02	5.29
4	1.41	0.151E+02	5.08
5	1.53	0.107E+02	4.93
6	1.99	0.589E+01	4.67
7	2.35	0.575E+01	4.66
8	2.70	0.407E+01	4.51
9	3.05	0.339E+01	4.43
10	3.40	0.105E+02	4.92
11	4.10	0.191E+01	4.18
12	4.57	0.107E+02	4.93
13	5.03	0.209E+03	6.22
14	5.50	0.120E+03	5.98
15	6.20	0.331E+03	6.42
16	8.31	0.490E+02	5.59
17	34.25	0.398E+03	6.50
18	35.01	0.102E+03	5.91
19	35.51	0.437E+02	5.54
20	35.89	0.115E+03	5.96
21	36.15	0.692E+02	5.74
22	36.53	0.151E+03	6.08
23	36.91	0.112E+03	5.95
24	37.29	0.575E+02	5.66
25	37.79	0.178E+03	6.15
26	38.30	0.955E+02	5.88
27	38.80	0.891E+02	5.85
28	39.56	0.589E+02	5.67
29	40.32	0.759E+02	5.78
30	41.08	0.661E+02	5.72
31	41.84	0.676E+02	5.73

Experiment 13

P17
0.5-mm silica beads
Column length = 20.0 cm
Average interstitial velocity = 11.11×10^{-3} cm s^{-1}
Dry bulk density = 1.72 g cm^{-3}
Porosity = 0.416
Input pH = 7.0 (No.1 - 9, P17)
Input pH = 7.0 (No.10 - PV=46.75, bacteria-free)
Input pH = 8.0 (PV=46.75 - No.24, bacteria-free)
Titer = 4.35 cfu mL^{-1}

No.	PV	C/Co	log C cfu/cm3
1	0.00	0.000E+00	0.00
2	0.58	0.000E+00	0.00
3	0.86	0.501E-01	3.05
4	1.15	0.724E-01	3.21
5	1.44	0.832E-01	3.27
6	1.73	0.813E-01	3.26
7	2.61	0.912E-01	3.31
8	3.48	0.933E-01	3.32
9	4.35	0.126E+00	3.45
10	5.23	0.112E+00	3.40
11	5.90	0.977E-01	3.34
12	6.57	0.166E+00	3.57
13	7.23	0.550E-01	3.09
14	8.24	0.288E-01	2.81
15	9.24	0.427E-01	2.98
16	10.24	0.468E-01	3.02
17	12.24	0.380E-01	2.93
18	17.05	0.912E-01	3.31
19	49.03	0.708E-01	3.20
20	50.11	0.525E-01	3.07
21	51.19	0.316E-01	2.85
22	52.28	0.380E-01	2.93
23	55.53	0.437E-01	2.99
24	57.70	0.646E-01	3.16

Experiment 14

P17
0.5-mm silica beads
Column length = 20.0 cm
Average interstitial velocity = 9.01×10^{-3} cm s^{-1}
Dry bulk density = 1.72 g cm^{-3}
Porosity = 0.432
Input pH = 5.5 (No.1 - 7, P17)
Input pH = 5.5 (No.8 - 15, bacteria-free)
Input pH = 8.2 (No.16 - 26, bacteria-free)
Titer = 5.36 cfu mL^{-1}

No.	PV	C/Co	log C cfu/cm3
1	0.00	0.000E+00	0.00
2	0.58	0.832E-03	2.28
3	0.87	0.132E+00	4.48
4	1.17	0.302E+00	4.84
5	1.46	0.372E+00	4.93
6	1.75	0.331E+00	4.88
7	2.62	0.447E+00	5.01
8	3.93	0.398E+00	4.96
9	4.47	0.437E+00	5.00
10	5.01	0.537E-01	4.09
11	5.54	0.501E-01	4.06
12	6.35	0.513E-01	4.07
13	7.16	0.398E-01	3.96
14	7.96	0.398E-01	3.96
15	8.77	0.347E-01	3.90
16	17.45	0.282E-01	3.81
17	18.84	0.155E-01	3.55
18	19.36	0.123E-01	3.45
19	19.88	0.851E-02	3.29
20	20.40	0.195E-02	2.65
21	20.92	0.151E-02	2.54
22	21.95	0.141E-02	2.51
23	22.99	0.102E-02	2.37
24	24.03	0.871E-03	2.30
25	25.07	0.871E-03	2.30
26	26.62	0.631E-03	2.16

Experiment 15

Bacillus
0.5-mm silica beads
Column length = 20.0 cm
Average interstitial velocity = 8.77×10^{-3} cm s^{-1}
Dry bulk density = 1.72 g cm^{-3}
Porosity = 0.438
Input pH = 7.0 (No.1 - 7, Bacillus)
Input pH = 7.0 (No.8 - 14, bacteria-free)
Input pH = 8.0 (No.15 - 24, bacteria-free)
Titer = 3.40 cfu mL^{-1}

No.	PV	C/Co	log C cfu/cm3
1	0.00	0.000E+00	0.00
2	0.53	0.000E+00	0.00
3	0.79	0.417E-01	2.02
4	1.06	0.195E+00	2.69
5	1.32	0.182E+00	2.66
6	1.59	0.204E+00	2.71
7	2.38	0.209E+00	2.72
8	3.18	0.200E+00	2.70
9	4.03	0.170E+00	2.63
10	4.60	0.407E-03	0.01
11	5.16	0.200E-02	0.70
12	6.01	0.603E-02	1.18
13	6.86	0.000E+00	0.00
14	7.71	0.000E+00	0.00
15	33.97	0.000E+00	0.00
16	34.50	0.200E-02	0.70
17	35.04	0.603E-02	1.18
18	35.57	0.200E-02	0.70
19	36.10	0.200E-02	0.70
20	37.17	0.200E-02	0.70
21	38.24	0.000E+00	0.00
22	39.30	0.000E+00	0.00
23	40.37	0.178E-01	1.65
24	41.97	0.257E-01	1.81

Experiment 16

Bacillus
0.5-mm silica beads
Column length = 20.0 cm
Average interstitial velocity = 8.77×10^{-3} cm s^{-1}
Dry bulk density = 1.72 g cm^{-3}
Porosity = 0.438
Input pH = 5.5 (No.1 - 7, Bacillus)
Input pH = 5.5 (No.8 - 15, bacteria-free)
Input pH = 7.0 (No.16 - 26, bacteria-free)
Titer = unknown

No.	PV	C/Co	log C cfu/cm3
1	0.00		0.00
2	0.52		0.00
3	0.78		3.09
4	1.04		3.51
5	1.30		3.53
6	1.56		3.35
7	2.33		3.47
8	3.11		3.54
9	3.65		3.45
10	4.20		1.40
11	4.74		0.01
12	5.56		0.01
13	6.38		1.18
14	7.19		1.18
15	8.01		1.40
16	37.76		0.00
17	38.29		1.18
18	38.83		0.70
19	39.36		0.01
20	39.89		0.01
21	40.96		0.00
22	42.03		0.00
23	43.09		1.30
24	44.16		0.00
25	45.76		0.70
26	47.36		1.18

Experiment 17

Bacillus
0.5-mm silica beads
Column length = 20.0 cm
Average interstitial velocity = 11.90×10^{-3} cm s^{-1}
Dry bulk density = 1.72 g cm^{-3}
Porosity = 0.438
Input pH = 7.0 (No.1 - 7, Bacillus)
Input pH = 7.0 (No.8 - 15, bacteria-free)
Input pH = 8.0 (No.16 - 26, bacteria-free)
Titer = 4.63 cfu mL^{-1}

No.	PV	C/Co	log C cfu/cm3
1	0.00	0.000E+00	0.00
2	0.61	0.302E-02	2.11
3	0.95	0.589E+00	4.40
4	1.22	0.110E+01	4.67
5	1.53	0.661E+00	4.45
6	1.83	0.794E+00	4.53
7	2.75	0.955E+00	4.61
8	3.67	0.631E+00	4.43
9	4.47	0.525E+00	4.35
10	5.28	0.759E-02	2.51
11	6.08	0.117E-02	1.70
12	7.29	0.589E-03	1.40
13	8.49	0.708E-03	1.48
14	9.70	0.589E-03	1.40
15	10.90	0.692E-03	1.47
16	53.14	0.000E+00	0.00
17	53.87	0.468E-03	1.30
18	54.60	0.000E+00	0.00
19	55.33	0.000E+00	0.00
20	56.06	0.000E+00	0.00
21	57.52	0.000E+00	0.00
22	59.05	0.117E-03	0.70
23	60.44	0.000E+00	0.00
24	61.90	0.000E+00	0.00
25	64.08	0.000E+00	0.00
26	66.27	0.000E+00	0.00

APPENDIX B

Results of Conservative-Tracer Column Experiments

NaCl-column experiment 1

Borden soil
Column length = 14.8 cm
Average interstitial velocity = 0.47×10^{-3} cm s^{-1}
Dry bulk density = 1.70 g cm^{-3}
Porosity = 0.322

No	Pore Vol	C/Co	No	Pore Vol	C/Co
1	0.00	0.000	31	1.65	0.990
2	0.13	0.000	32	1.73	1.000
3	0.26	0.000	33	1.92	1.000
4	0.39	0.000	34	1.99	0.990
5	0.53	0.000	35	2.07	0.990
6	0.68	0.000	36	2.14	0.980
7	0.79	0.000	37	2.22	0.975
8	0.81	0.015	38	2.26	0.970
9	0.84	0.040	39	2.30	0.924
10	0.87	0.081	40	2.31	0.894
11	0.89	0.141	41	2.33	0.843
12	0.92	0.197	42	2.35	0.778
13	0.94	0.283	43	2.37	0.697
14	0.97	0.374	44	2.39	0.616
15	0.99	0.470	45	2.41	0.530
16	1.02	0.571	46	2.43	0.429
17	1.04	0.662	47	2.45	0.333
18	1.07	0.742	48	2.47	0.253
19	1.10	0.813	49	2.48	0.187
20	1.12	0.864	50	2.50	0.126
21	1.15	0.899	51	2.52	0.096
22	1.18	0.919	52	2.54	0.066
23	1.21	0.934	53	2.56	0.045
24	1.26	0.949	54	2.58	0.030
25	1.31	0.955	55	2.60	0.015
26	1.36	0.960	56	2.62	0.010
27	1.41	0.965	57	2.64	0.005
28	1.46	0.975	58	2.65	0.000
29	1.50	0.980			
30	1.58	0.985			

NaCl-column experiment 2

Borden soil
Column length = 14.8 cm
Average interstitial velocity = 1.04×10^{-3} cm s^{-1}
Dry bulk density = 1.70 g cm^{-3}
Porosity = 0.306

No	Pore Vol	C/Co	No	Pore Vol	C/Co
1	0.00	0.000	46	1.52	0.995
2	0.83	0.000	47	1.54	1.000
3	0.85	0.010	48	1.57	1.000
4	0.86	0.020	49	1.77	1.000
5	0.87	0.035	50	1.78	1.000
6	0.89	0.066	51	1.80	1.000
7	0.90	0.096	52	1.81	0.995
8	0.91	0.131	53	1.82	0.985
9	0.92	0.177	54	1.84	0.975
10	0.94	0.227	55	1.85	0.960
11	0.95	0.283	56	1.86	0.934
12	0.96	0.323	57	1.87	0.904
13	0.97	0.389	58	1.88	0.869
14	0.99	0.449	59	1.90	0.818
15	1.00	0.510	60	1.91	0.768
16	1.01	0.571	61	1.92	0.707
17	1.02	0.626	62	1.94	0.641
18	1.04	0.682	63	1.95	0.576
19	1.05	0.727	64	1.96	0.510
20	1.06	0.768	65	1.97	0.439
21	1.08	0.803	66	1.99	0.384
22	1.09	0.833	67	2.00	0.323
23	1.10	0.859	68	2.01	0.278
24	1.11	0.879	69	2.03	0.237
25	1.13	0.894	70	2.04	0.197
26	1.14	0.909	71	2.05	0.167
27	1.15	0.919	72	2.06	0.141
28	1.16	0.929	73	2.08	0.121
29	1.18	0.939	74	2.09	0.106
30	1.19	0.944	75	2.10	0.091
31	1.20	0.949	76	2.11	0.076
32	1.22	0.955	77	2.13	0.066
33	1.23	0.960	78	2.14	0.056
34	1.24	0.965	79	2.15	0.045
35	1.25	0.970	80	2.16	0.040
36	1.26	0.970	81	2.18	0.035
37	1.29	0.975	82	2.19	0.030
38	1.32	0.980	83	2.20	0.025
39	1.34	0.980	84	2.21	0.020
40	1.37	0.985	85	2.23	0.015
41	1.39	0.990	86	2.24	0.010
42	1.42	0.990	87	2.25	0.005
43	1.44	0.990	88	2.27	0.005
44	1.47	0.995	89	2.28	0.000
45	1.49	0.995			

NaCl-column experiment 3

Borden soil
Column length = 14.8 cm
Average interstitial velocity = 2.65×10^{-3} cm s^{-1}
Dry bulk density = 1.70 g cm^{-3}
Porosity = 0.309

No	Pore Vol	C/Co	No	Pore Vol	C/Co
1	0.00	0.000	46	1.60	0.995
2	0.30	0.000	47	1.63	1.000
3	0.60	0.000	48	1.67	1.000
4	0.75	0.000	49	1.70	1.000
5	0.78	0.000	50	1.72	0.991
6	0.81	0.000	51	1.73	0.982
7	0.82	0.009	52	1.75	0.959
8	0.84	0.014	53	1.76	0.922
9	0.86	0.032	54	1.78	0.872
10	0.88	0.059	55	1.80	0.804
11	0.90	0.100	56	1.81	0.712
12	0.92	0.110	57	1.83	0.621
13	0.93	0.224	58	1.85	0.521
14	0.95	0.301	59	1.86	0.425
15	0.97	0.384	60	1.88	0.338
16	0.99	0.470	61	1.90	0.256
17	1.01	0.553	62	1.91	0.192
18	1.02	0.630	63	1.93	0.146
19	1.04	0.699	64	1.94	0.114
20	1.06	0.758	65	1.96	0.082
21	1.08	0.804	66	1.98	0.064
22	1.10	0.840	67	1.99	0.050
23	1.12	0.863	68	2.01	0.041
24	1.13	0.890	69	2.03	0.037
25	1.15	0.904	70	2.04	0.027
26	1.17	0.918	71	2.06	0.023
27	1.19	0.927	72	2.09	0.018
28	1.21	0.936	73	2.12	0.014
29	1.22	0.945	74	2.16	0.009
30	1.24	0.950	75	2.19	0.009
31	1.26	0.954	76	2.22	0.005
32	1.28	0.959	77	2.25	0.005
33	1.29	0.963	78	2.29	0.000
34	1.31	0.963			
35	1.33	0.968			
36	1.34	0.968			
37	1.36	0.973			
38	1.38	0.977			
39	1.39	0.977			
40	1.41	0.982			
41	1.44	0.986			
42	1.47	0.986			
43	1.50	0.991			
44	1.54	0.991			
45	1.57	0.991			

NaCl-column experiment 4

Borden soil
Column length = 14.8 cm
Average interstitial velocity = 3.50×10^{-3} cm s^{-1}
Dry bulk density = 1.70 g cm^{-3}
Porosity = 0.344

No	Pore Vol	C/Co	No	Pore Vol	C/Co
1	0.00	0.000	31	2.86	1.000
2	0.29	0.000	32	3.03	1.000
3	0.55	0.000	33	3.07	1.000
4	0.73	0.000	34	3.11	0.969
5	0.77	0.010	35	3.16	0.897
6	0.81	0.062	36	3.20	0.795
7	0.86	0.154	37	3.24	0.667
8	0.90	0.256	38	3.28	0.513
9	0.94	0.379	39	3.33	0.344
10	0.98	0.523	40	3.37	0.205
11	1.03	0.646	41	3.41	0.133
12	1.07	0.728	42	3.45	0.087
13	1.11	0.764	43	3.50	0.067
14	1.16	0.779	44	3.54	0.051
15	1.20	0.790	45	3.58	0.036
16	1.29	0.805	46	3.67	0.026
17	1.37	0.821	47	3.71	0.015
18	1.46	0.831	48	3.75	0.015
19	1.54	0.872	49	3.84	0.010
20	1.63	0.903	50	3.92	0.000
21	1.71	0.933			
22	1.80	0.949			
23	1.88	0.964			
24	1.97	0.974			
25	2.01	0.979			
26	2.05	0.985			
27	2.13	0.990			
28	2.22	1.000			
29	2.26	1.000			
30	2.55	1.000			

NaCl-column experiment 5

Cambridge soil
Column length = 14.8 cm
Average interstitial velocity = 2.07×10^{-3} cm s^{-1}
Dry bulk density = 1.68 g cm^{-3}
Porosity = 0.298

No	Pore Vol	C/Co	No	Pore Vol	C/Co
1	0.00	0.000	26	1.81	0.992
2	0.27	0.000	27	1.83	0.976
3	0.53	0.000	28	1.85	0.952
4	0.79	0.000	29	1.87	0.936
5	0.81	0.032	30	1.89	0.896
6	0.83	0.064	31	1.93	0.824
7	0.85	0.096	32	1.97	0.736
8	0.86	0.144	33	2.02	0.656
9	0.90	0.240	34	2.07	0.552
10	0.94	0.344	35	2.12	0.432
11	0.97	0.440	36	2.17	0.320
12	1.01	0.536	37	2.22	0.208
13	1.05	0.632	38	2.27	0.120
14	1.09	0.704	39	2.29	0.080
15	1.13	0.792	40	2.31	0.056
16	1.17	0.864	41	2.33	0.032
17	1.21	0.920	42	2.36	0.016
18	1.25	0.952	43	2.40	0.000
19	1.29	0.968			
20	1.33	0.976			
21	1.37	0.992			
22	1.41	0.992			
23	1.45	1.000			
24	1.73	1.000			
25	1.77	1.000			

NaCl-column experiment 6

Cambridge soil
Column length = 14.8 cm
Average interstitial velocity = 3.24×10^{-3} cm s^{-1}
Dry bulk density = 1.68 g cm^{-3}
Porosity = 0.307

No	Pore Vol	C/Co	No	Pore Vol	C/Co
1	0.00	0.000	26	2.28	0.980
2	0.71	0.000	27	2.31	0.973
3	0.75	0.015	28	2.35	0.959
4	0.78	0.037	29	2.38	0.912
5	0.81	0.105	30	2.41	0.864
6	0.85	0.151	31	2.45	0.796
7	0.88	0.233	32	2.51	0.646
8	0.91	0.301	33	2.58	0.517
9	0.94	0.376	34	2.65	0.401
10	0.98	0.444	35	2.71	0.272
11	1.04	0.580	36	2.78	0.150
12	1.11	0.722	37	2.82	0.102
13	1.17	0.842	38	2.85	0.068
14	1.21	0.880	39	2.88	0.048
15	1.24	0.917	40	2.92	0.027
16	1.27	0.932	41	2.95	0.014
17	1.31	0.955	42	2.98	0.000
18	1.34	0.970			
19	1.37	0.985			
20	1.41	0.992			
21	1.44	1.000			
22	2.04	1.000			
23	2.11	1.000			
24	2.18	0.993			
25	2.24	0.986			

NaCl-column experiment 7

Cape-Cod soil
Column length = 10.6 cm
Average interstitial velocity = 1.67×10^{-3} cm s^{-1}
Dry bulk density = 1.70 g cm^{-3}
Porosity = 0.345

No	Pore Vol	C/Co	No	Pore Vol	C/Co
1	0.00	0.000	21	1.72	1.000
2	0.68	0.000	22	1.77	1.000
3	0.75	0.029	23	1.82	0.990
4	0.82	0.107	24	1.86	0.922
5	0.87	0.223	25	1.95	0.786
6	0.93	0.359	26	2.05	0.660
7	0.99	0.495	27	2.13	0.544
8	1.04	0.602	28	2.21	0.456
9	1.10	0.689	29	2.29	0.379
10	1.16	0.786	30	2.36	0.311
11	1.21	0.835	31	2.43	0.272
12	1.27	0.883	32	2.50	0.233
13	1.33	0.922	33	2.57	0.204
14	1.38	0.951	34	2.64	0.175
15	1.44	0.961	35	2.71	0.146
16	1.50	0.981	36	2.78	0.117
17	1.54	0.990	37	2.85	0.087
18	1.59	0.990	38	2.91	0.049
19	1.63	1.000	39	2.98	0.019
20	1.68	1.000	40	3.06	0.010
			41	3.13	0.000

NaCl-column experiment 8

Cape-Cod soil
Column length = 10.6 cm
Average interstitial velocity = 2.95×10^{-3} cm s^{-1}
Dry bulk density = 1.70 g cm^{-3}
Porosity = 0.345

No	Pore Vol	C/Co	No	Pore Vol	C/Co
1	0.00	0.000	21	1.67	1.000
2	0.47	0.000	22	1.75	1.000
3	0.63	0.000	23	1.97	1.000
4	0.72	0.010	24	2.04	1.000
5	0.76	0.051	25	2.12	0.960
6	0.80	0.091	26	2.15	0.889
7	0.84	0.172	27	2.19	0.828
8	0.88	0.253	28	2.23	0.768
9	0.92	0.343	29	2.27	0.717
10	0.96	0.434	30	2.30	0.646
11	1.00	0.515	31	2.34	0.596
12	1.04	0.596	32	2.39	0.545
13	1.08	0.657	33	2.44	0.485
14	1.12	0.717	34	2.49	0.424
15	1.21	0.818	35	2.55	0.374
16	1.29	0.899	36	2.65	0.313
17	1.37	0.939	37	2.75	0.242
18	1.45	0.970	38	2.85	0.192
19	1.52	0.980	39	2.96	0.131
20	1.60	0.990	40	3.06	0.081
			41	3.16	0.030
			42	3.26	0.000

NaCl-column experiment 9

Cape-Cod soil
Column length = 10.6 cm
Average interstitial velocity = 2.01×10^{-3} cm s^{-1}
Dry bulk density = 1.68 g cm^{-3}
Porosity = 0.356

No	Pore Vol	C/Co	No	Pore Vol	C/Co
1	0.00	0.000	21	1.64	1.000
2	0.36	0.000	22	1.75	1.000
3	0.73	0.000	23	1.86	1.000
4	0.76	0.011	24	1.92	0.979
5	0.79	0.021	25	1.98	0.874
6	0.82	0.053	26	2.03	0.768
7	0.85	0.095	27	2.09	0.684
8	0.88	0.168	28	2.14	0.632
9	0.92	0.242	29	2.21	0.537
10	0.95	0.337	30	2.28	0.453
11	0.98	0.442	31	2.34	0.379
12	1.01	0.558	32	2.41	0.305
13	1.04	0.642	33	2.47	0.242
14	1.08	0.726	34	2.53	0.200
15	1.11	0.779	35	2.58	0.168
16	1.13	0.832	36	2.63	0.137
17	1.16	0.874	37	2.69	0.105
18	1.21	0.916	38	2.74	0.084
19	1.32	0.958	39	2.79	0.063
20	1.43	0.989	40	2.84	0.042
			41	2.88	0.032
			42	2.97	0.000

NaCl-column experiment 10

Cape-Cod soil
Column length = 10.6 cm
Average interstitial velocity = 2.37×10^{-3} cm s^{-1}
Dry bulk density = 1.68 g cm^{-3}
Porosity = 0.357

No	Pore Vol	C/Co	No	Pore Vol	C/Co
1	0.00	0.000	21	1.70	1.000
2	0.41	0.000	22	1.84	1.000
3	0.71	0.000	23	1.91	1.000
4	0.74	0.010	24	1.94	0.979
5	0.77	0.021	25	1.98	0.928
6	0.81	0.052	26	2.01	0.856
7	0.84	0.093	27	2.04	0.804
8	0.87	0.155	28	2.08	0.732
9	0.90	0.216	29	2.11	0.680
10	0.93	0.309	30	2.15	0.639
11	0.96	0.392	31	2.18	0.598
12	1.00	0.495	32	2.25	0.495
13	1.03	0.588	33	2.32	0.402
14	1.06	0.670	34	2.38	0.320
15	1.09	0.732	35	2.45	0.237
16	1.12	0.784	36	2.52	0.186
17	1.15	0.835	37	2.59	0.144
18	1.29	0.948	38	2.65	0.103
19	1.42	0.990	39	2.73	0.072
20	1.56	0.990	40	2.80	0.041
			41	2.87	0.021
			42	2.95	0.000

NaCl-column experiment 11

Silica beads (0.5 mm)
Column length = 20.0 cm
Average interstitial velocity = 5.42×10^{-3} cm s^{-1}
Dry bulk density = 1.72 g cm^{-3}
Porosity = 0.461

No	Pore Vol	C/Co	No	Pore Vol	C/Co
1	0.00	0.000	31	1.39	1.000
2	0.37	0.000	32	1.41	0.995
3	0.56	0.000	33	1.43	0.986
4	0.74	0.000	34	1.45	0.962
5	0.81	0.000	35	1.46	0.928
6	0.83	0.010	36	1.48	0.885
7	0.85	0.024	37	1.50	0.817
8	0.87	0.053	38	1.52	0.731
9	0.89	0.091	39	1.54	0.625
10	0.91	0.149	40	1.56	0.510
11	0.93	0.212	41	1.58	0.385
12	0.94	0.274	42	1.59	0.293
13	0.96	0.351	43	1.61	0.207
14	0.98	0.423	44	1.63	0.144
15	1.00	0.490	45	1.65	0.091
16	1.02	0.558	46	1.67	0.063
17	1.04	0.625	47	1.69	0.038
18	1.06	0.712	48	1.70	0.029
19	1.08	0.793	49	1.72	0.019
20	1.09	0.861	50	1.74	0.014
21	1.11	0.904	51	1.78	0.010
22	1.13	0.933	52	1.82	0.000
23	1.15	0.957			
24	1.17	0.971			
25	1.19	0.986			
26	1.20	0.990			
27	1.22	0.995			
28	1.24	1.000			
29	1.26	1.000			
30	1.37	1.000			

NaCl-column experiment 12

Silica beads (0.5 mm)
Column length = 20.0 cm
Average interstitial velocity = 6.95×10^{-3} cm s^{-1}
Dry bulk density = 1.72 g cm^{-3}
Porosity = 0.419

No	Pore Vol	C/Co	No	Pore Vol	C/Co
1	0.00	0.000	41	1.46	0.966
2	0.24	0.000	42	1.47	0.946
3	0.48	0.000	43	1.49	0.922
4	0.73	0.000	44	1.50	0.882
5	0.82	0.000	45	1.51	0.843
6	0.83	0.000	46	1.52	0.779
7	0.85	0.015	47	1.53	0.701
8	0.86	0.025	48	1.55	0.608
9	0.87	0.044	49	1.56	0.529
10	0.88	0.069	50	1.57	0.431
11	0.90	0.103	51	1.59	0.363
12	0.91	0.137	52	1.60	0.289
13	0.92	0.186	53	1.61	0.230
14	0.93	0.235	54	1.62	0.176
15	0.94	0.284	55	1.63	0.137
16	0.96	0.338	56	1.65	0.108
17	0.97	0.382	57	1.66	0.083
18	0.98	0.431	58	1.67	0.069
19	0.99	0.475	59	1.68	0.054
20	1.00	0.520	60	1.71	0.034
21	1.02	0.564	61	1.74	0.025
22	1.03	0.608	62	1.76	0.015
23	1.04	0.642	63	1.79	0.010
24	1.05	0.686	64	1.81	0.005
25	1.07	0.725	65	1.84	0.000
26	1.08	0.775			
27	1.09	0.824			
28	1.10	0.873			
29	1.11	0.907			
30	1.13	0.931			
31	1.14	0.951			
32	1.15	0.966			
33	1.16	0.975			
34	1.19	0.990			
35	1.21	1.000			
36	1.24	1.000			
37	1.41	1.000			
38	1.42	0.995			
39	1.43	0.990			
40	1.45	0.980			

NaCl-column experiment 13

Silica beads (0.5 mm)
Column length = 20.0 cm
Average interstitial velocity = 10.30×10^{-3} cm s^{-1}
Dry bulk density = 1.72 g cm^{-3}
Porosity = 0.432

No	Pore Vol	C/Co	No	Pore Vol	C/Co
1	0.00	0.000	46	1.63	0.995
2	0.78	0.000	47	1.65	0.995
3	0.80	0.010	48	1.67	1.000
4	0.82	0.029	49	1.82	1.000
5	0.83	0.064	50	1.83	0.995
6	0.86	0.118	51	1.84	0.990
7	0.87	0.176	52	1.85	0.980
8	0.89	0.235	53	1.86	0.971
9	0.91	0.294	54	1.87	0.951
10	0.93	0.353	55	1.88	0.936
11	0.95	0.402	56	1.89	0.912
12	0.97	0.456	57	1.90	0.882
13	0.99	0.505	58	1.91	0.824
14	1.01	0.554	59	1.92	0.775
15	1.03	0.618	60	1.94	0.706
16	1.05	0.676	61	1.95	0.637
17	1.07	0.725	62	1.96	0.569
18	1.09	0.755	63	1.97	0.515
19	1.11	0.775	64	1.98	0.456
20	1.13	0.784	65	1.99	0.412
21	1.15	0.804	66	2.00	0.373
22	1.16	0.814	67	2.01	0.333
23	1.18	0.828	68	2.02	0.299
24	1.20	0.843	69	2.03	0.279
25	1.22	0.853	70	2.04	0.250
26	1.24	0.868	71	2.05	0.230
27	1.26	0.877	72	2.07	0.191
28	1.28	0.887	73	2.10	0.162
29	1.30	0.902	74	2.12	0.132
30	1.32	0.912	75	2.14	0.113
31	1.34	0.922	76	2.16	0.093
32	1.36	0.926	77	2.18	0.078
33	1.38	0.936	78	2.20	0.069
34	1.40	0.941	79	2.22	0.054
35	1.42	0.951	80	2.24	0.049
36	1.44	0.956	81	2.27	0.039
37	1.46	0.961	82	2.29	0.034
38	1.48	0.966	83	2.31	0.029
39	1.50	0.971	84	2.33	0.025
40	1.51	0.975	85	2.35	0.020
41	1.53	0.980	86	2.37	0.015
42	1.55	0.985	87	2.39	0.010
43	1.57	0.985	88	2.41	0.005
44	1.59	0.990	89	2.43	0.000
45	1.61	0.990			

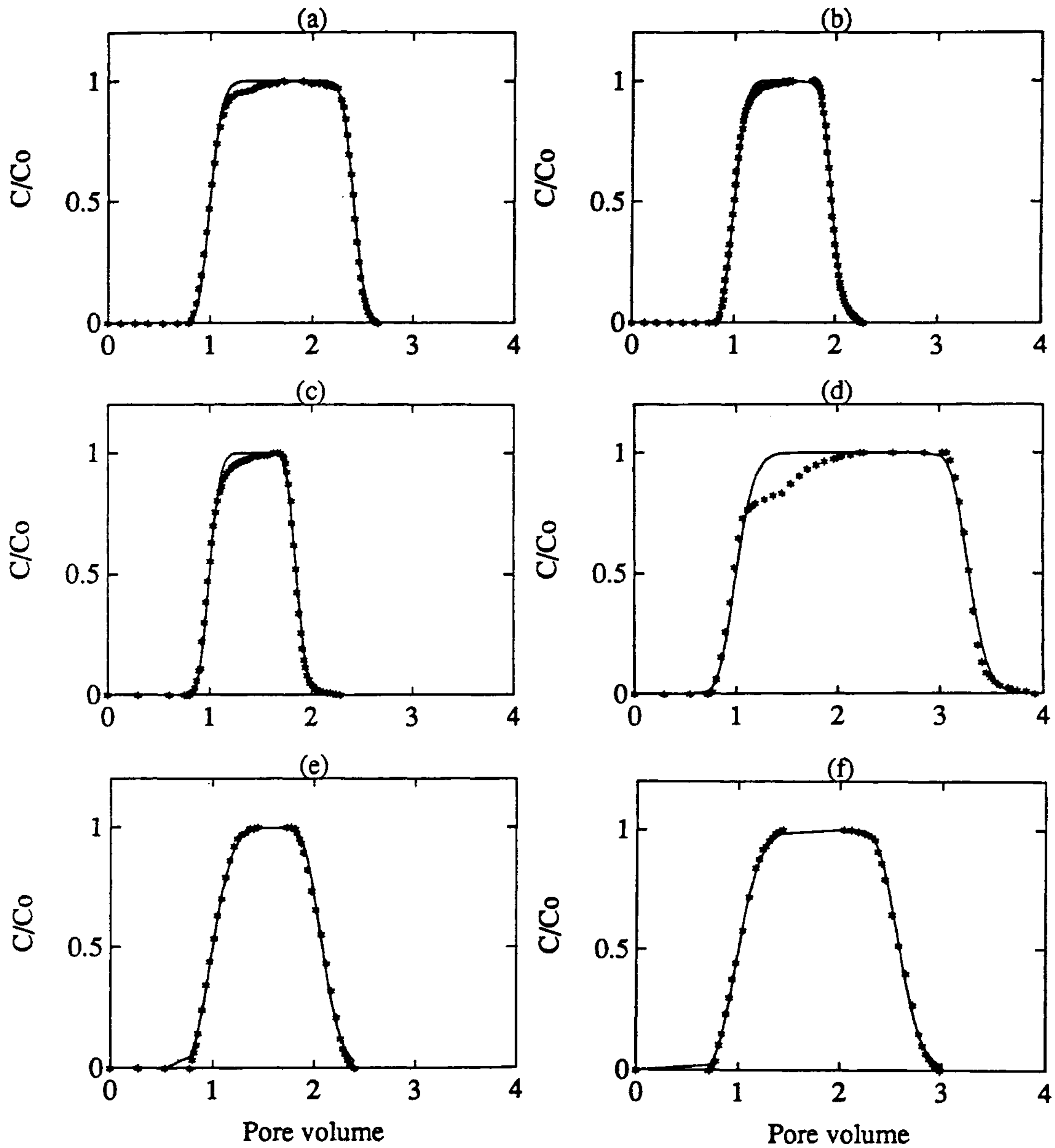

Figure 1. Equilibrium model fits to the break curve of NaCl: a) experiment 1, Borden soil; b) experiment 2, Borden soil; c) experiment 3, Borden soil; d) experiment 4, Borden soil; e) experiment 5, Cambridge soil; f) experiment 6, Cambridge soil. * observed; – fitted line.

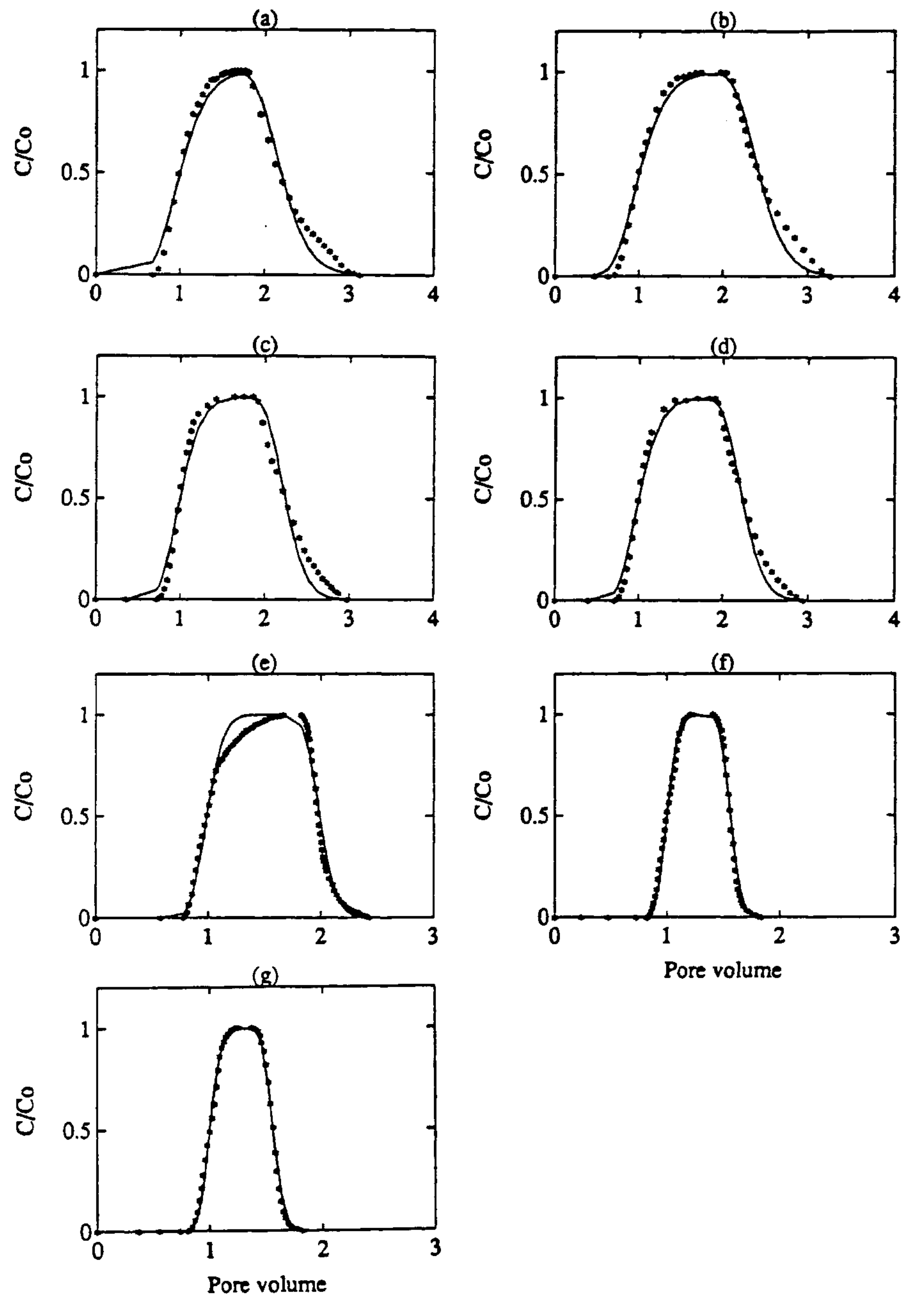

Figure 2. Equilibrium model fits to the breakthrough curve of NaCl: a) experiment 7, Cape-Cod soil; b) experiment 8, Cape-Cod soil; c) experiment 9, Cape-Cod soil; d) experiment 10, Cape-Cod soil; e) experiment 11, 0.5-mm silica beads; f) experiment 12, 0.5-mm silica beads; g) experiment 13, 0.5-mm silica beads. * observed; – fitted line.

LITERATURE CITED

Bergey's Manual of Determinative Bacteriology, 18th ed., The Williams and Wilkins Co., Baltimore, 1974.

Standard Methods For the Examination of Water and Wastewater, 1268 pp., American Public Health Association, 1985.

Adams, M. H., *Bacteriophages,* Interscience Publishers, New York, 1959.

Bales, R. C., C. P. Gerba, G. H. Grondin, and S. L. Jensen, Bacteriophage transport in sandy soil and fractured tuff, *Applied and Environmental Microbiology, 55,* 2061-2067, 1989.

Bales, R. C., S. R. Hinkle, T. W. Kroeger, K. Stocking, and C. P. Gerba, Bacteriophage adsorption during transport through porous media: chemical perturbations and reversibility, *Submitted for publication*, 1991.

Barber, L. B., Geochemical heterogeneity in a glacial outwash aquifer: Effects of particle size and mineralogy on sorption of nonionic organic solutes, Ph.D.dissertation, 237 pp., University of Colorado, 1990.

Bitton, G., in *Introduction to Environmental Virology,* p. 326, John Wiley & Sons, New York, 1980.

Cameron, D. and A. Klute, Convective-Dispersive solute transport with combined equilibrium and kinetic adsorption model, *Water Resources Research, 13,* 183-188, 1977.

DeMarsily, C., in *Quantitative Hydrogeology,* p. 440, Academic Press, San Diego, 1986.

Doyle, R J., F. Nedjat-Haiem, and J. S. Singh, Hydrophobic characteristics of Bacillus spores, *Current Microbiology, 10,* 1984.

Drever, J. I., in *The Geochemistry of Natural Waters,* p. 437, Prentice Hall, Inc, Englewood Cliffs, New Jersey, 1988.

Duboise, S. M., B. E. Moore, C. A. Sorber, and B. P. Sagik, Viruses in soil systems, in *CRC Critical Reviews in Microbiology,* edited by H. D. Isenberg, vol. 7, pp. 245-285, CRC Press, West Palm Beach, FL, 1979 .

Farrah, S., D. O. Shah, and L. O. Ingram , Effects of chaotropic and antichaotropic agents on elution of poliovirus adsorbed on membrane filters, *Proceedings of the National Academy of Science of the United States of America, 78,* 1229-1232, 1981.

Freeze, R. and J. Cherry, *Groundwater,* 604 pp., Prentice Hall, Inc., Englewood Cliffs, New Jersey, 1979.

Garabedian, S. P. and D. R. LeBlanc, Overview of contaminant hydrology, geochemistry, and microbiology at the Cape Cod Toxic Waste Research Site, in *U.S. Geological Survey Toxic Substances Hydrology Program-- Proceedings of the Technical Meeting, Phoenix, Arizona, September 26-30, 1988: U.S. Geological Survey Water-Resources Investigations Report 88-4220,* U.S. Geological Survey, 1989.

Gerba, C. P. and G. Bitton, Microbial pollutants, their survival and transport pattern to groundwater, in *Groundwater Pollution Microbiology,* edited by C. P. Gerba, pp. 65-88, John Wiley and Sons, NY, 1984.

Harvey, R. W. and S. P. Garabedian, Use of colloid filtration theory in modeling movement of bacteria through a contaminated sandy aquifer, *Environmental Science and Technology, 25,* 178-185, 1991.

Hinkle, S., Modeling Colloid Transport in Saturated Porous Media, M.S. Thesis, 68 pp., Department of Hydrology and Water Resources, University of Arizona, Tucson, AZ, 1990.

Keswick, B. H., D. S. Wang, and C. P. Gerba, The use of microorganisms as groundwater tracers: a review, *Ground Water*, *20*, 142-149, 1982.

LeBlanc, D. R., in *Open File Report 84-475*, pp. 1-46, U. S. Geological Survey, Reston, VA, 1984.

Lemon, L. A., J. R. Barbaro, and J. F. Barker, Biotransformation of BTEX under anaerobic denitrifying, in *Proceedings of the FOCUS Conference On Eastern Regional Ground Water Issues, Kitchener, Ontario, Canada*, National Water Well Association, October 17-19, 1989.

Lips, A. and N. E. Jessup, Colloidal aspects of bacterial adhesion, in *Adhesion of Microorganisms to Surfaces*, pp. 5-27, New York, 1979.

MacFarlane, D. S., J. A. Cherry, R. W. Gillham, and E. A. Sudicky, Migration of contaminants in groundwater at a landfill: A case study, 1. groundwater flow and plume delineation, *Journal of Hydrology*, *63*, 1-29, 1983.

Mackay, D. M., D. L. Freyberg, and P. V. Roberts, A natural gradient experiment on solute transport in a sand aquifer, 1. Approach and overview of plume movement, *Water Resources Research*, *22*, 2017-2029, 1986.

McDowell-Boyer, L. M., J. R. Hunt, and N. Sitar, Particle transport through porous media, *Water Resources Research*, *22:13*, 1901-1921, 1986.

Murray, J. P. and G. A. Parks, Poliovirus adsorption on oxide surfaces: correspondence with the DLVO-Lifshitz theory of colloid stability, in *Particulates in Water*, edited by M. C. Kavanaugh and J. O. Leckie , Advances in Chemistry Series 189, pp. 97-133, American Chemical Society, Washington, D.C. , 1980.

O'Melia, C. R., Aquasols: the behavior of small particles in aquatic systems, *Environmental Science and Technology*, *14*, 1052-1060, 1980.

Olsen, R. H., J. Siak, and R. Gray, Characteristics of PRD1, a plasmid-dependent broad host range DNA Bacteriophage , *Journal of Virology*, *14*, 689-699, 1974.

Parks, G. A., The isoelectric points of solid oxides, solid hydroxides, and aqueous hydroxo complex systems, *Chemistry Reviews*, *65*, 177-198, 1965.

Rao, P. S. C., J. Davidson, R. Jessup, and H. Selim, Evaluation of conceptual models for describing nonequilibrium adsorption-desorption of pesticides during steady flow in soils, *Journal of the Soil Science Society of America*, *43*, 22-28, 1979.

Richmond, D. V. and D. J. Fisher, The electrophoretic mobility of micro-organisms, in *Advances in Microbial Physiology*, vol. 9, 1973.

Robertson, W. D., J. A. Cherry, and E. A. Sudicky, Ground water contamination from two small septic systems on sand aquifers, *For publication in Ground Water*, 1990.

Rogers, H. J., Adhesion of Microorganisms to Surfaces: Some General Considerations of the Role of the Envelope., in *Adhesion of Microorganisms to Surfaces*, pp. 29-55, New York, 1979.

Rose, D., Hydrodynamic dispersion in porous materials, *Soil Science*, *123*, 277-283, 1977.

Rosenberg, M., D. Gutnick, and E. Rosenberg, Adherence of bacteria to hydrocarbons: A simple method for measuring cell-surface hydrophobicity, *FEMS Microbiology Letters*, *9*, 29-33, 1980.

Shutter, S. B., E. A. Sudicky, and W. D. Robertson, Numerical analysis of chemical migration from a domestic septic system in a sandy aquifer, *For publication in Ground Water*, 1990.

Snyder, L. R. and J. J. Kirkland, *Introduction to Modern Liquid Chromatography, 2nd ed.*, 863 pp., Wiley, New York, 1979.

Stocking, K., Adsorption of MS-2 Bacteriophage to Silica, M.S. Thesis, 91 pp., Department of Hydrology and Water Resources, University of Arizona, Tucson, AZ, 1989.

Stotzky, G., Mechanisms of adhesion to clays, with reference to soil systems, in *Bacterial Adhesion, Mechanisms and physiological significance*, edited by M. Flecher, pp. 195-245, Plenum Press, New York, 1985.

Stumm, W. and J. J. Morgan, *Aquatic Chemistry*, 780 pp., Wiley, New York, 1981.

Tanford, C., in *The Hydrophobic Effect, Formation of Micelles and Biological Membranes*, p. 200, Willey-Interscience Publication, New York, 1973.

VandeVen, T. G. H., in *Colloidal Hydrodynamics*, p. 582, Academic Press, London, 1989.

VanGenuchten, M. Th., Non-equilibrium transport parameters from miscible displacement experiments, *Research Report 119*, 88 pp., U. S. Salinity Lab, Riverside, CA, 1981.

VanLoosdrecht, M. C. M., J. Lyklema, W. Norde, and A. J. B. Zehnder, Bacterial adhesion: A physicochemical approach, *Microbial Ecology*, *17*, 1-15, 1989.

Wicken, A. J., Bacterial Cell Walls and Surfaces, in *Bacterial Adhesion, Mechanisms and Physiological Significance*, edited by M. Flecher, pp. 45-67, Plenum Press, New York, 1985.

Yates, M. V. and S. R. Yates, Modeling microbial fate in the subsurface environment, in *CRC Critical Reviews in Environmental Control*, edited by C. P. Straub, vol. 17, pp. 307-344, CRC Press , Boca Raton, FL, 1988 .

Zerda, K. S., Adsorption of viruses to charge-modified silica, Ph.D. dissertation, 128 pp., Baylor College of Medicine, Houston, TX, 1982.